https://ntrs.nasa.gov/search.jsp?R=19660020690 2020-03-16T20:56:20+00:00Z

NSG-228

# RECOMBINATION LIFETIMES IN GAMMA-IRRADIATED SILICON

Ralph Allan Hewes
Department of Physics
University of Illinois
Urbana, Illinois

GPO PRICE $ ______

CFSTI PRICE(S) $ ______

Hard copy (HC) 5.00

Microfiche (MF) 1.25

ff 653 July 65

Ph.D. Dissertation

June, 1966

N66 29980

(ACCESSION NUMBER) (THRU)

188 (PAGES) 1 (CODE)

CR-76090 (NASA CR OR TMX OR AD NUMBER) 24 (CATEGORY)

FACILITY FORM 602

# RECOMBINATION LIFETIMES IN GAMMA-IRRADIATED SILICON*

Ralph Allan Hewes

This report is based on a thesis submitted in partial fulfillment of the requirements for the degree of Doctor of Philosophy in Physics in the Graduate College of the University of Illinois, 1966.

*This research was supported in part by the National Aeronautics and Space Administration, Grant NSG 228-62.

RECOMBINATION LIFETIMES IN GAMMA-IRRADIATED SILICON

Ralph Allan Hewes, Ph.D.
Department of Physics
University of Illinois, 1966

The small-signal recombination lifetimes of minority carriers were measured as a function of temperature in silicon before and after irradiation at room temperature by cobalt 60 gamma rays. The resistivity of the boron doped samples ranged between 10 and 5000 ohm-cm, and the resistivity of the phosphorus doped samples was between 20 and 220 ohm-cm. Both crucible and floating zone grown materials were investigated.

The radiation induced lifetime changes were interpreted by the theory of Hall, and Shockley and Read. The lifetime changes in n-type material were interpreted to be due to two energy levels, one 0.17 ev from the conduction band edge, which was assumed to be the substitutional oxygen (A center) defect, and the other at 0.4 ev from the conduction band edge. On the basis of annealing data, it appeared that the 0.4 ev level could be due to several defects whose energy levels coincided, but that most of the recombination in the float-zoned material occured through the donor-vacancy complex (E center). The introduction rates of the levels were not strongly influenced by differences in resistivity, but the introduction rate of the 0.4 ev level was much less in material containing large oxygen concentrations.

Defects controlling the lifetime in irradiated p-type material were placed at 0.18 ev above the valence band edge and at 0.3 ev below the conduction band edge. The former level could possibly be located 0.18 ev below the conduction band edge, but it is most unlikely that it is the A center because of the ratio of the hole and electron capture cross-sections. The

0.18 ev level controlled the lifetime in the room temperature region in the pulled material, and the 0.3 ev level controlled the lifetime at all measured temperatures in float-zoned material whose resistivity was 70 ohm-cm or greater. The ratio of the hole to electron capture cross-section for the 0.3 ev level was about 20. No strong effect of resistivity was seen in either of the p-type silicon, but the effect of the larger oxygen content of the pulled material was to reduce the introduction rate of the 0.3 ev level.

## ACKNOWLEDGMENTS

It is a pleasure for the author to thank Professor W. Dale Compton for suggesting this problem, and especially for his guidance, advice, encouragement, and patience throughout the endeavor.

He is indebted to Dr. E. A. Davis and Mr. R. J. Spry for many invaluable discussions, and to Professor F. C. Brown for the loan of certain equipment.

He wishes to thank Mr. James Pfaff and Mr. E. J. West of the U. S. Naval Research Laboratory in Washington, D. C., for performing the Cobalt 60 irradiations.

He is grateful to Mr. Morris Firebaugh for assistance with the computer analysis.

He thanks Mr. R. MacFarlane for preparing the illustrations, and Mrs. Divona Keel for typing the final manuscript.

He is grateful for the support and encouragement of his wife, Judy, during his graduate studies.

# TABLE OF CONTENTS


I. INTRODUCTION . . . . . . . . . . . . . . . . . . . . . . . . . 1

A. Chemical and Structural Defects in Silicon and Germanium . . . . . . . . . . . . . . . . . . . . . . . 1
B. Irradiation Induced Defects in Silicon . . . . . . . . 5
C. Effects of Source of Radiation . . . . . . . . . . . . 13
D. Purpose of the Investigation . . . . . . . . . . . . . 15

II. THEORY . . . . . . . . . . . . . . . . . . . . . . . . . . . 17

III. PROCEDURE . . . . . . . . . . . . . . . . . . . . . . . . . 51

A. Measurements . . . . . . . . . . . . . . . . . . . . . 51

1. Sample Preparation and Preliminary Measurements. . 51
2. Lifetime Measurement Procedure -- Pre-Irradiation 59
3. Irradiation Procedure . . . . . . . . . . . . . . 69
4. Post-Irradiation Measurements . . . . . . . . . . 69
5. Anneal Procedure . . . . . . . . . . . . . . . . . 70
6. Equipment Calibration Procedure . . . . . . . . . 70

B. Analysis of Data . . . . . . . . . . . . . . . . . . . 71

1. Raw Data Analysis . . . . . . . . . . . . . . . . 71
2. Analysis of Lifetime-Temperature Data . . . . . . 82

IV. DISCUSSION OF RESULTS . . . . . . . . . . . . . . . . . . . 90

A. Phosphorus Doped Floating Zone Grown Silicon . . . . . 90
B. Phosphorus Doped Crucible Grown Silicon . . . . . . . 109
C. Boron Doped Crucible Grown Silicon . . . . . . . . . . 121
D. Boron Doped Float-Zoned Silicon . . . . . . . . . . . 134

V. SUMMARY AND RECOMMENDATIONS . . . . . . . . . . . . . . . . 150

APPENDIX I. LIFETIME IN THE VALIDITY OF THE SHOCKLEY-READ FORMULA . . . . . . . . . . . . . . . . . . . . . . . . . 153

APPENDIX II. VERIFICATION OF THE VALIDITY OF THE SHOCKLEY-READ FORMULA . . . . . . . . . . . . . . . . . . . . . . 161

REFERENCES . . . . . . . . . . . . . . . . . . . . . . . . . . 166

VITA . . . . . . . . . . . . . . . . . . . . . . . . . . . . . 170

# I. INTRODUCTION

## A. Chemical and Structural Defects in Silicon and Germanium

The diamond lattice semiconductors, germanium and silicon, are among the most important materials in the electronic age. Most electronic instruments use solid state devices extensively, if not exclusively. The vacuum tubes which served technology well for over a quarter of a century have been supplanted by transistors and diodes in many applications. The much larger power requirements of vacuum tubes, together with their fragility make them unsuitable for uses ranging from portable radios to scientific instruments used in space vehicles.

Although silicon and germanium can be prepared with greater purity than most, if not all, other substances, it is only when they contain regulated amounts of certain impurities that they are useful. Pure silicon is a very poor conductor, with a resistivity of 23,000 ohm-centimeters at room temperature. When elements from group V(P, As, Sb) are present in concentrations of one part in 100 million, silicon has a resistivity of about 8 ohm-centimeters. This drop in resistivity is due to electrons thermally ionized into the conduction band from the impurities, which have energy levels in the forbidden gap slightly below the conduction band. Similarly, the introduction of one part per million of group III impurities (B, Al, Ga, In) reduces the resistivity to about 25 ohm-centimeters. The difference in resistivity between n-type (Group V doped) and p-type (Group III doped) silicon is due to the difference in mobility between electrons and holes as charge carriers.

Other defects, besides those mentioned previously, are often present in silicon and germanium, and can greatly change the usefulness of the material

for transistors, even though their concentrations may be many orders of magnitude below that of the major impurity. Transistors depend upon the diffusion of excess minority carriers for their operation, and the distance a minority carrier is able to diffuse depends greatly upon the defects present.

If the concentration of minority carriers is increased beyond the thermal equilibrium value in a non-uniform manner in an infinite crystal, the two processes of recombination and diffusion will occur simultaneously. Because the concentration is larger than the equilibrium value, it will decrease toward that value, and for small deviations from equilibrium, the decay will be nearly exponential. If the excess minority carriers are holes and their concentration is denoted by $\delta p$, the time constant $\tau$ determined by the logarithmic derivative $-\frac{1}{\delta p}\frac{d(\delta p)}{dt} = 1/\tau$ is called the lifetime.

The excess holes will also tend to diffuse away from each other, so that in the absence of recombination the excess hole concentration would be uniform over the volume of the crystal at the end of an infinite period of time. Since recombination occurs, excess holes introduced at a surface will travel on the average a distance $L_d$ from the surface before recombining with an electron. The quantity $L_d$ is known as the diffusion length, and is related to the lifetime and the diffusion constant D by $L_d = \sqrt{D\tau}$, where D is given by $D = \mu kT/q$, with k the Boltzmann's constant, T the Kelvin temperature, $\mu$ the minority carrier drift mobility (ratio of the drift velocity in an applied electric field to the applied electric field), and q the charge of the minority carrier. The mobility is decreased when defects are introduced

into the crystal due to scattering of the charge carriers by the defects, but at temperatures at which these devices are used, mobility changes are quite small compared to changes in the lifetime. Measurable changes in the lifetime can be detected with defect concentrations two orders of magnitude less than can be detected by other means.

The defects can be classified into two categories: intrinsic defects and extrinsic defects. Intrinsic defects include vacancies and interstitials and all complexes formed by these two primary defects. A vacancy is the defect formed when an atom is removed from its lattice site, and an interstitial is the defect formed when the atom is placed in the crystal at any non-lattice point. Both vacancies and interstitials are present in a pure crystal according to entropy and energy considerations.[1] Free electrons and holes can also be considered imperfections, since they arise from the same considerations that cause vacancies and interstitials. Extrinsic defects include structural defects, such as surfaces, twin planes, edge and screw dislocation lines, as well as chemical impurities. Crystal growth has been shown to occur fastest along screw dislocations,[2] and edge dislocation lines can easily be introduced by the application of stress.[3] The usual techniques of growth produce large concentrations of edge dislocations due to thermal stresses arising from the large thermal gradients present.[4]

The presence of chemical impurities is unavoidable, since crystals must be prepared from impure ores. In preparing crystals from the chemically purest material available, it is often possible to greatly reduce the impurity concentrations during the process of single crystal growth by making use of the fact that most elements are more soluble in the molten

phase of silicon or germanium that in the solid.[5] For such substances, techniques which do not allow the molten mass to cool uniformly, but which cause solidification to proceed from one end of the crystal to the other, result in most of the impurity being found in the portion of the crystal that was last to freeze. Boron can not be removed from germanium by this technique, since it is about twenty times as soluble in the solid as in the melt. In silicon, boron has a solubility in the melt about 1.5 times that in the solid, and all other impurities are much less soluble in the solid than in the melt, so it is relatively easy to purify silicon.

Originally silicon was grown by dipping a seed, a small crystal, into a melt contained in a quartz crucible, and then pulling the seed slowly out of the melt. The melt would then freeze onto the seed, resulting in fairly large single crystals.[6] About 1955 it was discovered that large concentrations of oxygen were present in silicon crystals grown in this manner due to the large solubility of oxygen in silicon.[7] Ordinarily the oxygen in such crystals is in the form of interstitial molecules and is electrically inactive, but if the silicon is subjected to heat treatment,[8] and under certain other conditions, the oxygen becomes electrically active, changing the resistivity and the lifetime.

The floating zone process of growing silicon was then developed by Keck and van Horn.[9] In this process the solid crystal is placed in an inert atmosphere or vacuum, held vertically at the ends, and a molten zone is created by induction heating. This zone is then moved up or down the crystal, and the material is refined by the freezing process mentioned before. The zone length is dependent upon the crystal diameter, since the molten mass is supported

solely by surface tension. The oxygen concentration of crystals prepared in this manner is about one percent of that found in crystals pulled from the melt.[7]

B. Irradiation Induced Defects in Silicon

This is also the nuclear and space age, and high energy radiation has been found to introduce defects into silicon.[10] In order that precautions might be taken against degradation by radiation from nuclear sources or outer space, so that semiconductor devices operated in or near such environments would not undergo changes in operating characteristics that would render them useless, it is necessary to know the effect of radiation upon the material.

A great many studies have been made upon irradiated silicon and germanium. The principle techniques used to study silicon and germanium are electron spin resonance, optical absorption, Hall effect and resistivity studies as a function of temperature, photoconductivity, and many types of lifetime measurements. Spin resonance is a powerful technique to determine the microscopic structure of a defect. However, it is not possible to determine the location of the energy level in the forbidden gap that gives rise to a particular resonance signal by use of resonance techniques alone, since some other technique must be used to determine the position of the Fermi level, which in turn determines which defects are occupied by electrons. Many unidentified resonances exist in silicon.[11] Another shortcoming of spin resonance is that it is difficult to ascertain whether or not a particular defect that exhibits a resonance has an important effect upon any of the other properties of the material.

Optical absorption readily gives the energy separation of a particular defect level from a band edge, if the transition between the defect level and a band edge is favored by symmetry and population considerations. However, it is not possible to determine directly which band is involved in the transition. Transitions between two bound states of a defect can be very difficult to interpret.

Photoconductivity is in a sense an extension of optical absorption. It is difficult to accurately measure small changes in the absorption coefficient. If the transition is between a bound state and either the conduction or valence bonds, it may be possible to detect the transition by means of photoconductivity even though the absorption coefficient for the transition is unmeasurable. The increased sensitivity of photoconductivity measurements is accomplished by use of a modulated excitation source, which produces an ac signal capable of amplification.

The Hall effect, combined with resistivity data, provides a fairly straightforward method for determining the energy levels and charge states of the major electrically active levels, since the Hall coefficient is inversely proportional to the electron (hole) concentration in the conduction (valence) band. The Hall mobility, the ratio of the Hall coefficient and the resistivity, provides information about the charge states of the defects since the mobility is affected by the scattering of the mobile charge carriers by the defects. Since the energy level positions are determined by the change of the Hall coefficient with temperature, only level positions in the upper (lower) half of the gap can be determined in n-type (p-type) material, making the Hall effect a majority carrier technique.

In order to obtain data easily interpreted by the above techniques, it is necessary to damage the semiconductor much more than is necessary to cause great changes in the lifetime. Since some studies have shown that the introduction rates of some defects are not linear, care must be taken in interpreting data taken at different total doses.

Changes in the minority carrier lifetime can be measured by many methods. Among those used most on silicon are "junction" methods[12,13] and various bulk methods. The junction techniques utilize the fact that various parameters of p-n junctions are strongly dependent on the lifetime. The most common bulk methods are the microwave techniques,[14] which measure the decay of the free-carrier absorption of microwaves by a pulse of excess carriers, the photoconductivity or photo-decay methods which measure the decay of the change in the conductivity due to a pulse of excess carriers, and other conductivity decay methods. The excess carriers in the microwave study are usually generated by exposing the crystal to a burst of light. Bursts of fast electrons are also used to create electron-hole pairs, and the measurement of the decay of the conductivity created by this method is identical to photo-decay measurements.

Each technique has its advantages, but a review of the literature shows that the number of energy levels reported is only slightly less than the number of experimenters reporting. Part of the difficulty in assessing whether such a multiplicity of levels is due to technique or to minor impurities in the samples is that no single experimenter has investigated a broad range of samples. If minor impurities are the source of the defects introduced by irradiation, then a variety of samples investigated by one technique would

show a variety of defect levels. If, on the other hand, the differences in levels positions are due to differences in techniques, samples containing the same basic defects would give different results if measured by different methods. Vavilov and Plotnikov[15] investigated a number of samples of irradiated silicon by both the Hall effect and photoconductivity. By comparing the changes in both the Hall coefficients and photoconductivity spectra which occured when the samples were annealed, they concluded that the energy levels in the lower half of the gap, as determined by photoconductivity, were related to levels differing in energy by 0.03 ev from those obtained by Hall measurements. They pointed out that their results did not agree entirely with the earlier photoconductivity results of Fan and Ramdas.[16] Some discrepancies are to be expected between the results of lifetime measurements and photoconductivity measurements, since, as will be seen, lifetime measurements yield the level positions at $0^{o}K$, while the levels as determined by photoconductivity measurements are for the temperature of measurement. Some studies have shown that junction methods and photo-decay methods give nearly identical results for the same crystals.[17] Few comparisons have been done between microwave and photo-decay or junction methods, and examination of the data published for microwave measurements shows that it does not appear to fit the Shockley-Read theory as well as that obtained by the other methods.[18,19]

Originally it was assumed that the defects resulting from radiation damage would be the simplest possible,[20] the vacancy and the interstitial, and early studies attempted to explain the defects found on this basis.[21] It was soon realized that this was not the case, and that the primary defects

are not stable even at reduced temperatures, and that they disappear, forming complexes, in the case of vacancies, or by annihiliation at structural defects, as has been supposed for interstitials.[22,23] Conclusive evidence has been presented that the activation energy for motion of vacancies in silicon is less than a third of an electron volt, allowing migration even at liquid nitrogen temperatures.[24] The interstitial has remained unobserved to date, but is assumed to be able to move at much lower temperatures than the vacancy, due to the open nature of the diamond lattice.

The defect levels discovered in silicon irradiated by electron and gamma rays that are stable in the room temperature region are listed in Tables 1 to 3, along with the experimentors, the material used (insofar as can be determined from the literature), the type of damage, either gamma or electron, and the technique used to locate the energy level position.

Conclusive evidence exists for models for several of the above levels. It should be noted that more than one center may contribute levels at a particular energy in the forbidden gap. This seems to be the case for levels at $E_c$ - .4 ev, for at least three different defects have been shown to have levels near that position, the divacancy, the donor-vacancy complex (E-center), and the B-center, whose model is less well known that the other two. Evidence that these are distinct defects was given by Watkins and Corbett, who observed that the E-center EPR signal annealed at much lower temperatures than the divacancy EPR signal,[37,39] and that the B-center EPR signal is not always seen when the others are.[38] By examining various materials, Watkins and Corbett concluded that the divacancy has two other levels, one at about $E_v$ + .27 ev, and one slightly below midgap. The four

Table I

Shallow Levels in the Upper Half of the Forbidden Gap

| Level Position ($E_c$-$E_r$) (ev) | Material Class | Resistivity (ohm-cm) | Technique | Irradiation Source | Reference |
|---|---|---|---|---|---|
| .10 | nFZ | 10 | Hall | e | 25 |
| .10 | n | -- | $\tau$(MW) | $\gamma$ | 26 |
| .146 to .173 | nP, nFZ | .1-56 | Hall | $\gamma$ | 22,27 |
| .16 | n | -- | Hall,$\tau$(MW) | $\gamma$ | 26 |
| .16 | nFZ | 10 | Hall | e | 25 |
| .17 | nFZ | 2.8-140 | Hall | $\gamma$ | 28 |
| .16 | nP, nFZ | 80 | Hall | $\gamma$ | 18 |
| .16 | n | 10,70 | Hall | e | 29 |
| .16 | nP, nFZ | 60-250 | Hall | $\gamma$ | 31 |
| .16 | n | -- | Hall | e | 30 |
| .17 | nP | .43 to .043 | ESR, IA | e | 23,32 |
| .17 | n | -- | IA,PC | e | 16 |
| .16 | pP | 5 | $\tau$(CD) | e | 21 |
| .16 | nP | 5 | $\tau$(J) | e | 33 |
| .16 | nFZ | 32,77 | $\tau$(PD) | $\gamma$ | 34 |
| .18 to .20 | nP | 1,3 | $\tau$(CD) | e | 35 |
| .16 | pFZ | 400 | PC | e | 36 |
| .21 | n | -- | IA,PC | e | 16 |
| .23 | n | -- | $\tau$(MW) | $\gamma$ | 26 |

nFZ: n-type float-zoned silicon
pFZ: p-type float-zoned silicon
nP: n-type pulled silicon
pP: p-type pulled silicon

Hall: Hall effect; IA: infrared absorption; PC: photoconductivity; ESR: electron spin resonance; $\tau$(J): junction lifetime; $\tau$(PD): photo-decay lifetime; $\tau$(CD): conductivity decay (van de Graaf method); e: electron bombardment; $\gamma$: Cobalt 60 gamma ray bombardment; $\tau$(MW): microwave lifetime.

Table 2

Deep Levels in the Upper Half of the Forbidden Gap

| Level Position ($E_c$-E) in ev | Material Class | Resistivity (ohm-cm) | Technique | Irradiation Source | Reference |
|---|---|---|---|---|---|
| .38 | nFZ | 10 | Hall | e | 25 |
| .38 | n | -- | Hall | γ | 31 |
| .40 | nFZ | 2.8-140 | Hall | γ | 28 |
| .40 | nP,nFZ | 80 | Hall,τ(MW) | γ | 18 |
| .40 | n | 10,70 | Hall | e | 29 |
| .40 | n | -- | Hall | e | 30 |
| .40 | n | -- | EPR | e | 37 |
| .40 | nFZ | 32,77 | τ(PD) | γ | 34 |
| .40 | nP | -- | EPR | e | 38 |
| .42 | n | -- | Hall | γ | 31 |
| .43 | n | -- | EPR | e | 39 |
| .43 | n* | -- | Hall | γ | 27 |
| .47 | n† | -- | Hall | γ | 27 |

nFZ: n-type float-zoned silicon
nP : n-type pulled silicon
pFZ: p-type float-zoned silicon
pP : p-type pulled silicon

Hall: Hall effects; EPR: electron paramagnetic resonance; τ(MW): microwave lifetime; τ(PD): photo-decay lifetime; e: electron bombardment; γ: Cobalt 60 gamma ray bombardment.

* doped with Sb.
† doped with P.

Table 3

Energy Levels in the Lower Half of the Forbidden Gap

| Level Position ($E-E_V$) in ev | Material Class | Resistivity (ohm-cm) | Technique | Irradiation Source | Reference |
|---|---|---|---|---|---|
| ≈ .5 | -- | -- | EPR | e | 37 |
| .45 | pFZ | 400;11,000 | PC | e | 36 |
| .40 | nP | -- | EPR | e | 38 |
| .36 | p | 40;600 | Hall | e | 29 |
| .35 | pP | -- | Hall | γ | 40 |
| .30 | pFZ | 400 | PC | e | 36 |
| .30 | pP | 32 | PC | e | 41 |
| .28 | pFZ | -- | Hall | γ | 40 |
| .28 | -- | -- | τ(MW) | γ | 26 |
| .27 | pP | -- | τ(MW) | γ | 19 |
| .27 | n | 3 | τ(PD) | e | 35 |
| .27 | pP,pFZ | -- | Hall | γ | 42 |
| .27 | pP | -- | Hall | e | 41 |
| .27 | pP | .04 | Hall | e | 43 |
| .27 | nP | 7 | τ(CD) | e | 21 |
| .25 | pFZ | -- | PC | e | 41 |
| .22 | pFZ | 32 | PC | e | 41 |
| .21 | pP | -- | τ(MW) | γ | 19 |
| .21 | pFZ | -- | Hall | γ | 40 |
| .21 | pFZ | 2.5 | Hall | e | 43 |
| .21 | pFZ | 32 | Hall | e | 41 |
| .19 | pFZ | 32 | Hall | e | 41 |
| ..18 | pP | 1;2 | τ(CD) | e | 35 |
| .15 | p | 40;600 | Hall | e | 29 |
| .13 | p | -- | τ(MW) | γ | 26 |

nFZ: n-type float-zoned silicon; nP: n-type pulled silicon
pFZ: p-type float-zoned silicon; pP: p-type pulled silicon

EPR: electron paramagnetic resonance; PC: photo-conductivity; Hall: Hall effect; τ(MW): microwave lifetime; τ(PD); phto-decay lifetime; τ(CD): conductivity decay lifetime (Van de Graaf)

charge states of the levels were found to be positive, neutral, negative, and double negative.[37]

The level at about $E_c$ - .17 ev has been shown to be due to the A-center, whose model is a substitutional oxygen atom. Spin resonance,[23] optical absorption,[32] Hall effect,[22,23] and lifetime measurements[33,34] all are compatible with this model.

C. Effects of Source of Radiation

The type of damage created in the material depends to a large part upon the type of radiation to which the material is exposed. Neutrons and heavy charged particles tend to create large disordered regions as well as isolated point defects.[46] The mass of the incident particles is close enough to the mass of a silicon atom that an appreciable fraction of the energy of the incoming particles can be transferred to the struck particle. Unless the energy of the particles is very low, the displaced atom usually possesses enough energy to displace many other atoms in the lattice.

Electrons and gamma rays, because of their much smaller mass, can transfer much less of their energy to the silicon atoms, so that in the average collision the energy transferred is too small for the displaced atom to remove any other atoms from their lattice sites, even for fairly large (1 Mev) energies of the electrons or photons. The cross section for direct displacement of a silicon atom by a gamma ray is very small compared to that of the cross section for interaction of the gamma rays with electrons by the processes of Compton scattering and the photoelectric effect, or the cross section for pair production. The latter process cannot occur for gamma ray energies less than two electron rest masses, and the maximum energy of an

electron or hole created is the energy difference between the gamma ray energy and the energy of formation of the pair.

For gamma rays with energies between 0.06 and 15 Mev[45] the cross section in silicon for Compton scattering is larger than for pair production (which dominates for energies greater than 15 Mev) or for the photoelectric effect (which dominates at energies less than 0.06 Mev).

The high energy electrons created by gamma rays by the above processes have energies ranging downward from the Compton maximum, which is given by

$$E_{max} = \frac{2\ E^2}{2\ E + mc^2}$$

where E is the energy of the gamma ray, m is the electron rest mass, and c is the velocity of light. Due to the design of high activity gamma ray sources, the gamma rays must travel through an appreciable thickness of sample container and source coolant, so that some of the gamma rays are degraded in energy by Compton scattering. Instead of a monoenergetic gamma source, gamma rays of a range of energy are incident upon the material to be irradiated.

Electron irradiation avoids this problem, but only at the expense of less uniform damage. Beams of monoenergetic electrons are readily obtained from Van de Graaf accelerators, permitting damage (at the surface struck by the beam) to be done by particles of the same energy. Due to the high absorption coefficient of these electrons, they are rapidly degraded and unless the sample thickness is kept less than the range of the electrons in the material, the damage will be non-uniform as well as due to electrons having a range of energies. For effects depending reciprocally on the number

of defects, such as the Hall effect or lifetime measurements, the average effect will not be related in a simple manner to the average number of defects created, because of the uniform damage is required in material to be investigated by these methods. The thin samples required for uniform damage by electrons make lifetime measurements more difficult, since the surface lifetime (the lifetime of the sample if no other recombination mechanisms were present) is proportional to the square of the thinnest dimension of the sample if that dimension is much less than any other, posing both theoretical and experimental problems in analysis of lifetime data. Experimentally, the difficulty is posed by the need to cause large changes in the lifetime in order to reduce measurement errors, but yet to have the lifetime much longer than the duration of the pulse used to create the electron-hole pairs whose decay is to be measured.[46] For samples thin enough that electron damage would be sufficiently uniform, the surface lifetime would be of the same order of magnitude as the pulse duration of the flashtube used in this experiment. Theoretical complications arise because the theories derived for relating the lifetime as a function of temperature to the energy levels of the defects are dependent upon the number of defects for the large concentrations necessary to cause the required changes in the lifetime for such thin samples.

## D. Purpose of the Investigation

The purpose of this thesis was to investigate a large variety of samples by one technique to determine, if possible, the extent to which radiation induced lifetime changes are due to major impurities such as the dopant and oxygen, rather than to minor impurities whose concentrations might vary from sample to sample. This required measurement of the temperature dependence of

the lifetime, from which the level positions were determined by use of the Shockley-Read lifetime formula and its generalizations. Cobalt 60 irradiation was used because of its ability to cause uniform damage in large samples.

# II. THEORY

In an infinite, pure crystal the recombination of excess electrons and holes would occur by three processes: band-to-band radiative recombination, band-to-band multiphonon recombination, and band-to-band Auger process. The subject of recombination is comprehensively covered by Blakemore, who points out that for silicon, radiative recombination is the limiting process at reasonably low temperatures.[47] Van Roosbeck and Shockley[48] have predicted that the lifetime from this process should be several tenths of a second in germanium, and since silicon has a wider forbidden energy gap than germanium, the lifetime in silicon should be even longer. Since the observed lifetimes in silicon are of the order of microseconds, recombination is not controlled by band-to-band processes, but by processes involving crystal defects. Of course, every physical crystal possesses a surface and often times several of the other types of defects mentioned in the introduction.

The first theories of recombination via defects were derived by Hall,[49] and Shockley and Read.[50] They considered recombination through a single type of monovalent defect, using the processes shown in Figure 1, but limited themselves to the case of negligible trap adjustment time and to steady state conditions. The trap adjustment time is the time necessary for a defect that has captured a carrier and is in an excited state to make a transition to the ground state. Sandiford[51] and Wertheim[52] showed that the Shockley-Read result (hereafter indicated as S-R) is identical to the result obtained for transient conditions if the concentration of recombination defects is small compared to the thermal equilibrium majority carrier concentration. In his paper, Wertheim also considered recombination in the presence of several types of monovalent defects, and showed that in the limit of small defect concentrations the net

Figure 1. Processes occurring at a Shockley-Read recombination center: (a) free electron captured from the conduction band by the defect; (b) electron emitted from the defect into the conduction band; (c) free hole captured by the defect from the valence band; (d) hole emitted into the valence band by the defect. Processes (a) and (c) result in annihilation of an electron-hole pair; processes (b) and (d) result in generation of an electron-hole pair.

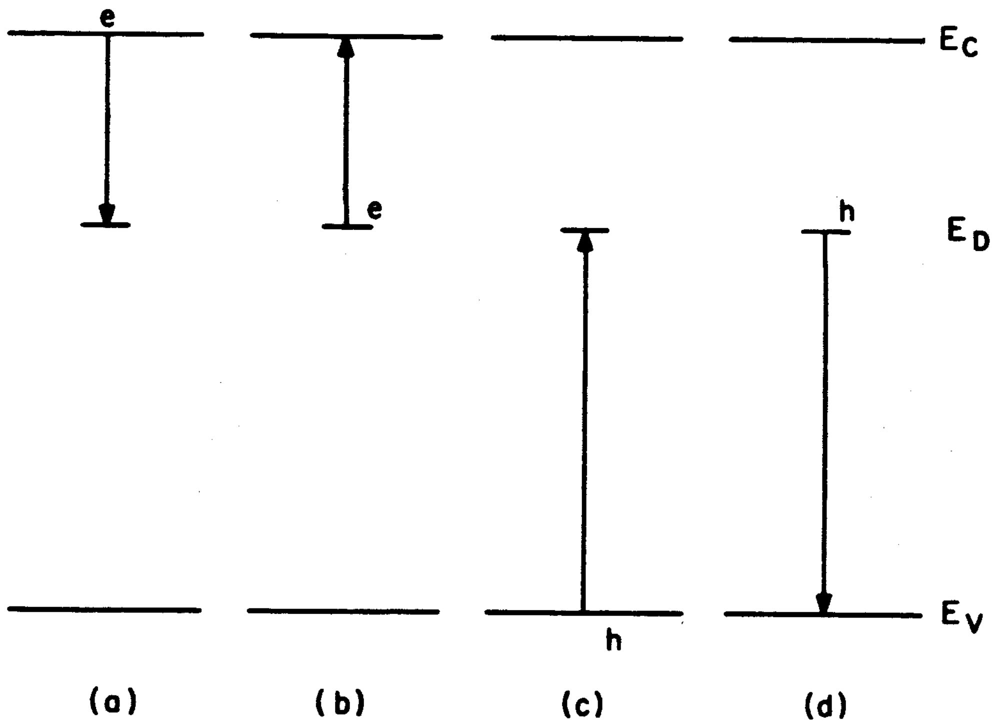


Figure 1

recombination rate $1/\tau$ was given by

$$1/\tau = \sum_j 1/\tau_j \tag{2.1}$$

where $\tau_j$ is the lifetime due to defects of type j. This result permits the calculation of changes in lifetime if defects of various types are introduced or removed, as is possible with radiation damage and annealing, respectively.

Wertheim[6] considered the topic of trapping, in which one of the types of defects present has such a small probability of capturing carriers of one type, that carriers of the opposite type must be thermally excited back into the band from which they were captured by the traps, and then be captured by an active recombination center before they can recombine. Trapping was shown to exist at room temperature in pulled silicon by Hornbeck and Haynes.[53,54] Traps can also be introduced into silicon by irradiation.

The most complete treatment of transient recombination through a monovalent set of defects is due to Nomura and Blakemore,[55] who solved the S-R differential equations exactly for certain limiting cases, and employed a computer to obtain solutions for the general case. They showed that the S-R result was valid for all concentrations of excess carriers if the recombination defect concentration was less than a certain limit.

Experiments have shown that many elements not in the third or fifth columns of the periodic table introduce several energy levels in the forbidden gap of silicon and germanium,[56] and that some radiation-induced defects also introduce several levels.[37,38] Steady-state theories for recombination in the presence of defects of this type have been derived by Sah and Shockley,[57] M. Bernard,[58] Zhdanova, Kalashnikov, and Morozov,[59] and Nagae.[60]

Before discussing the case of recombination through defects, it is appropriate to briefly discuss the subject of surface recombination. Unless the surface is treated to remove or somehow inactivate the surface states, surface recombination will make it impossible to achieve the condition of uniform excess carrier populations that would make possible the unambiguous interpretation of the experimental data, particularly for the case of "large" excess carrier densities. It is also difficult experimentally to obtain reproducible results with such surface treatments. It is generally held that the surface states have a range of energies,[61] so that if one were disposed to treat them by means of Eq. (2.1) and the various S-R lifetimes $\tau_j$, the experimental data would be most difficult to analyze. However, since the ground or polished surfaces have so many recombination defects, the surface lifetime is limited by the rate at which the excess carriers diffuse to the surface.

Shockley first treated the problem of surface recombination in this way. The present treatment is adopted from that of Blakemore.[62] By assuming that the surface and bulk lifetimes add reciprocally, we can neglect recombination in the bulk, and solve the equation of continuity for excess electrons, $n_e$, in p-type material

$$\frac{\partial n_e}{\partial t} = D_n \nabla^2 n_e \tag{2.2a}$$

where $D_n$ is electron diffusion coefficient $\mu_n kT/e$, together with the boundary condition

$$D_n \nabla_{n_e} = - \vec{S}\, n_e \tag{2.2b}$$

where $\vec{S}$ is the surface recombination velocity and is related to the surface recombination rate. The sample dimensions will be 2A, 2B and 2C. The solution is

$$n_e = \sum_{ijk} n_{ijk} = \sum_{ijk} \alpha_{ijk} \, e^{-\nu_{ijk} t} \sin[\frac{\xi_i x}{A} + \delta_i] \sin[\frac{\eta_i y}{B} + \delta_j]$$

$$\sin[\frac{\zeta z}{C} + \delta_k] \qquad (2.3a)$$

where

$$\nu_{ijk} = D_n [\frac{\xi_i^{\,2}}{A^2} + \frac{\eta_j^{\,2}}{B^2} + \frac{\zeta_k^{\,2}}{C^2}] \qquad (2.3b)$$

and the quantities $\xi_i$, $\eta_j$, $\zeta_k$ and the phase angles $\delta_i$, $\delta_j$, $\delta_k$ are determined by the boundary conditions. The boundary condition on $\eta_j$ requires that $-\tan(2\eta_j + \delta_j) = D_n \eta_j / sB$ and the analogous conditions hold for $\xi_i$ and $\zeta_k$. For ground surfaces $\vec{S}$ is so large that to an excellent approximation $\xi_i$, $\eta_j$, $\zeta_k$ are given by

$$\xi_i, \eta_j, \zeta_k = \frac{n\pi}{2} \, , \quad n = 1, 2, \ldots, m, m+1 \ldots$$

The quantities $\alpha_{ijk}$ will be determined by the condition that $\sum_{ijk} n_{ijk} = n_e$ at time $t = 0$. If the quantity $N_{ijk}$ is defined by

$$N_{ijk}^{(t)} = \int_0^{2A} \int_0^{2B} \int_0^{2C} n_{ijk}^{(t)} \, dx \, dy \, dz \qquad (2.4)$$

and if $F(t)$ is given by

$$F(t) = \sum_{ijk} N_{ijk}^{(t)} / \sum_{ijk} N_{ijk}^{(0)}$$

the surface decay can be described by the surface decay rate

$$\nu_s = - \frac{1}{F(t)} \cdot \frac{dF(t)}{dt} \qquad (2.5)$$

the dimension A is much larger than B or C, and if we let B equal C, the fundamental decay rate $N_1$ is then $\nu_{11} = \pi^2 D_n / 2B^2$. The surface decay rate will approximate $\nu_{11}$ for times longer than $1/2\nu_{11}$, but is much larger than $\nu_{11}$ for times less than $1/5\nu_{11}$. Thus the surface lifetime is strictly time dependent rather than concentration dependent.

The lifetime is usually defined as the reciprocal of the recombination rate. Thus, if the excess electron concentration is defined by $\delta_n = n - n_o$, where n is the instantaneous electron concentration in the conduction band, and $n_o$ is the thermal equilibrium concentration, the lifetime of the electron, $\tau_n$, is given by

$$\tau_n = - \frac{\delta n}{\frac{d}{dt}\delta_n} \quad . \tag{2.6}$$

If $\tau_n$ is a constant, this expression can be integrated to give

$$\delta n = \delta n_o e^{-t/\tau_n} \tag{2.7}$$

If Eq. (2.7) is used to calculate the mean time an electron spends in the conduction band before it recombines with a hole, the result is that the mean time $T_m$, is equal to $\tau_n$. The lifetime of a free hole is given by a similar expression. As noted by Nomura and Blakemore[55], however, unless the defect concentration is small, the electron and hole lifetimes will generally be unequal, even if no other types of defects are present, due to trapping by the recombination centers themselves.

Since the S-R differential equations, or modifications thereof, will be used in all later derivations in this thesis, it is of interest to investigate their formulation. The net electron capture rate $U_{cn}$, that is, the net

removal rate of electrons from the conduction band, is equal to $-d\delta n/dt$, and is given by the difference in the rate at which electrons are captured by defects and the rate at which they are emitted back into the conduction band. The capture rate must be equal to the product of the concentration of electrons in the conduction band, n, the number of defects not already containing electrons, $N_o$, and the rate constant for the capture of an electron by an empty defect, $C_n$. The emission rate will be equal to the product of the number of defects containing electrons, $N_e$, the number of empty states in the conduction band, $N_c - n \approx N_c$, and the emission rate constant for an electron trapped at a defect to be returned to an empty conduction band $E_n$. In material in which the defects are always empty, the lifetime will be given by $1/C_nN$ which will be defined as $\tau_{n_o}$. This situation is seen to occur for p-type material at low temperature, for then the emission of electrons back into the conduction band will be negligible, and if the Fermi level lies below the defect level, the defects will all be empty. Due to the large concentration of free holes, any center that captures an electron will capture a hole, annihilating the electron, in a time short compared to the electron capture time. At higher temperatures, due to excitation of the electrons back into the conduction band, or to the fact that the Fermi level has moved above the defect level, decreasing the concentration of empty defects, the lifetime will increase above the value $1/C_nN$. The constant $C_n$ is given by the average over all energies of initial states (in the conduction band) and all final states (ground and excited states) of the product of the capture cross-section of the defect for an electron of energy E, $\sigma(E)$, and the electron speed v. This constant is usually used to define the average capture cross-section

of the defect for electrons, $\sigma_n$, by means of the equation

$$C_n = \sigma_n v_n \tag{2.9}$$

where $v_n$ is the thermal velocity of the electron, $\sqrt{3kT/m_{ce}}$, k is Boltzmann's constant, T is the kelvin temperature, and $m_{ce}$ is the conductivity effective mass of the electron. The emission constant $E_n$ is similarly the average overall energies of the probability for an electron trapped at the defect to be excited to some state in the conduction band. It is possible to eliminate this constant from the equations by considering the case of thermal equilibrium, when the net capture rate must be zero. Thus,

$$U_{cn} = C_n N_o n_o - E_n N_e N_c = 0 \tag{2.10a}$$

or

$$E_n = C_n n_o N_o / N_e N_c \ . \tag{2.10b}$$

The number of empty defect states $N_o$ will be given by $N-N_e$, and $N_e/N$ is equal to the Fermi-Dirac distribution function $f_o(E_R)$,

$$\frac{N_e}{N} = f_o(E_R) = [1 + \omega \exp(E_r - E_f)/kT]^{-1} \tag{2.11}$$

where $\omega$ is the degeneracy of the defect, $E_r$ the energy level of the defect, and $E_f$ the Fermi energy (all energies will be measured relative to the valence band edge). The degeneracy $\omega$ arises from the requirement that the defect has an energy level which contains only one more electron when fully occupied than when fully empty. The degeneracy will be 1/2 or 2 depending upon whether an occupied defect has an unpaired electron or no unpaired electrons, respectively.

Thus $E_n$ is given by

$$E_n = C_n n_o \omega \exp[E_r - E_f)/kT]/N_c \tag{2.12}$$

If $n_{10}$ is defined to be the electron concentration in the conduction band when the Fermi level is at the defect level,

$$n_{10} = N_c \exp[-(E_c - E_R)/kT] \tag{2.13}$$

where $E_c$ is the energy of the lowest conduction band level, then

$$E_n = C_n n_{10} \omega/N_c \tag{2.14}$$

since

$$n_o = N_c \exp[-(E_c - E_f)/kT.] \tag{2.15}$$

If $n_1$ is defined as the product $\omega n_{1o}$, the net electron capture rate becomes

$$U_{cn} = -d(\delta n)/dt = C_n N[(n_o + \delta_n)(1 - f) - n_1 f] \tag{2.16}$$

where f is the fraction of recombination sites occupied by electrons, and under conditions of thermal equilibrium reduces to the Fermi-Dirac distribution $f_o = n_o/n_o + n_1$ = (equation 2.11). By identical considerations the net capture rate for holes is given by

$$U_{cp} = -d\delta p/dt = C_p N[(p_o + \delta p)f - (1 - f)p_1] \tag{2.17}$$

where $C_p$, $p_o$, $p_1$ are defined analogously to $C_n$, etc. above. Note also that $f_o = \frac{p_1}{p_o + p_1}$ since $n_1 p_1 = n_o p_o$. This equation can also be obtained from the net capture rate for electrons by replacing n's by p's, interchanging f and (1 - f), due to the symmetry in the electron-hole formalism.

The S-R result is now obtained by noting that for steady-state conditions, the net electron and hole capture rates must be equal. This allows the

determination of f, and the lifetime is then found from $\tau = \delta n/U_{cn}$.

The transient solution is obtained with the two equations for the net capture rates and the additional requirement of charge conservation: $\delta f = (\delta p - \delta n)/N$, where $\delta f = f - f_o$. The differential equations now are

$$-d\delta n/dt = C_n[\delta n(n_o + n_1 + Nn_1/(n_o + n_1)) - \delta p(n_o + n_1 + n) + \delta n^2] \tag{2.18a}$$

and

$$-d\delta p/dt = C_p[\delta p(p_o + p_1 + \delta_p + Np_1/(p_o + p_1)) - \delta_n(p_o + p_1 + p)]. \tag{2.18b}$$

Nomura and Blakemore[55] found it convenient to transform to a set of dimensionless variables, and to discuss the solutions for p-type material only, noting that the solutions for n-type material could be obtained from the symmetry between electrons and holes. They defined $x = \delta n/p_o$, $y = \delta p/p_o$, $n^* = N/p_o$, $a = n_1/p_o$, $b = p_1/p_o$, $\gamma = C_p/C_n = \tau_{no}/\tau_{po}$, and used the dimensionless time scale $T = t/\tau_{no}$, so that $x' = dx/dT$. Equations (2.18a) and (2.18b) are then

$$-n^*x' = (x-y)[x + a + ab] + n^*x/(1 + b) \tag{2.19a}$$

$$-(n^*/\gamma)y' = (y-x)[1 + y + b] + n^*by/(1 + b) . \tag{2.19b}$$

Simultaneous solution of these equations yields

$$n^*[y''(y+1+b)-y'^2(1-1/\gamma)]+y'[y^2(1+\gamma)+y[(1+b)(1+a+2\gamma)+n^*(1+2b)/(1+b)]$$
$$+ [(1+b)^2(a+\gamma)+n^*(1+\gamma b)]] + \gamma y[y^2+y[(2+b+ab)+n^*b/(1+b)]$$
$$+ [(1+b)(1+ab)+n^*b/(1+b)]] = 0 \tag{2.20a}$$

$$n^*\{x''[x+a(1+b)]-x'^2(1-\gamma)\} + x'(x^2(1+\gamma) + x[(1+b)(2a+\gamma a+\gamma)$$
$$+ \gamma n^*(2+b)/(1+b)] + a[(1+b)^2(a+\gamma)+n^*(1+\gamma b)]\} + \gamma x\{x^2$$
$$+ x[(1+a+2ab) + n^*/(1+b)] + a[(1+b)(1+ab) + n^*b/(1+b)]\} = 0 \qquad (2.20b)$$

They discussed the case of trapping of a fraction of electrons or holes by the defects in the process of transient decay, and defined a quantity r,

$$r = \lim_{\substack{x\to 0\\ y\to 0}} (x/y) = dx/dy|_{x=y=0}$$

and showed that trapping occured for r <u>unequal</u> to one. They solved equations (2.19a) and (2.19b) for r, and found that the upper limit on defect density consistent with $r \approx 1$ was

$$n^* \ll [(1+b)^2(a+\gamma)]/|1-\gamma b|, \text{ or } N \ll \frac{(p_o+p_1)^2(n_1\tau_{p_o}+p_o\tau_{n_o})}{p_o|\tau_{p_o}p_o - \tau_{n_o}p_1|} \qquad (2.21)$$

If n satisfies this condition, then terms in $n^*$ in Equation (2.20a) and (2.20b) can be neglected, and Equation (2.20a) becomes

$$y'[(1+b)(a+\gamma)+y(1+\gamma)]+\gamma y[1+ab+y] = 0$$

and the hole lifetime, which is now equal to the electron lifetime, is

$$\tau_p = -\tau_{n_o}(y/y') = \tau_{p_o}[(1+b)(a+\gamma)+y(1+\gamma)]/[1+ab+\gamma]$$
$$= \frac{\tau_{n_o}(p_o+p_1)+\tau_{p_o}(n_o+n_1)+\delta p(\tau_{n_o}+\tau_{p_o})}{p_o+n_o+\delta p} \qquad (2.22)$$

which is exactly the S-R result. This is also the result obtained by Wertheim[52], in the limit of small defect concentration, but he found it necessary to place restrictions on $\delta n$ and $\delta p$ for conditions of large N that could not be lifted as N was made very small.

If more than one type of defect is present, the total net electron capture rate is the sum of the net capture rates for all the types of levels involved, with the quantities $n_{1_j}$, $C_{n_j}$ etc. The total net hole capture rate is similarly the sum of the net hole capture rates, and the charge conservation equation is now

$$\delta p - \delta n = \sum_{i=1}^{M} N_i \delta f_i \ ,$$

where the sum runs over the M types of levels present. As mentioned previously, Wertheim considered the problem (for M = 2). The result is given in Appendix I, for the recombination case (both $C_{pi}$,$C_{ni}$ non-zero) and the trapping case (one of the four rate capture constants zero).

The result of Sah and Shockley[13] for a multivalent center is that the steady-state lifetime will be given by

$$1/\tau = \sum_{s=1}^{M} 1/\tau_s \left( \frac{N_s + N_{s-1}}{N} \right) \tag{2.23}$$

in the case of small excess carrier densities. The quantity $N_s/N$ is the fraction of defects occupied by s electrons, M is the maximum number of electrons that are bound to the defect, and $\tau_s$ is the S-R lifetime for a monovalent defect having an energy level at $E_s$. The quantity $N_s/N$ is given by

$$\frac{N_s}{N} = \frac{\sum_{k=0}^{s} \frac{p_k}{p_o}}{\sum_{s=0}^{M} \prod_{k=0}^{s} \frac{p_k}{p_o}} \tag{2.24}$$

where $p_k$ is the quantity $p_1$ corresponding to the kth energy level, and when $k = 0$, $p_k = p_o$.

The temperature dependence of the lifetime is shown in Figures 2 through 8. Figure 2 shows the logarithm of the lifetime plotted against reciprocal temperature under the assumptions that 1) the majority carrier concentration is constant, 2) the quantity $\tau_o$ is temperature independent, 3) the defect level is in the same half of the gap as the Fermi level, and 4) the excess carrier density is small. The effect of the degeneracy factor $\omega$ is demonstrated by plotting the lifetime for $\omega = 1/2$, 1, and 2. Figure 3 shows the variation of lifetime with injection level, where the injection level is defined by $\delta n/(n_o+p_o)$. At sufficiently low temperatures, the small signal lifetime will be given in n type material by

$$\tau_o = \frac{\tau_{p_o}(n_o+n_1)+\tau_{n_o}(p_o+p_1)}{n_o+p_o} \approx \tau_{p_o} \tag{2.25}$$

and since $\tau_{p_o} < \tau_{p_o} + \tau_{n_o}$, the lifetime will increase as the injection level is raised. This behavior will persist until $\tau_o = \tau_{n_o} + \tau_{p_o}$, at which temperature $\tau$ is independent of injection level. At yet higher temperatures, $\tau$ will decrease as the excess carrier density increases. However, at all temperatures the slope of $\tau\ (1 + \delta n/n_o+p_o)$ will be equal to $\tau_{n_o} + \tau_{p_o}$.

The behavior of the small signal lifetime in the presence of two types of defects is shown in Figure 4, along with the lifetime expected if only one type of defect were present at a time. If the injection level is varied, the result will be similar to that shown in Figure 5. Note that now $\tau(1 + \delta n/(n_o+p_o))$ does not give any useful information, and that data taken at large injection levels cannot be extrapolated back to zero for meaningful interpretation. Figure 6 and 7 illustrate respectively the effects of varying the resistivity of the material and the ratio of the quantities $\tau_{po}$ for the two levels upon the net lifetime.

Figure 2. Variation of lifetime with reciprocal temperature according to the Shockley-Read theory. The curves were calculated for a recombination level 0.4ev from the conduction band in extrinsic n-type material. $\tau_{po}$ and the energy level position have been assumed constant. The three curves illustrate the effect of the spin degeneracy ratio, denoted here by $\alpha$, upon the lifetime-temperature relationship.

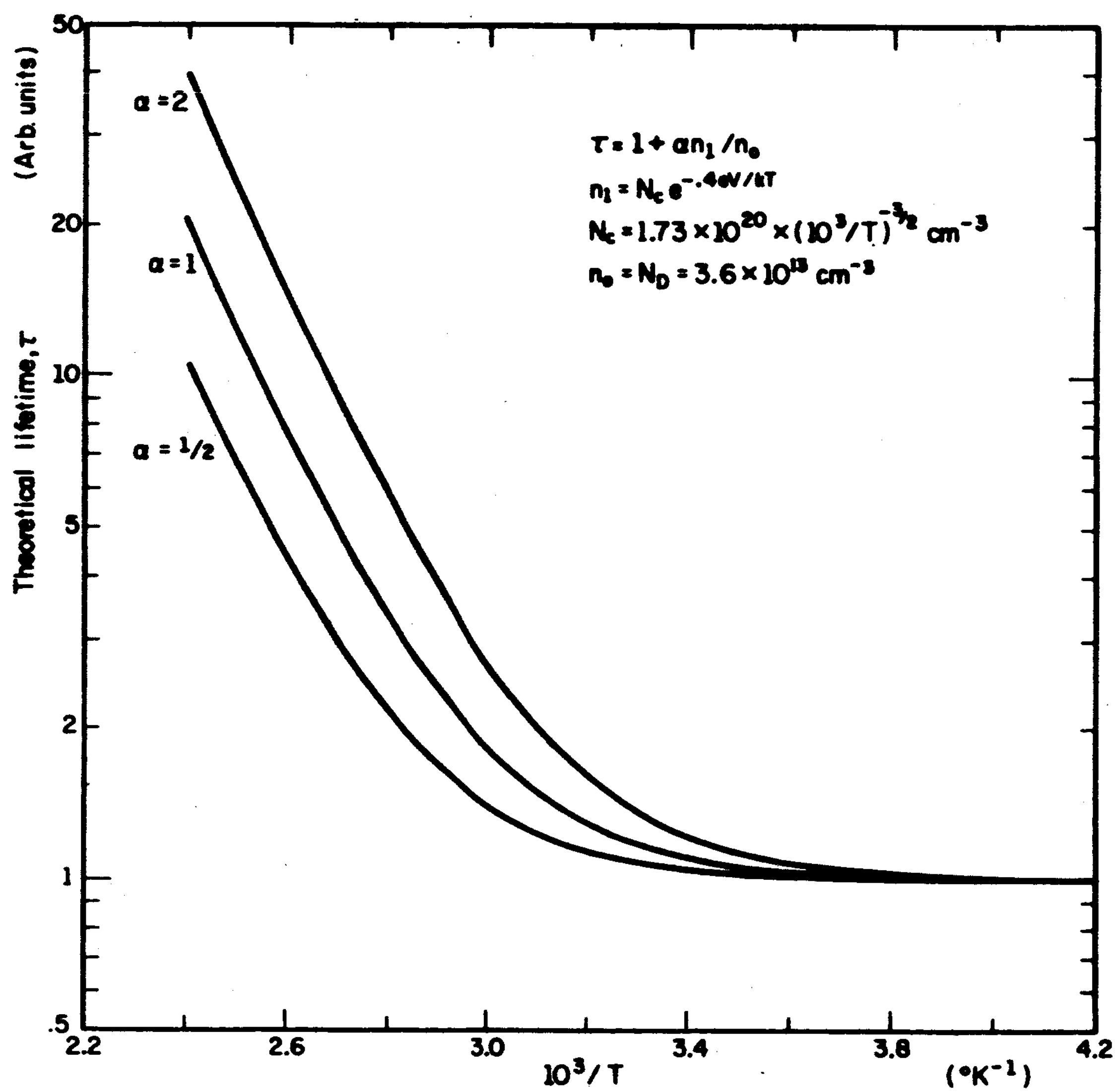


Figure 2

Figure 3. Variation of lifetime $\tau$ and the quantity $\tau(1+x)$ with injection level. The quantity $\tau(1+x)$ is linear in the injection level x with an intercept $\tau_o$ and slope $\tau_{no} + \tau_{po}$, where $\tau_o$ is the small-signal Shockley-Read lifetime. At low temperature ($\tau = \tau_1$), $\tau$ is less than $\tau_{no} + \tau_{po}$, and the lifetime increases with increasing injection level to $\tau_{no} + \tau_{po}$. At the transition temperature ($\tau = \tau_2$), $\tau$ equals $\tau_{no} + \tau_{po}$ and the lifetime is independent of injection level. At higher temperature ($\tau = \tau_3$), $\tau_o$ is greater than $\tau_{no} + \tau_{po}$, and the lifetime decreases to $\tau_{no} + \tau_{po}$ with increasing injection level.

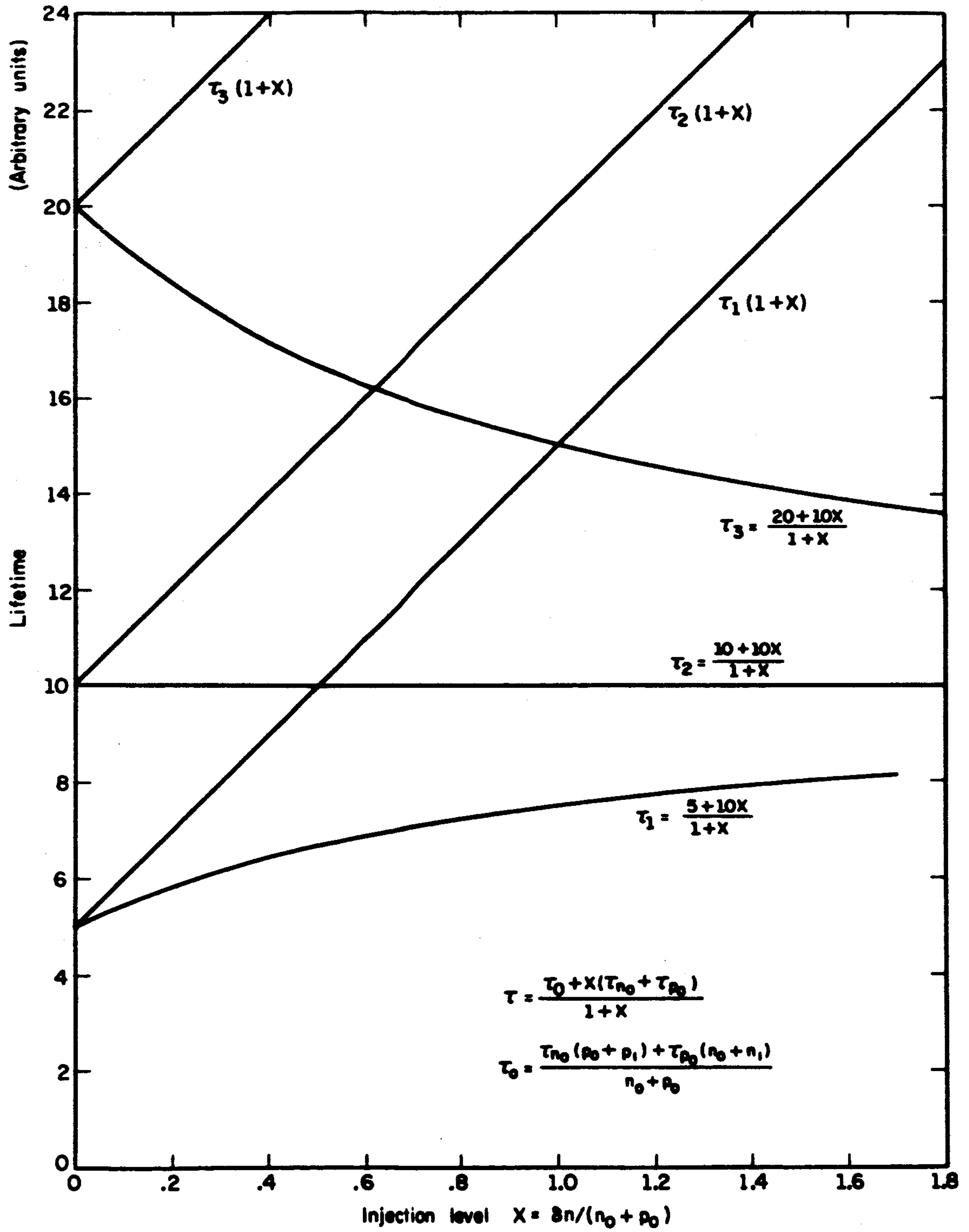


Figure 3

Figure 4. Variation of net lifetime $\tau$ with reciprocal temperature for a system of two Shockley-Read levels in extrinsic n-type silicon. The variation of lifetime with temperature of each of the levels is also shown. Both levels are in the upper half of the gap, in the positions indicated by the formulae for $\tau_1$ and $\tau_2$. Level 1 has a spin degeneracy ratio of 1/2 and level 2 has a ratio of 2. The ratio of $\tau_{po}$ for level 1 to that of level 2 is .08, and $\tau_{po}$ for level 2 was set at 1.

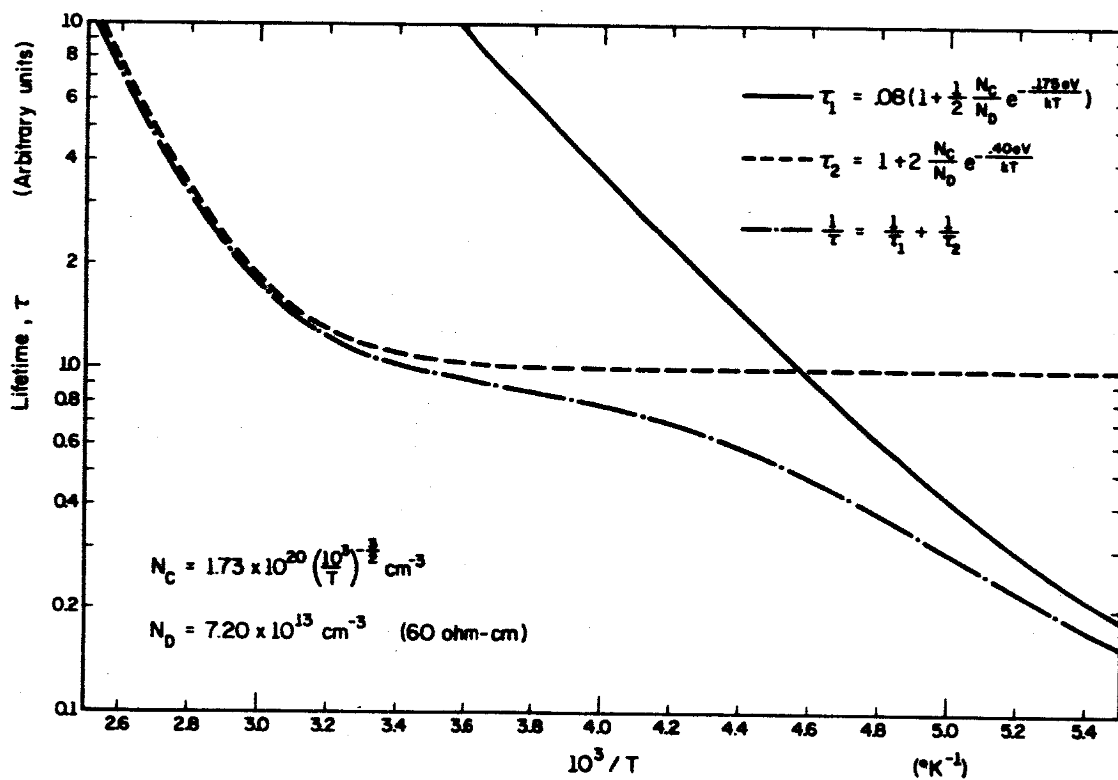


Figure 4

Figure 5. Variation of net lifetime $\tau$ and $\tau(1+x)$ with injection level x for a system of two Shockley-Read levels. The small-signal lifetime $\tau_o$ for level 1 is 1; for level 2 it is 5. The quantity $\tau_{no} + \tau_{po}$ for level 1 is 25; for level 2 it is 1. It is seen that level 1 is in its low temperature condition and that level 2 is in its high temperature state.

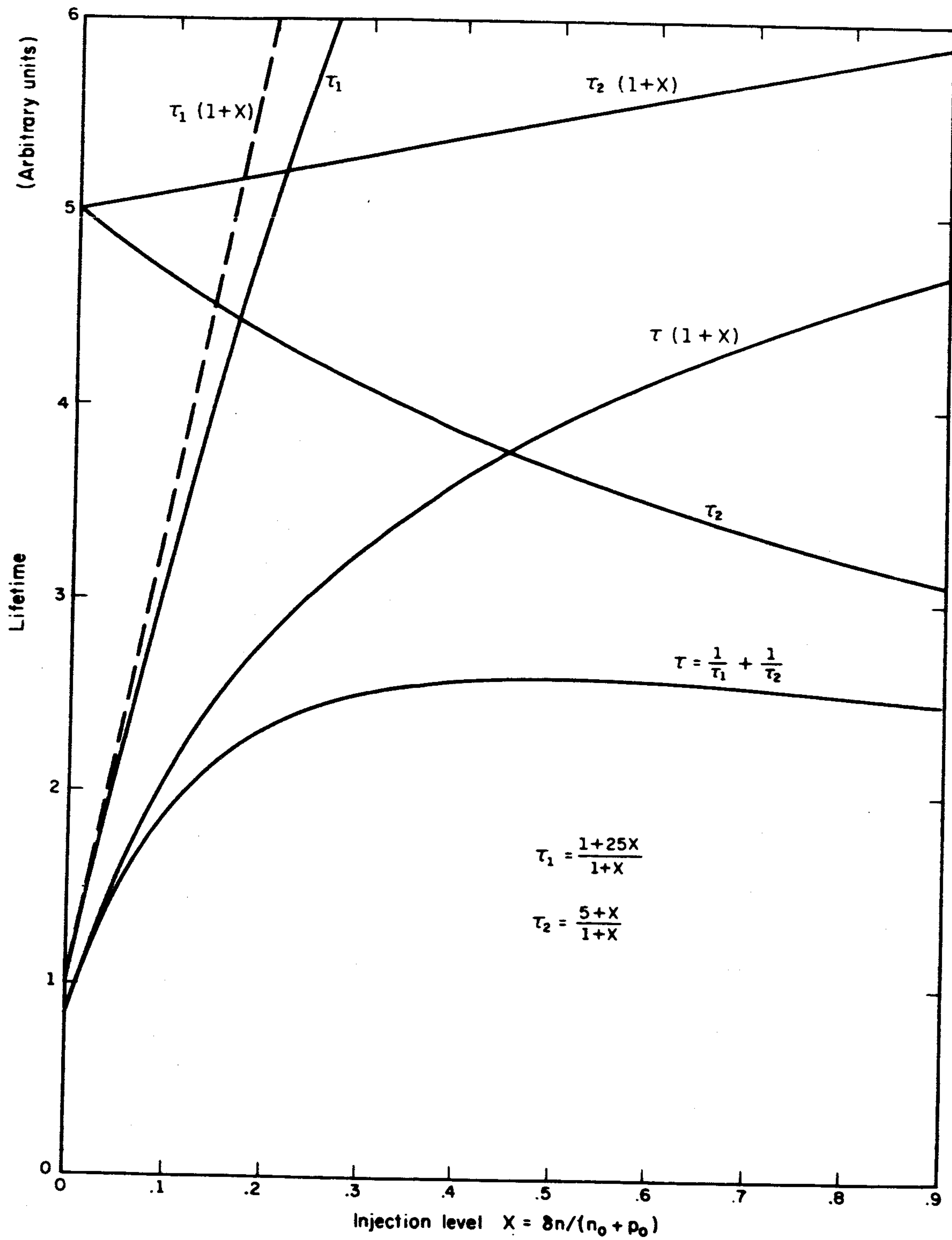


Figure 5

Figure 6. The effect of the sample resistivity upon the lifetime is shown for the levels used in Figure 4.

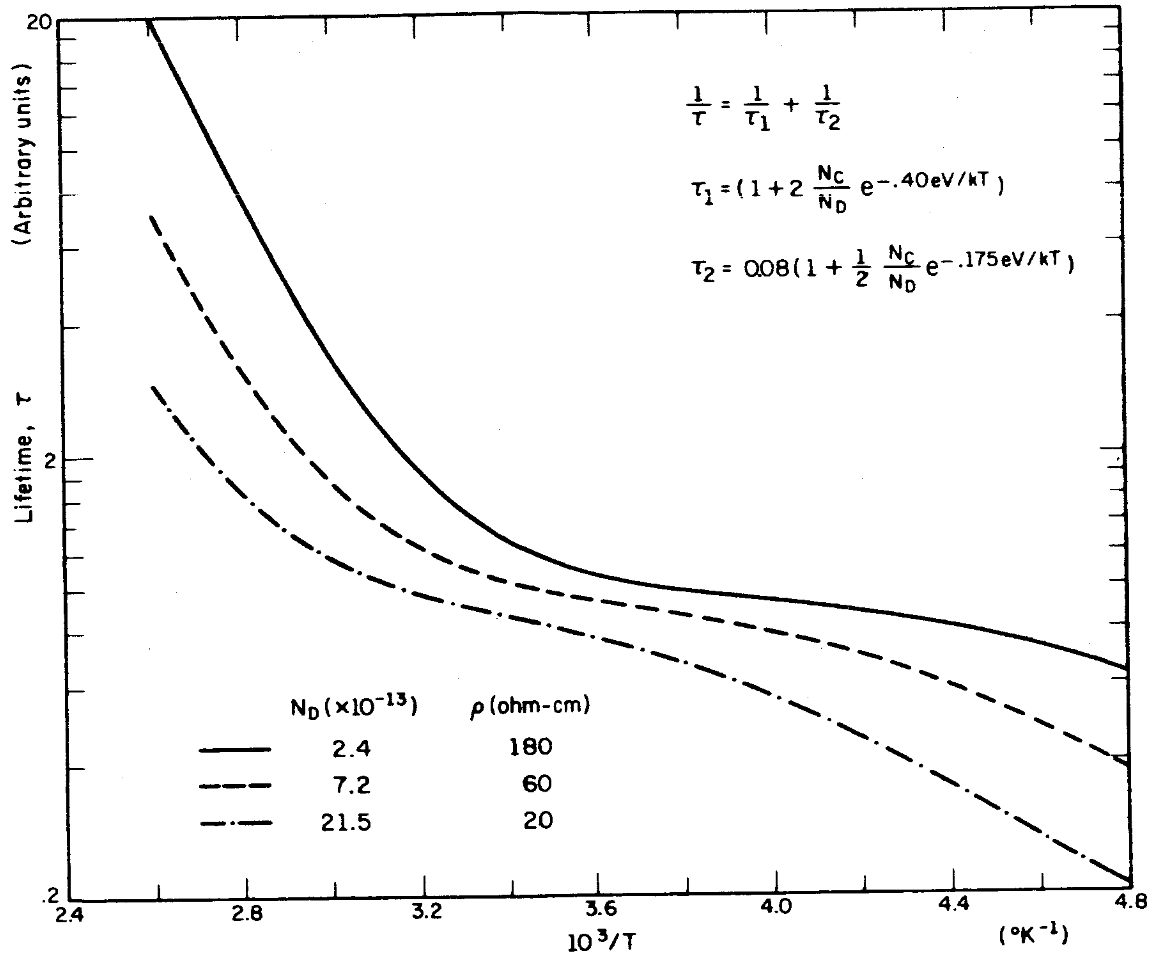


Figure 6

Figure 7. The effect of varying the ratio of the quantities $\tau_{po}$ upon the lifetime for the two levels of Figure 4. Here $\alpha$ is the ratio of $\tau_{po}$ for the 0.175ev level to $\tau_{po}$ of the 0.4ev level. Small $\alpha$ corresponds to a larger relative concentration of the shallower level.

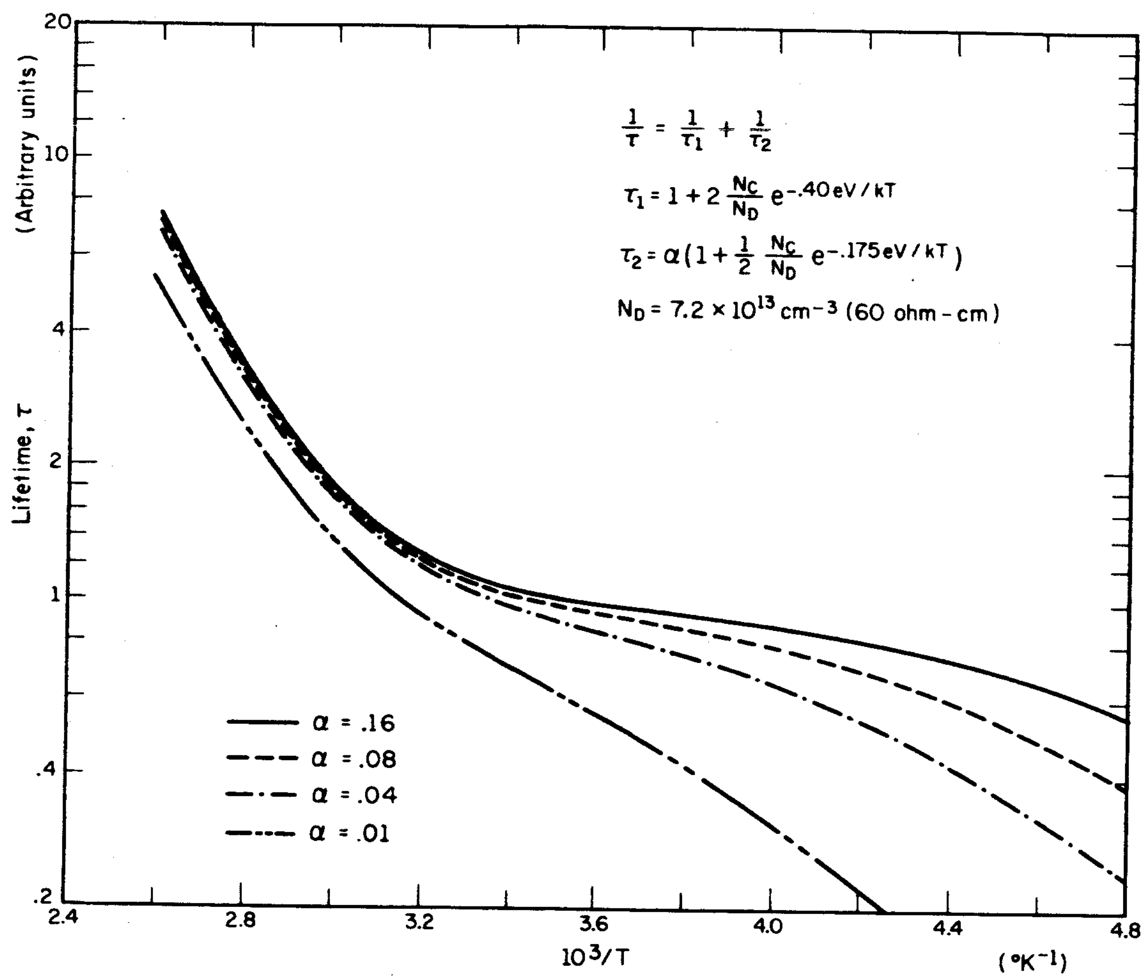


Figure 7

Figure 8. Variation of small-signal lifetime with reciprocal temperature for recombination through a set of Sah-Shockley centers. (a) n-type silicon. (b) p-type silicon. The energy level positions $E_j$ and spin degeneracy ratios $\omega_j$ of this three level defect were chosen to correspond to those determined by Watkins and Corbett for the divacancy. The capture cross-section ratios used in the computation were chosen to be of the same order of magnitude as determined for similar charge states of monovalent defects. The Sah-Shockley formulae are given in the upper figure. The quantity $n_j$ is given by

$$n_j = \omega_j N_c e^{-(E_c-E_j)kT} = \omega_j (10^3/T)^{-1.5} \exp[47.1-11.6(1.12-E_j)(10^3/T)]$$

and $p_j$ is given by

$$p_j = N_v e^{-E_j/kT} \omega_j = \omega_j^{-1} (10^3/T)^{-1.5} \exp[46.1-11.6E_j(10^3/T)]$$

where $N_c(N_v)$ is the effective density of states of the conduction (valence) band, $E_j$ is measured from the top of the valence band, T is the Kelvin temperature, and k is Boltzman's constant. The quantity $(n_o+p_o)$ is given by

$$(n_o+p_o) = [N^2+4N_vN_c e^{-E_g/kT}]^{1/2} = \{N^2 \times 10^{-26} + (10^3/T)^{-3} \exp[38.63-11.6(10^3/T)1.12]\}^{1/2} \times 10 .$$

N is the absolute value of the difference of the donor and acceptor concentrations $N_d-N_a$, and $E_g$ is the width of the forbidden gap (1.12 ev). The lowest level (j=1) at $E_v$ +0.25ev has $\omega$ = 2, $\tau_{n1}$ = 1 and $\tau_{po}$ = 20. The middle level at $E_v$ +0.45ev has $\omega$ = 1/2, $\tau_{n2}$ = 20. and $\tau_{p2}$ = 1/2. The upper level at $E_c$ - 0.4 ev has $\omega$ = 2, $\tau_{n3}$ = 20, and $\tau_{p3}$ = 1/2.

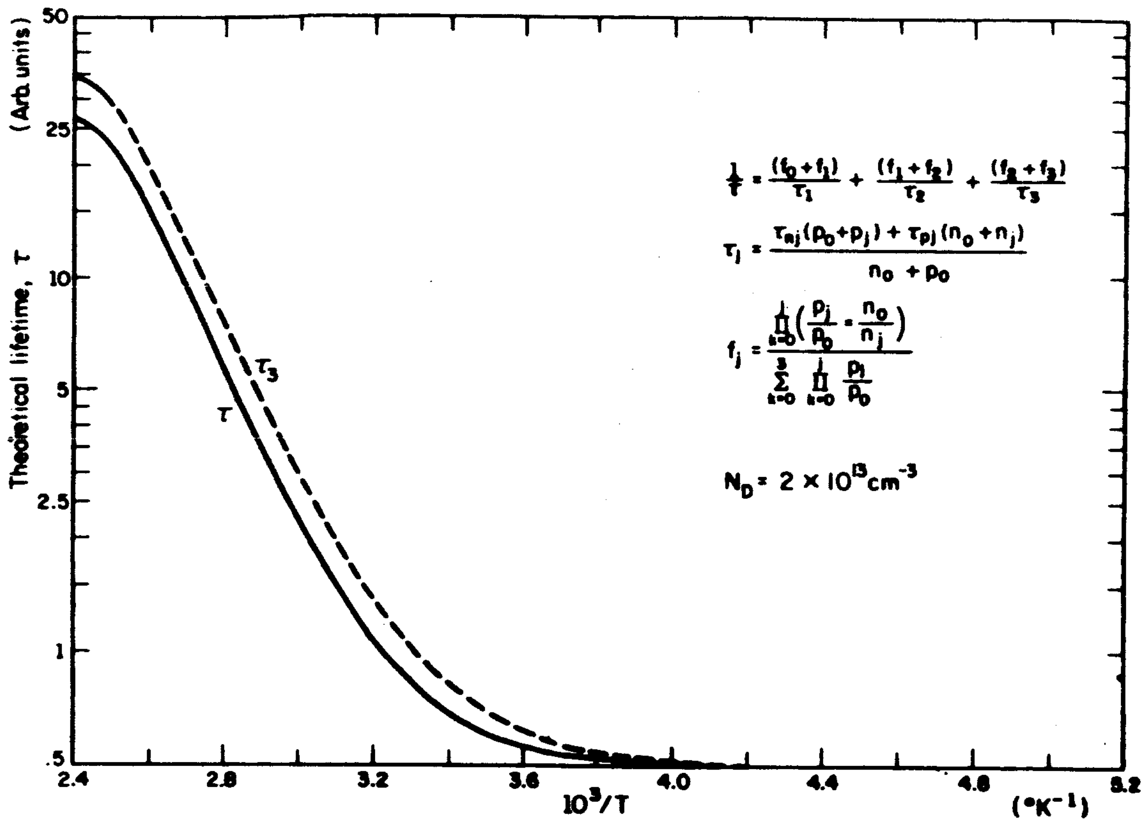


Figure 8(a)

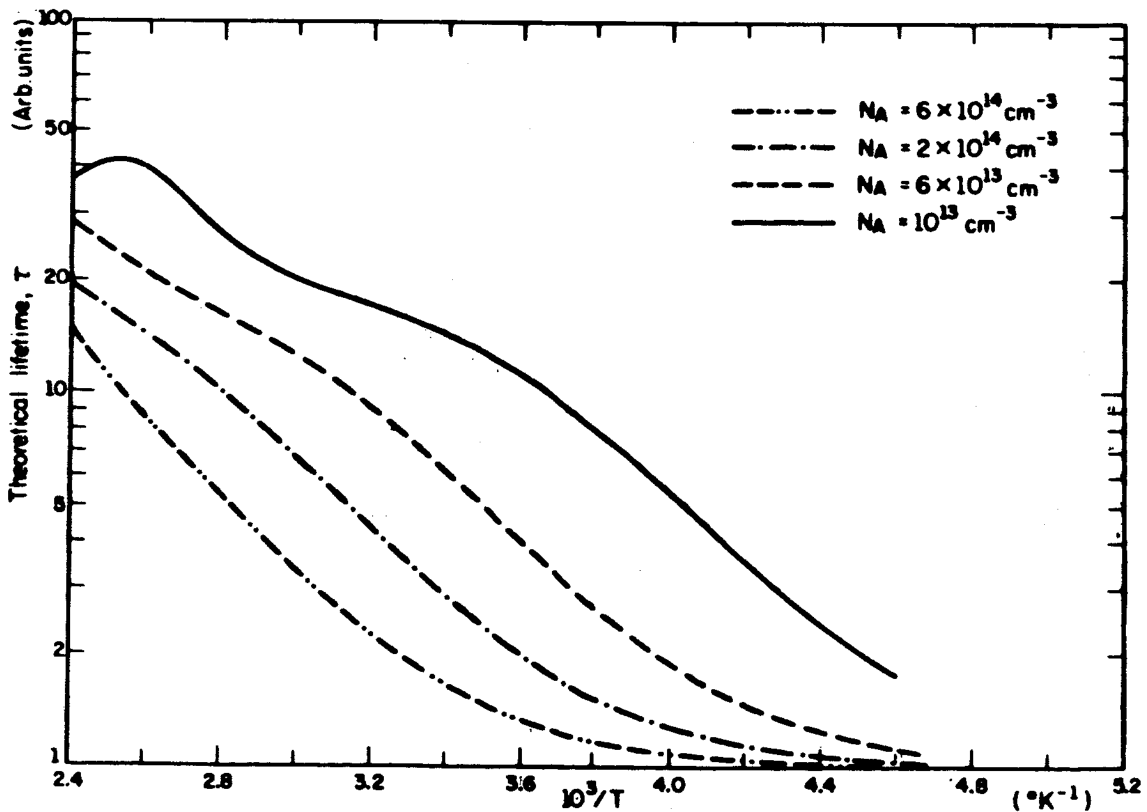


Figure 8(b)

The lifetime in a material containing multilevel defects is shown in Figure 8 again for small-signal conditions. The defect is assumed to have three energy levels, corresponding to those attributed to the divacancy. The lifetimes $\tau_1$, $\tau_2$, and $\tau_3$ are the lifetimes that would result if each of the levels were due to separate monovalent defects.

In order to measure the lifetime of excess carriers by the decay of the photoconductivity, it is necessary to relate the time decay of the photoconductivity to the time decay of the excess carrier population. This is easily done if one assumes 1) that the current in all portions of the circuit shown in Figure 9 is the same at a given instant of time, 2) that the hole and electron lifetimes are equal, and 3) that the component of the electric field in the sample which is parallel to the sample length does not have a significant dependence upon position in a plane perpendicular to that direction. If a set of coordinate axes are defined so that the z direction falls along the sample length, if the conductivity at a point (x,y,z) and time t is given by $\sigma(xyzt)$ with J the current density, and if we assume n-type material, then the current I will be given by

$$I = \int_A J_z \; dxdy = \int_A \sigma(xyzt) E_z(z,t) \, dxdy$$

If a cross-section is chosen where $\sigma = \sigma_o = n_o e\mu_n$, it follows that

$$I = n_o e\mu_n E_{zo}(t) A \tag{2.26}$$

where $n_o$ is the thermal equilibrium electron concentration, $\mu_n$ is the electron mobility, A is the cross-sectional area, and e is the electronic charge.

Figure 9. Circuit and conditions used to derive the relationship between excess carrier concentration and voltage across the sample terminals. The sample of length L has electron-hole pairs created in the shaded area of length $\beta L$ by the exciting light pulse. The current I is kept nearly constant by the resistor $R_s$ which is much larger than the sample resistance R(t).

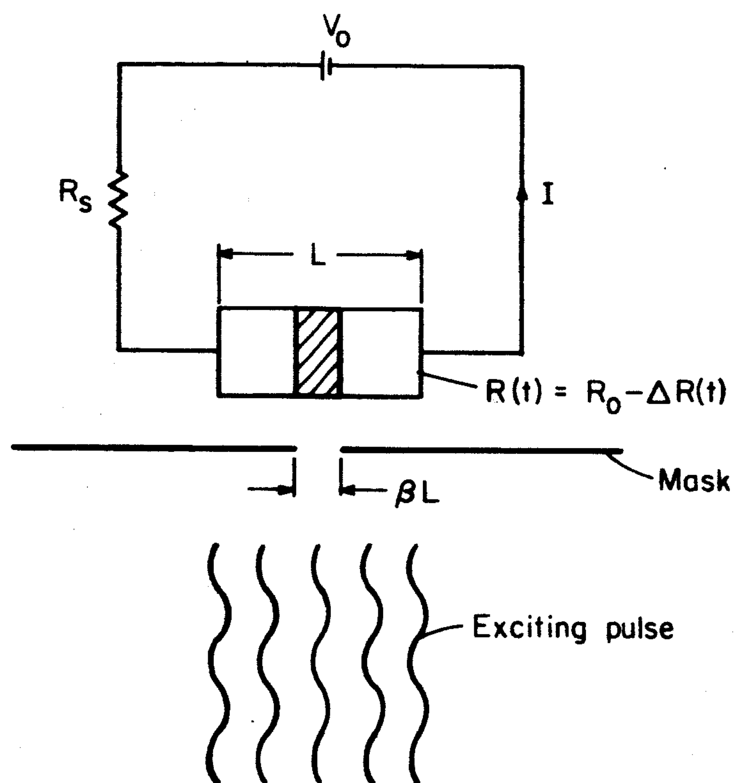


**Figure 9**

At a point in the crystal where the excess electron concentration is given by $\delta n$ and the excess hole concentration by $\delta p$

$$I = \int_A \sigma E_z dxdy = e\mu_n E_z \int [(n_o + \delta_n + \delta_p \mu_p/\mu_n]dxdy \tag{2.27}$$

where the hole mobility is given by $\mu_p$.

If the excess carrier population is described by

$$\alpha\delta_n = \delta_n + \delta p/b \tag{2.28}$$

where $b = \mu_n/\mu_p$, then $\alpha\delta n$ describes the effective excess electron concentration. Because of surface recombination, $\delta n$ and $\delta p$ will depend on x and y, and it is useful to calculate the average value of $\delta n$ over the area of the sample:

$$\langle \delta n \rangle = \int \delta n \; dxdy/A \equiv \eta n_o$$

Equation (2.27) then becomes

$$I = e\mu_n E_z(z,t) A[n_o + \alpha n_o \eta(z,t)] \tag{2.29}$$

By comparing the above expression to Eq. (2.26) we see that $E_{zo}(t) = E_z(z,t)\ (1 + \alpha\eta(zt))$. The voltage across the sample will be given by

$$V(t) = \int_o^L E_z(z,t)\,dz = E_{zo}(t) \int_o^L \frac{dz}{1+2\eta(z,t)} \equiv E_{zo}L' \tag{2.30}$$

and by

$$V(t) = \frac{V_o R(t)}{R_s + R(t)} = IR(t) = E_{zo}(t)\ \sigma_o AR(t) \tag{2.31}$$

where $V_o$ is the battery potential, $R_s$ is the resistance in the circuit exclusive of the specimen, $R(t)$ is the resistance of the sample, and L is the sample length. Thus

$$R(t) = \frac{L'}{\sigma_o A} = \frac{L-\delta L}{\sigma_o A} = R_o - \Delta R \tag{2.32}$$

and

$$V(t) = \frac{V_o L'}{L' + R_s \sigma_o A} . \tag{2.33}$$

If the voltage across the sample when no excess carriers are present is given by

$$V_D = I_o R_o = \frac{I_o L}{\sigma_o A} = \frac{V_o R_o}{R_o + R_s} ,$$

then

$$V(t) = V_o \left(1 + \frac{R_s}{R_o} \frac{L}{L'}\right)^{-1} \tag{2.34}$$

and the transient portion of the voltage across the sample is

$$V_{tr} = V(t) - V_D = - V_D \frac{1 - \frac{L'}{L}}{1 + \frac{R_o}{R_s} \frac{L'}{L}} . \tag{2.35}$$

Thus

$$\frac{V_{tr}}{V_D} = - \frac{L - \int_o^L \frac{dz}{1+(1+1/b)\, 1/n_o \int_A \delta n(xyzt)\, dxdy}}{L + \frac{R_o}{R_s} \int_o^L \frac{dz}{1+(1+1/b)\, 1/n_o \int_A \delta n(xyzt)\, dxdy}} \tag{2.36}$$

For lifetime measurements in this experiment, the maximum value of $\delta n$ was kept small enough that the lifetime was essentially constant over the sample. If it is desired to measure the lifetime for large injection levels, it must be remembered that the result will always be somewhat incorrect due to the physical averaging over the sample area.

In this experiment $R_o/R_s$ was $\leq 0.1$, and $\delta n/n_o \leq 0.05$, so that the approximation

$$\frac{V_{tr}}{V_D} = [1 - \int_0^L dz(1- \frac{\alpha\langle\delta n\rangle}{n_o})][1 - \frac{R_o}{R_s}\int_0^L dz(1- \frac{\alpha\langle\delta n\rangle}{n_o})] \tag{2.37}$$

is valid. In practice, only a portion of the sample is exposed to the source of excitation. If the fraction of the sample length exposed is $\beta$, then

$$\frac{V_{tr}}{V_D} = -\beta\frac{\alpha}{n_o}\langle\langle\delta n(xyzt)\rangle_{xy}\rangle_z\,[1 - \frac{R_o}{R_s}(1 + \frac{\beta\alpha}{n_o}\langle\langle\delta n\rangle\rangle] \;, \tag{2.38}$$

and if only the first order term is retained, then

$$\frac{V_{tr}}{V_D} = \beta\alpha\frac{\langle\langle\delta n\rangle\rangle}{n_o} \;. \tag{2.39}$$

Since

$$\langle\langle\delta n(t)\rangle\rangle = \langle\langle\delta n(0)\rangle\rangle\, e^{-t/(\tau_s+\tau_b)} \;, \tag{2.40}$$

where $\tau_s$ is the surface lifetime and $\tau_b$ is the bulk lifetime, a plot of the logarithm of the transient voltage versus time will have a slope inversely proportional to the lifetime.

For p-type material the relation between transient voltage and excess carrier concentration is

$$\frac{V_{tr}}{V_D} = -\beta(1+b)\frac{\langle\langle\delta p\rangle\rangle}{p_o} \;. \tag{2.41}$$

# III. PROCEDURE

## A. Measurements

### 1. Sample Preparation and Preliminary Measurements

Samples with dimensions 2 to 5 x 5 x 20 to 25 mm were cut from cylindrical boules of 2 to 3 cm diameter and 3 to 8 cm in length by a diamond saw and were polished on two or three of the larger faces until few, if any, scratches or pits were visible. The samples were given a code letter designating the boule from which they were cut and a number that identified the various samples cut from the same boule.

In order to verify that the float-zoned samples contained relatively small amounts of oxygen, the oxygen concentration was determined by measuring the optical absorption of the samples in the 9 micron region, according to the method of Kaiser, Keck, and Lange.[7] The infra-red absorption of some pulled specimens was measured also for comparison.

Electrical contacts were usually applied by ultrasonic soldering of indium, although electroless nickel plating was occasionally used. The contacts were tested by measurement of the sample conductance as a function of temperature. It was found that in all samples, the decay of the photo-conductivity became non-exponential at temperatures in the neighborhood of 200°K due to trapping, and contacts ohmic to 200°K were therefore regarded as adequate. Poor contacts revealed themselves by a decrease in the conductivity as the temperature decreased, by noisiness of the photo-decay signal, and by "trapping-like" behavior of the photo-decay signal. It was found in the course of the experiment that the contact quality tended to

degrade, but whether this was due to aging, heat treatments, or irradiation was not determined.

The room temperature resistivity $\rho$ was determined from $\rho = RA/L$ where R is the sample resistance, A the cross-sectional area, and L the sample length. The majority carrier concentration was estimated from the resistivity by means of the formulae

$$1/\rho = N_d e \mu_e \quad (1/\rho = N_a e \mu_h) \tag{3.1}$$

for n-type (p-type) materials with $N_d (N_a)$ the majority carrier concentration, $\mu_e (\mu_h)$ the majority carrier mobility, and e the electronic charge. The mobilities used were those reported by Morin and Maita.[63]

The crystals were measured for uniformity of resistivity and lifetime along the crystal length by means of the apparatus shown in Figure 10. The voltage was adjusted so that the pulse of minority carriers would drift less than three slit widths. The drift distance D is related to the minority carrier mobility $\mu$, the measurement time T, the sample length L, and the applied voltage V by $D = \mu TV/L$. In order to obtain as much information as possible, the drift distance was minimized. Eq. (2.39) or Eq. (2.41) was used to relate the lifetime and majority carrier density to the dc and transient voltages measured. Inspection of these formulae shows that the signal amplitude for the conditions of measurement is proportional to the resistivity, and that the lifetime can be found by plotting the logarithm of the transient voltage versus time. Some samples, cut so that their longest dimension was a boule diameter, had such large lifetime (Fig. 11) or resistivity variations (Fig. 12) that it was necessary to cut another sample which had its longest dimension along the boule axis. Samples cut

Figure 10. Schematic of apparatus used to measure the variation of lifetime and resistivity along the length of the sample. The silicon sample was mounted in a simple bakelite jig (not shown) that secured it to the micrometer stage. The electrical connections were identical to those in other lifetime experiments.

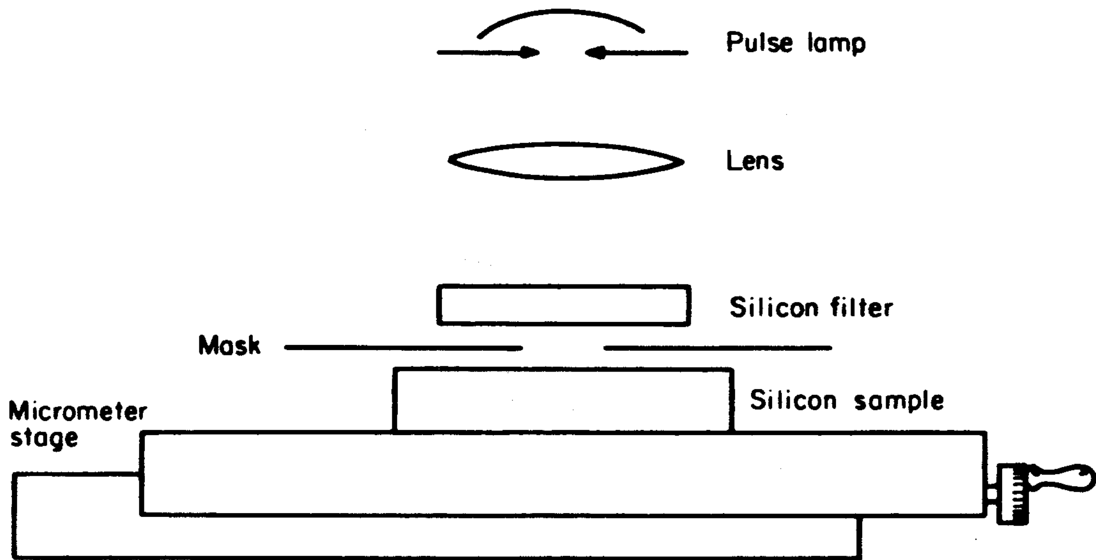


**Figure 10**

Figure 11. Variation of pre-irradiation lifetime with portion of sample exposed to excitation for three classes of material. Sample C6, n-type float-zoned, and sample H2, n-type pulled, show little dependence of lifetime on the region exposed. Sample F3, p-type float-zoned, shows moderate-to-large variations, and sample L3, n-type float-zoned, shows severe variation of lifetime with the region exposed. The length of the exposed portion of the sample in all cases was 0.1 inches, and the pulse of minority carriers was allowed to drift less than 0.1 inches during the time of measurement.

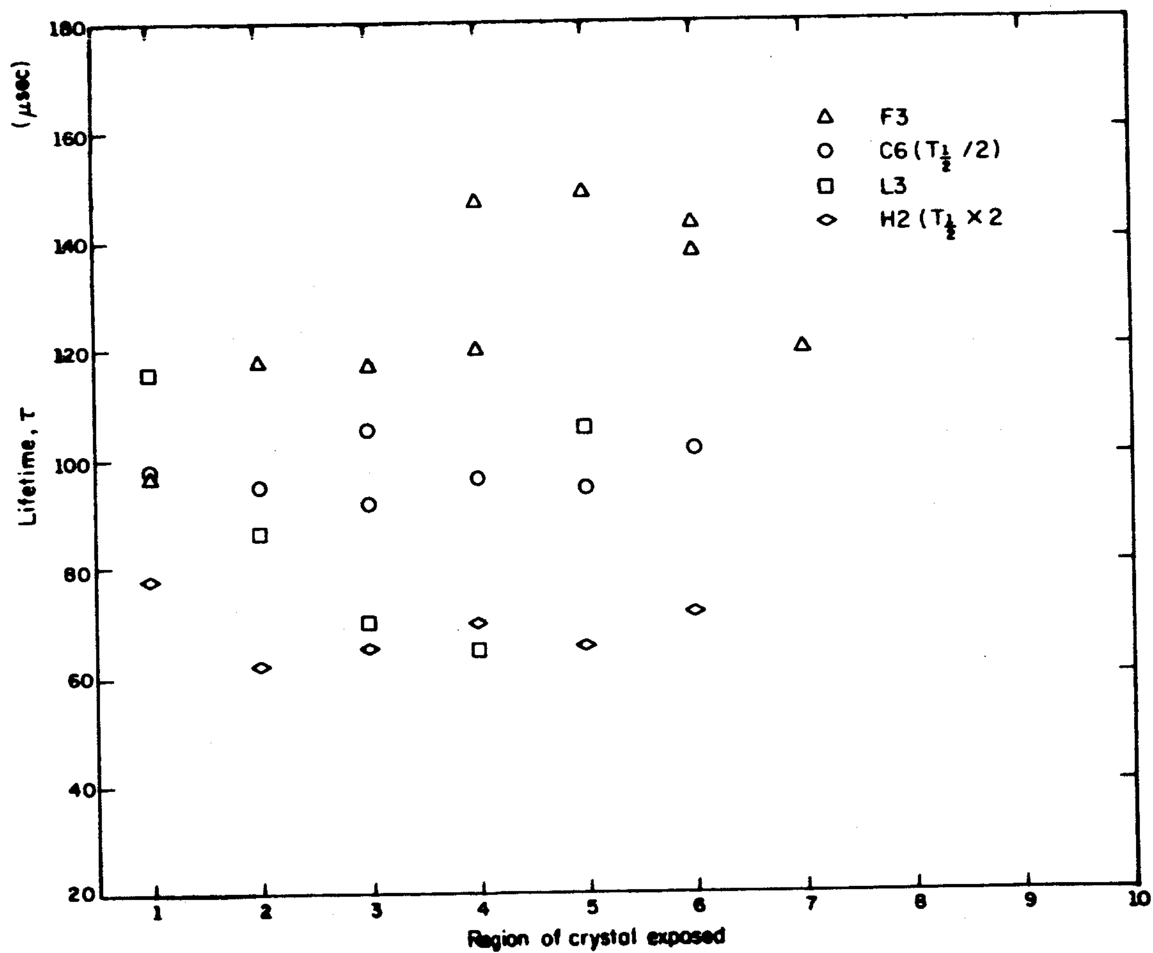


Figure 11

Figure 12. Variation of the voltage ratio with the region of the crystal exposed to excitation for a sample cut from boule T. The longest dimension of the sample was a boule diameter. The voltage ratio is proportional to the resistivity of the material. The difference in the voltage ratio for the two voltage polarities is due to the sweeping of the minority carrier pulse from the common excitation region into the two regions on either side during the time of measurement.

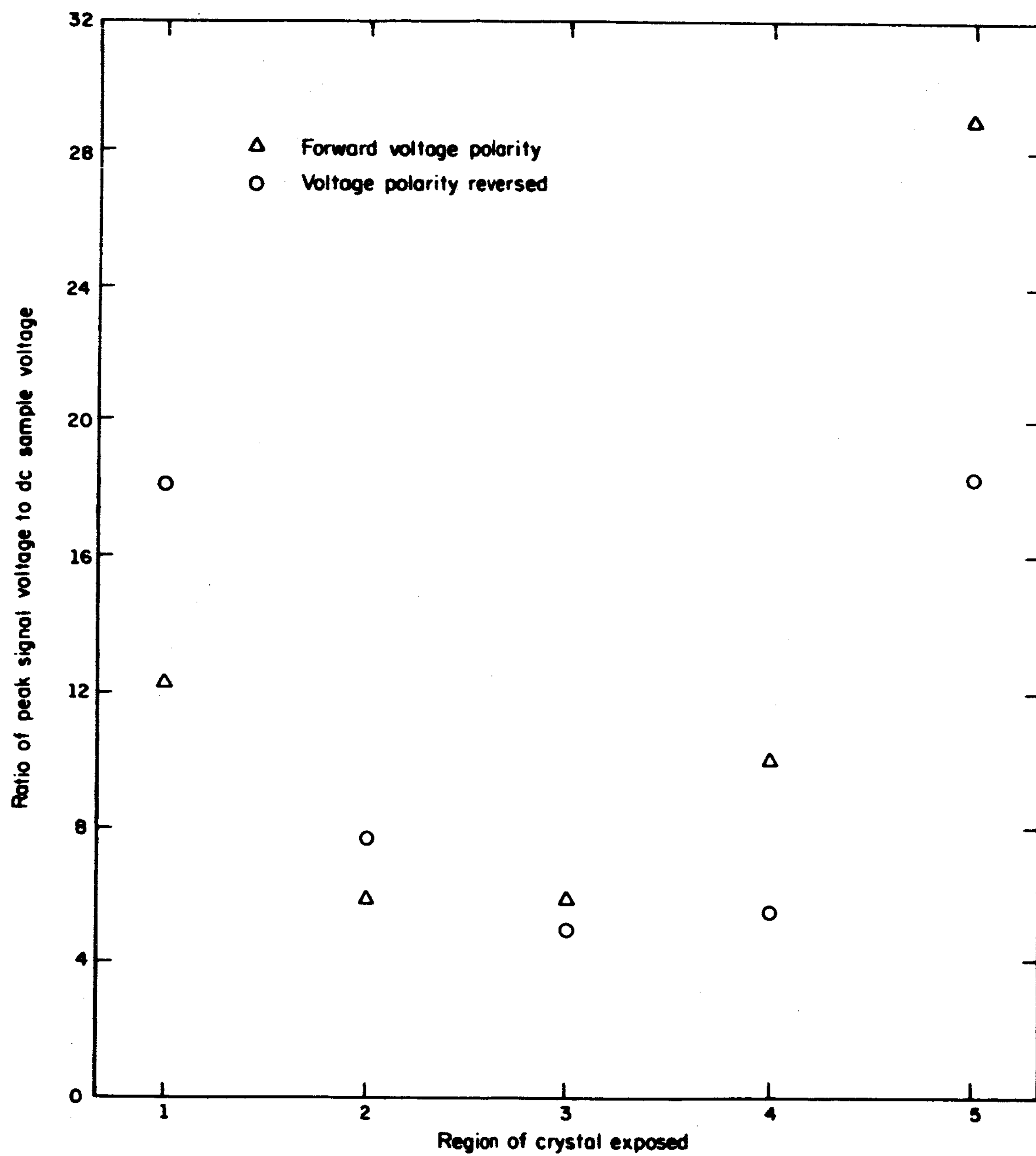


Figure 12

in this manner showed no significant variations in lifetime or resistivity. On samples showing minor variations in lifetime, a region was selected for lifetime measurements. During measurements on these crystals the dc voltage was adjusted so that the minority carrier pulse remained in this region during the time of measurement.

The conductivity type was measured by determining the sign of the thermoelectric coefficient.[64]

2. Lifetime Measurement Procedure -- Pre-Irradiation

The half-decay time of the photoconductivity, hereafter synonymous with the lifetime, was measured before and after irradiation by the apparatus shown in Figures13 to 16. The pulse lamp was similar to the one developed by Swank[65], except that the capacitance was tripled, the spark gap increased, and a gas mixture of 80% nitrogen and 20% air was used. The gas pressure was one atmosphere.

The silicon filter shown in Figure 14 between the pulse lamp and the sample was mounted on the dewar as shown in Figure 16, and actually consisted of two filters, one of 1.5 mm thickness and one of 5 mm thickness, mounted on a sliding port so that either could be used. For high resistivity material additional silicon filters were placed in the optical path. The minimum amount of filter consistent with no injection level effects was chosen. The lens was used in all cases except on resistivity samples or those exhibiting severe injection level effects.

The Tektronix type 1121 amplifier shown connected across the sample terminals in Fugure 11 amplified the transient portion of the voltage across the sample. The amplified signal then passed into the plug-in vertical amplifier of the oscilloscope. A type O plug-in was used for measurements

Figure 13. Schematic of electrical circuit and apparatus used to measure the lifetime. Si is the silicon sample being measured, $V_b$ is a dry-cell battery, and $R_s$ is the large series resistor.

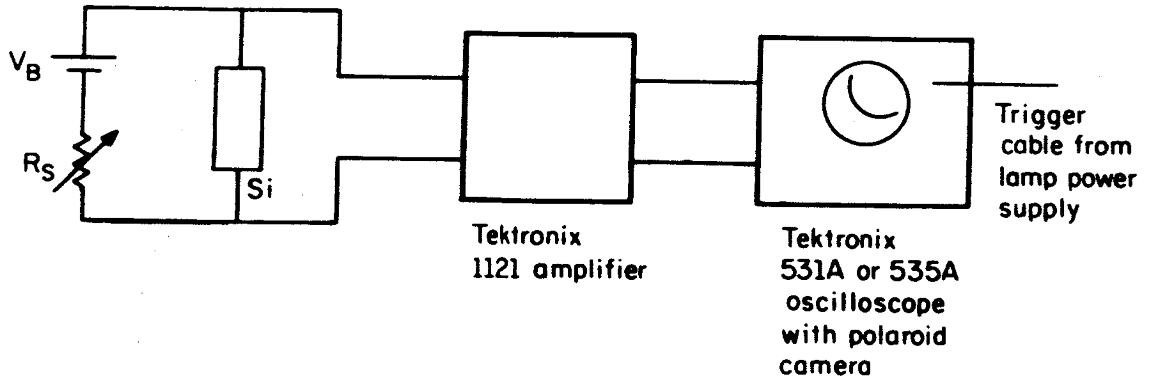


Figure 13

Figure 14. Schematic of optical arrangement for lifetime measurements.

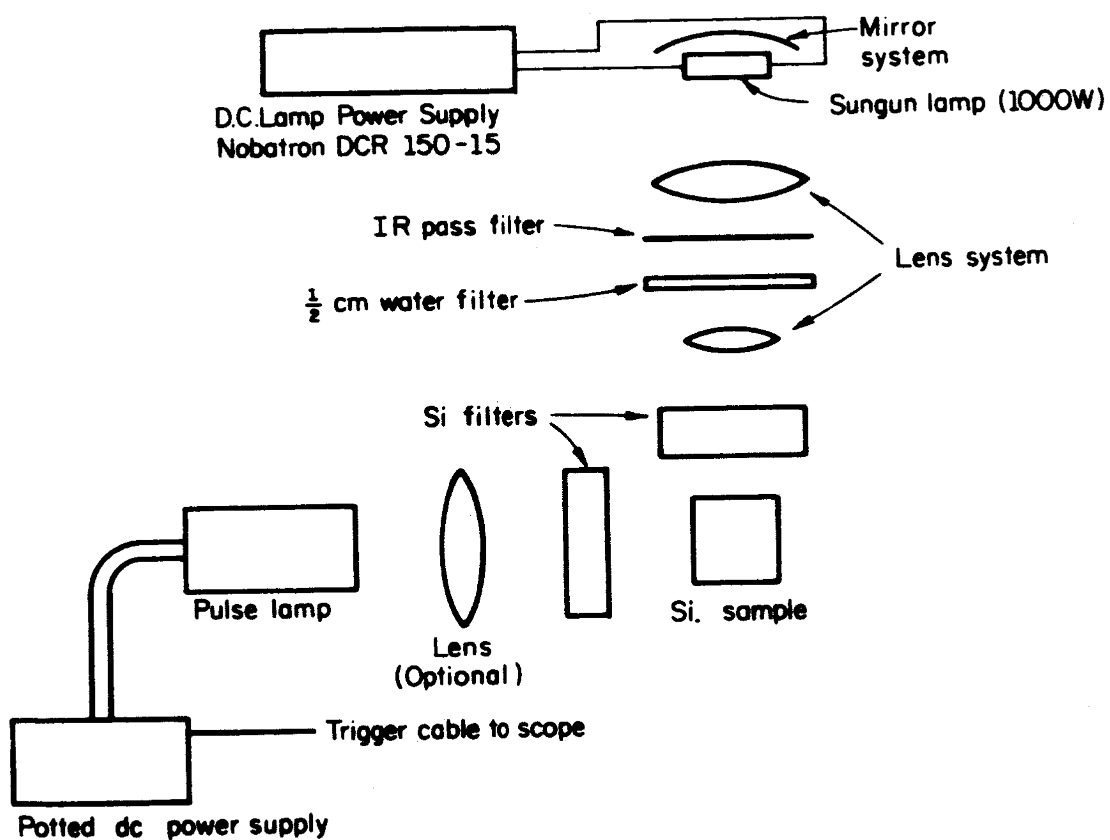


Figure 14

Figure 15. Sample holder used for lifetime measurements. A: copper rod from dewar and heater. B: setscrew to fasten sample holder to rod A. A coating of Apiezon N vacuum grease was used between the rod and the holder to increase thermal contact. C: copper leads from sample. D: copper sample holder body. E: electrical contact on silicon sample. F: 1/2 mil mylar electrical insulation between thermocouple and sample. G: thermocouple. H: 1/2 mil mylar between sample and sample mount. I: silicon sample. J: screw to hold thermocouple to mount. K: 8 mil mylar between thermocouple and mount. L: brass washer. M: photographic masking tape to limit portion of sample exposed to pulse light. General Electric Co. #7031 Insulating Varnish was used to glue mylar, sample, sample mount, and thermocouple together and to provide thermal contact.

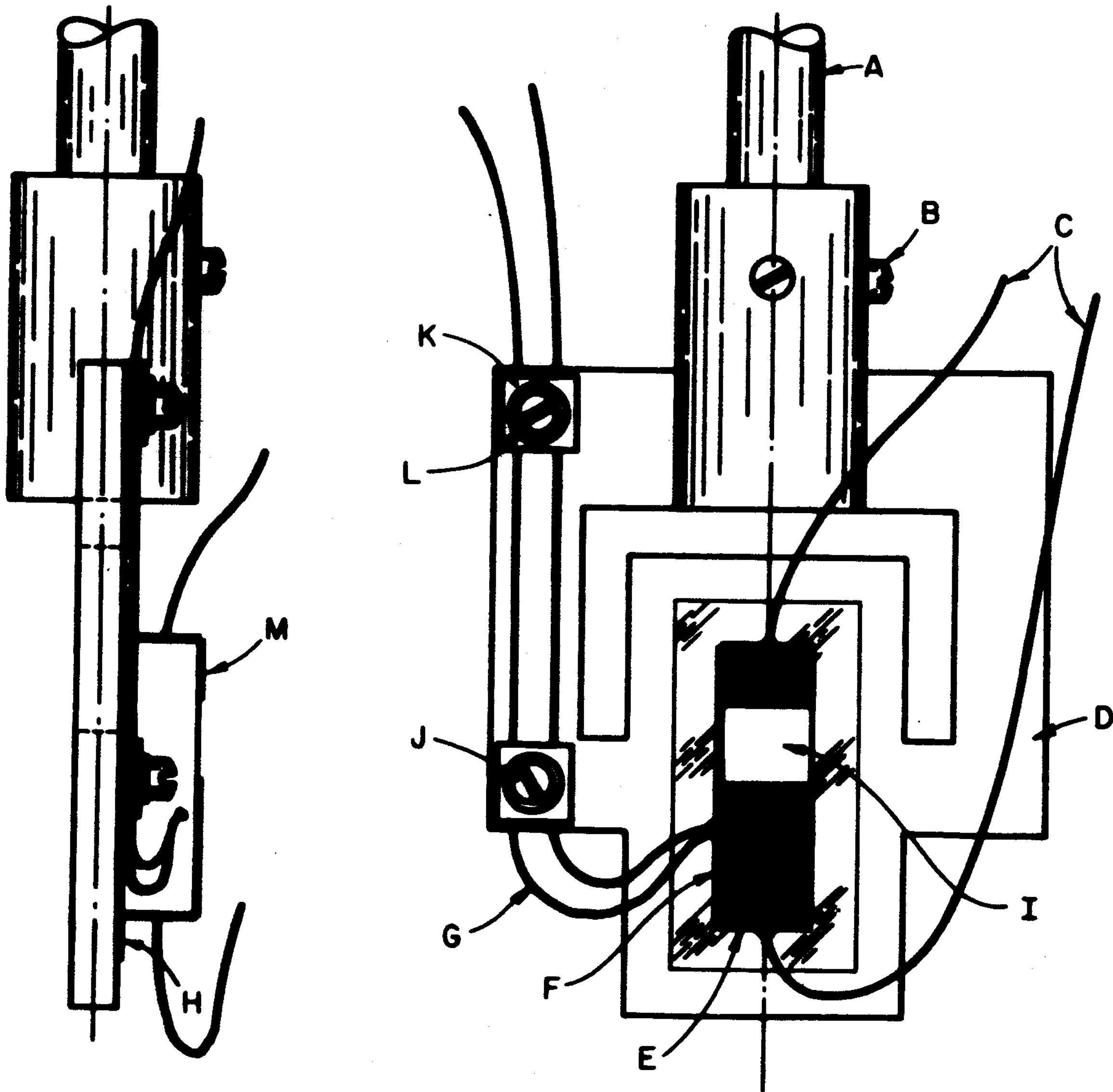


Figure 15

Figure 16. Schematic of dewar used in lifetime-temperature measurements. Two of the three BNC connectors were used to apply voltage to the sample and for connections to the amplifier and oscilloscope, and the third was used to supply power to the heater assembly. For low temperature measurements a dry ice-methanol mixture was placed in the monel can. The heater assembly consisted of 8 one watt resistors buried in the copper block shown. The circles on the rod between the heater and the dewar bottom indicate holes drilled in the rod to decrease thermal contact between heater and dewar. The filter not shown on the dewar bottom consisted of two filters mounted on a sliding port so that either could be used without opening the dewar to atmospheric pressure.

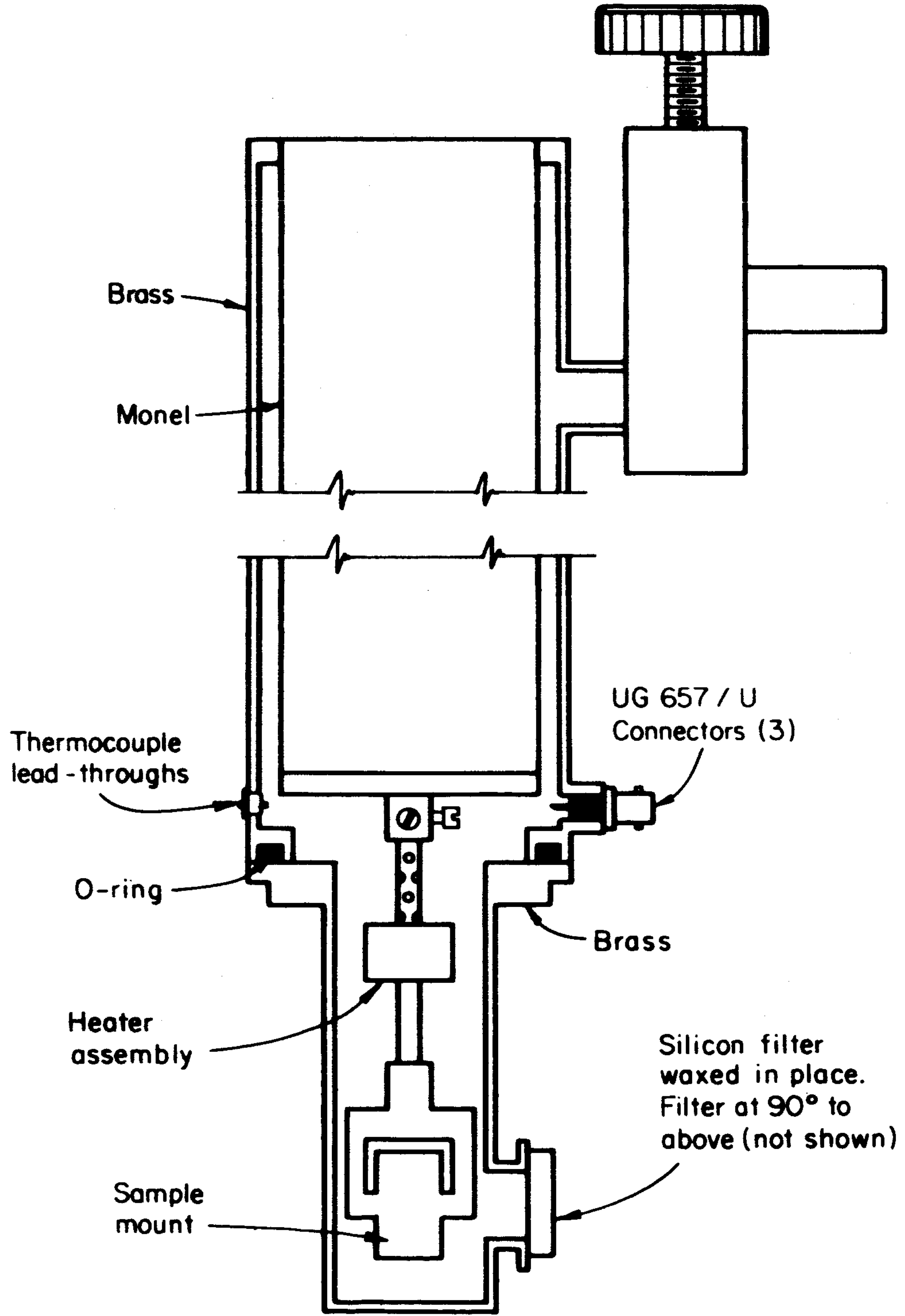


Figure 16

on specimens whose lifetimes were in excess of 50 microseconds, since its internal gain of 100 and 1Mc bandwidth permitted amplification of the signal with little attendant amplifier noise, compared to the type L and type 1A1 units. These latter plug-ins had bandwidths in excess of 17 Mc, and it was necessary to use one of these units on samples with lifetimes less than 50 microseconds to prevent signal distortion. The oscilloscopes used were Tektronix types 531A and 535A. These were nearly identical except that the type 535A, which was used for the latter half of the measurements, had a calibrated sweep delay. This feature eliminated the problem of signal distortion due to measurement of the lifetime at times such that the pulse lamp was still creating electron-hole pairs, and was most useful on irradiated samples whose lifetimes were on the order of 5 microseconds.

The display of the photo-decay was photographed with a Dumont model 353 camera unit, and the Polaroid photographs were measured to obtain the lifetime. The vertical amplifier gain of the oscilloscope was adjusted so that the initial signal amplitude was from 3 to 6 cm, referred to the signal amplitude at times long compared to the lifetime. The film was exposed for several settings of the sweep rate. For specimens showing injection level effects, photographs were taken with a variety of sweep delays in order to measure the lifetime at various times during the decay.

The 1000 watt lamp indicated in Figure 14 was used for specimens showing noticeably non-exponential decay due to the fact that the lifetime and the trap-empty time (see Appendix I) were not greatly different. This technique was effective for samples with a concentration of traps small enough that the dc light could fill them and thus make them ineffective without causing any change in the lifetime by injection level effects.

For measurement of the lifetime as a function of temperature, the samples were mounted on the sample holders shown in Figure 15. The sample holder was then mounted in the dewar as shown in Figure 16, and the dewar was evacuated. The sample temperature was measured with a thormocouple having an ice point reference junction and a Leeds and Northrup model 8637 potentiometer. The temperature was controlled by varying the voltage applied to the heater indicated in Figure 16. The heater consisted of 8 resistors glued into holes drilled into a copper block, and was powered by a Sorensen QB6-30 Nobatron. For temperatures below 25$^{o}$C a dry ice-methanol mixture was placed in the dewar top.

3. Irradiation Procedure

The samples were wrapped in facial tissue and placed in plastic pill capsules before they were sent to the U. S. Naval Research Laboratory in Washington, D. C. were all irradiations were performed. The intensity of the cobalt 60 source varied between 6 x $10^4$ and 2 x $10^6$ Roentgens per hour, with the intensity dependent upon the location of the sample in the source. The temperature of the samples during irradiation was approximately room temperature.

4. Post-Irradiation Measurements

An attempt was made to determine the annealing behavior of the defects introduced by irradiation, on the first sample from each boule to be measured after irradiation. The lifetime was measured by the method described for pre-irradiation measurements, starting at the lowest temperature for which the lifetime had been measured prior to irradiation. Since exploratory measurements had indicated that annealing occurred in float-zoned samples at temperatures above 80$^{o}$C, once temperatures in this neighborhood

were reached, the lifetime was measured as a function of time at constant temperature as the temperature was increased by steps. After the upper limit of the non-anneal temperature region had been established, measurements on all other samples from that boule were made at temperatures less than the lowest temperature for which anneal had been seen. Following measurements at temperatures above room temperature, the lifetime was remeasured at room temperature and compared to the room temperature lifetime measured before the high temperature measurement.

5. Anneal Procedure

The samples were annealed in two other ways besides any annealing done while the samples were in the dewar. For anneals at less than 200°C, the samples were wrapped in aluminum foil, and placed in an aluminum capsule which was sealed by a teflon O-ring. The capsule was then immersed in a bath of diffusion pump oil whose temperature was regulated to within 1/2°C. For anneals at temperatures above 200°C, the specimens were annealed in a tube furnace lined with a quartz tube which was flushed with nitrogen. The samples were wrapped in aluminum foil and placed in a platinum boat which could be drawn into the furnace for the anneal.

6. Equipment Calibration Procedure

The decay rate of the pulsed light was measured with a 7102 photomultiplier filtered by several millimeters of silicon. The circuit used with the 7102 is the same as used by Swank[65]. The power supply was a John Fluke model 402M Power Supply, the output from the photomultiplier circuit was connected to a Tektronix type 531A oscilloscope, and the display of photomultiplier voltage versus time was photographed by the camera assembly mentioned above. The photograph was measured and the decay time calculated from the slope of the log voltage versus time curve.

The photon output of the lamp was determined by the use of Eq. (2.39), and data taken during measurements of resistivity and defect gradients in pre-irradiated crystals. The photon output was capable of exciting approximately $10^{12}$ electron-hole pairs per cubic centimeter if the lens and a 1.5 mm silicon filer were used.

The sweep rates of the oscilloscope were calibrated by use of a Tektronix type 180 time mark generator, and all sweep rates were within 2%. The thermocouples were calibrated in boiling water, in a dry ice-methonal mixture, and in liquid nitrogen. The measured emf's were compared to the published (1938 calibration) tables for copper-constantan thermocouples, and errors were $2^{o}C$ or less at all temperatures.

## B. Analysis of Data

### 1. Raw Data Analysis

The raw data consisted of the photographs taken of the photo-decay traces on the oscilloscope, together with information on the experimental conditions.

The photographs were measured with a metal scale calibrated in 1/50ths of inches, and the value of the supposed exponential read at the point where the decay curve crossed the vertical graticule marks on the film. Figure 17 and 18 show examples of the photographs, and the calculation of lifetime from the films.

If the signal were a true exponential, the time behavior would be given by $V = V_o \exp(-t/\tau)$ where $\tau$ is the lifetime. To determine $\tau$ from a photograph of the trace, it is necessary to know the baseline, that is, the zero point. This may be accomplished by using a sweep rate such that $t = 5\tau$ in one centimeter or less of horizontal display. From such a trace,

Figure 17. Variation of transient voltage with time, and determination of lifetime from the transient voltage-time curves. (a) 3/4 reproduction of Polaroid film 14-23-11-65, taken during measurement of sample L5 after the first irradiation. The vertical scale is 0.2 mv/cm, resulting from an oscilloscope setting of 20 mv/cm and an amplifier gain of 100. The time scale is 5, 10, and 50 μsec/cm for the top, middle, and bottom traces, respectively. The sweep delay was 10 μsec, the dc voltage across the sample was 2.04 volts, and $10^3/T$ was 4.30. This film shows trapping-like effects in that two time constants are apparent. (b) 3/4 reproduction of film 38-23-11-65, taken during the same measurement. The vertical scale is 1/2 mv/cm, resulting from an oscilloscope setting of 50 mv/cm and an amplifier gain of 100. The time scale is 20, 50, and 200 μsec/cm for the top, middle, and bottom group of traces, respectively. The sweep delay was 10 μsec, the sample voltage 2.00 volts, and $10^3/T$ was 2.68. This film is typical of all float-zoned samples at temperatures greater than $250^{\circ}K$. (c) 5/16 reproduction of semilog authmic plot of transient voltage amplitude at successive vertical centimeter lines on the above Polaroid photographs. All values of $\tau$ obtained were plotted against $10^3/T$ (see Figure 21b).

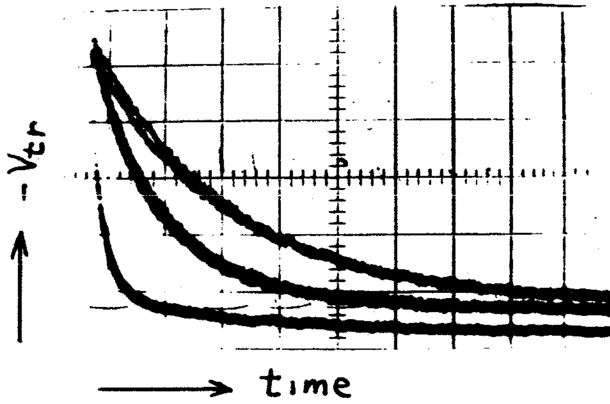


Figure 17(a)

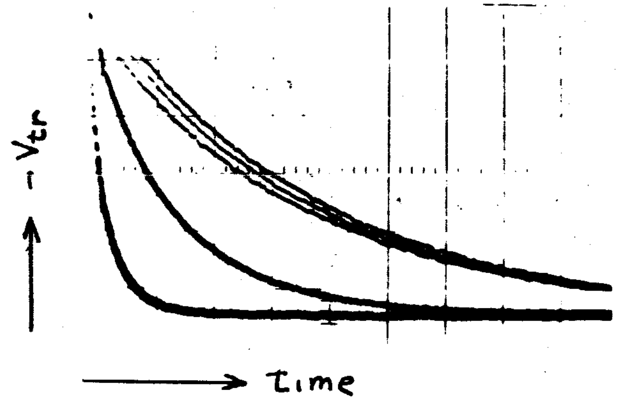


Figure 17(b)

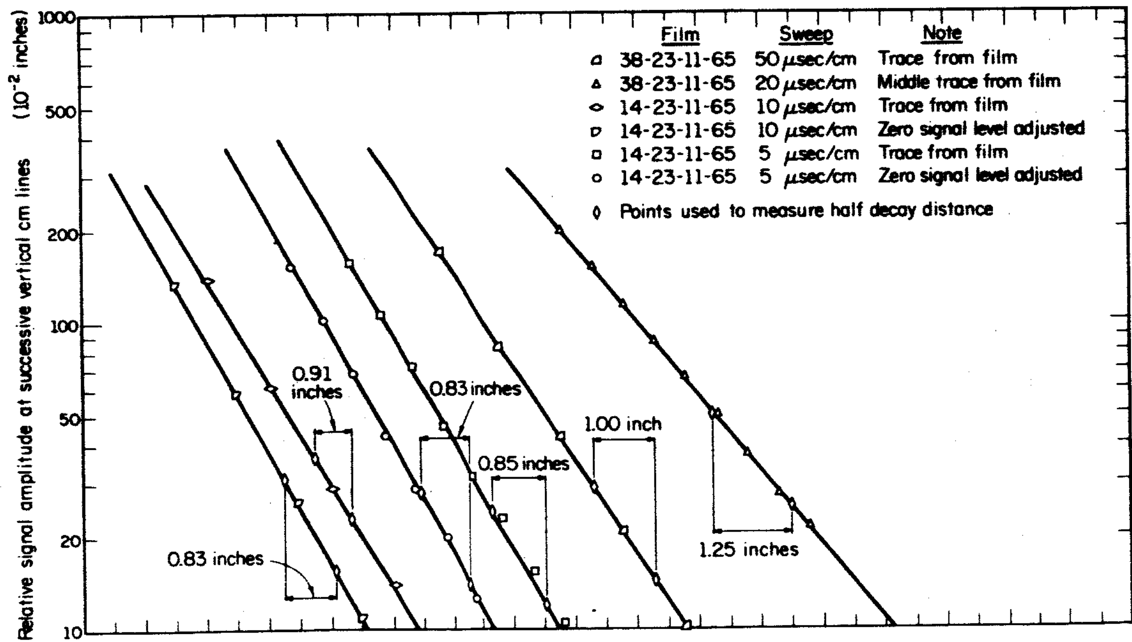


Figure 17(c)

Figure 18. Variation of transient voltage with time, and determination of lifetime from transient voltage-time curves. (a) 3/4 reproduction of Polaroid film 1-9-10-65 taken during second post-irradiation measurement on sample S2. The vertical scale is 100 μvolt/cm, resulting from an oscilloscope setting of 10 mv/cm and an amplifier gain of 100. The time scale is 5, 10, and 50 μsec/cm for the top, middle, and bottom group of traces, respectively. The sweep delay was 10 μsec, the dc sample voltage was 1.30 volts, and $10^3/T$ was 3.87. Trapping-like effects evident in the photograph were due to the contacts. Many traces were recorded and the mean position estimated to eliminate the effects of the noise present. (b) 3/4 reproduction of film 38-9-10-65 taken during the same measurement. The vertical scale is 200 μvolt/cm resulting from an oscilloscope setting of 20 mv/cm and an amplifier gain of 100. The time scale is 50, 100, and 500 μsec/cm for the top, middle, and bottom traces, respectively. The sweep delay was μ100 sec, the dc sample voltage 2.57 volts, and $10^3/T$ was 2.49. This film was typical of all pulled samples above room temperature. (c) 23/64 reproduction of semilogarithmic plot of transient voltage ampltiude at successive vertical centimeter lines on the above Polaroid photographs. All values of $\tau$ were plotted versus $10^3/T$ (see Figure 29b).

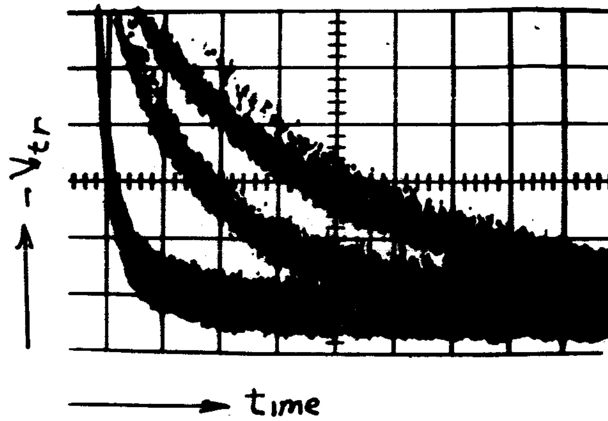


Figure 18(a)

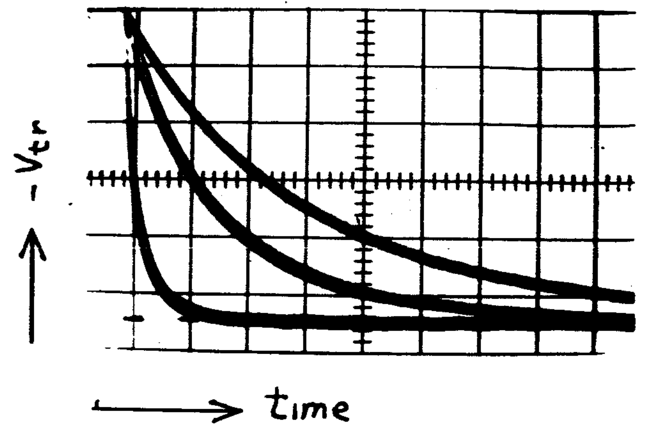


Figure 18(b)

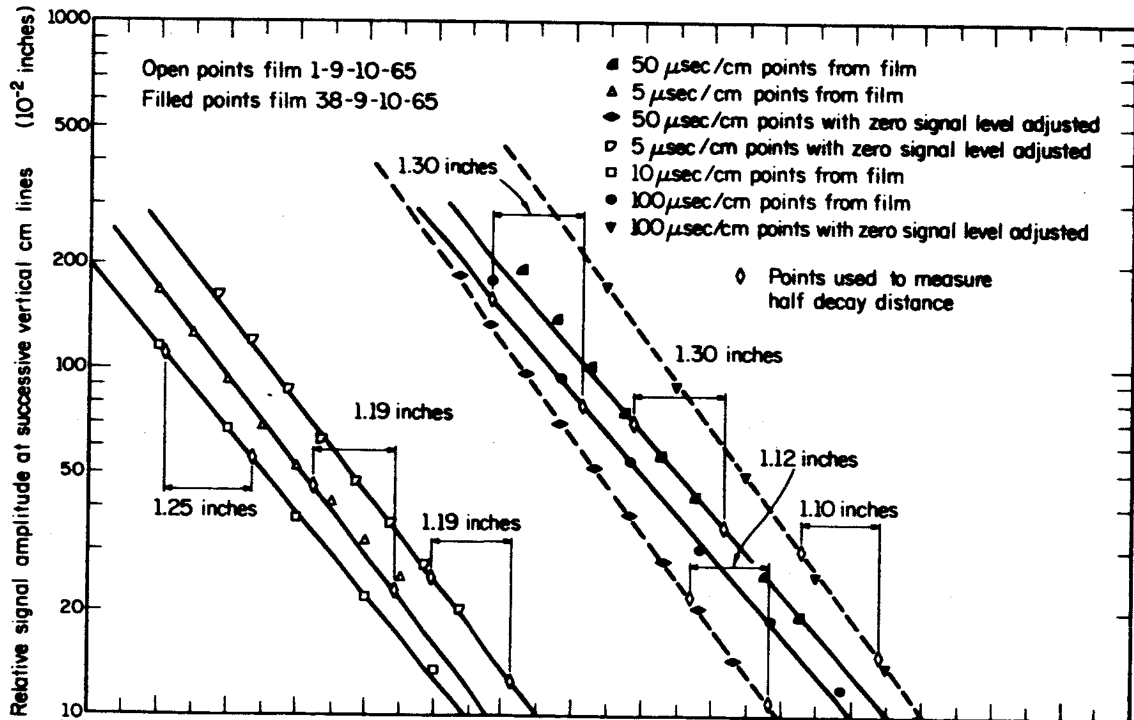


Figure 18(c)

which was always taken for samples which showed no trap decay for times comparable to the time of the photodecay, the baseline was determined and marked on the film at all vertical graticule lines. Using this baseline, the vertical distance to the trace was measured and the ordinate values plotted on semilog paper (see Figures 17c and 18c). The points plotted should fall near a straight line. The half-decay time is then found by means of the formula $T_{1/2} = (H.D.D.)(P/I)(S)$ where H.D.D. is the half decay distance on the graph (in inches), P/I is the number of film measurements at succeeding centimeter marks plotted per inch on the graph paper, and S is the oscilloscope sweep in microseconds per centimeter. If the baseline was incorrectly determined due to a high noise to signal ratio, the slope of the decay curve would change from its constant value determined at times for which the error was negligible, increasing in absolute value to infinity if the baseline had been set too high, and decreasing to zero for large times if the baseline had been set too low. This is illustrated in Figure 19 where the function $\ln(A + Be^{-t})$ is plotted against time.

Trapping can cause an increase in apparent lifetime, as was mentioned earlier, and if the pulse drifts into a region of increased defect concentration or if injection level effects are important, the lifetime can decrease with time. The delay feature of the oscilloscope display, as was mentioned above, was used to examine the second possibility, and knowledge of the sample characteristics was used to decide if injection level effects were the cause of the non-exponentiality, or if the cause was a mismeasurement of the baseline. If it was decided that mismeasurement were far more probable,

Figure 19. Semilogarithmic plot of $y = A + \exp(-t/\tau)$ against $t/\tau$ to illustrate the effect of baseline mis-measurement upon the lifetime. The lifetime indicated on the figure was measured in the region $y = 0.6$ to $y = 0.3$.

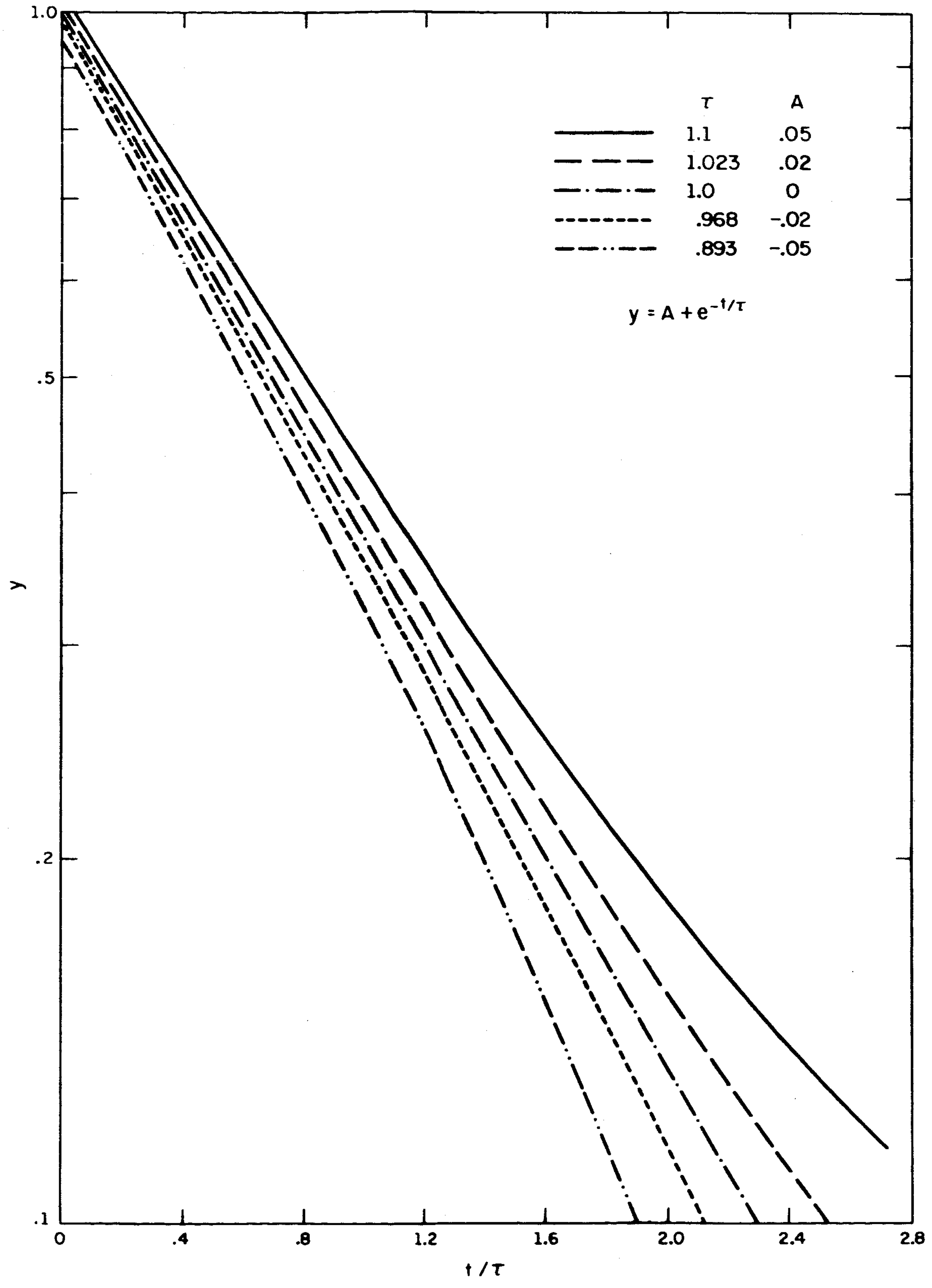


Figure 19

the film would be reexamined to see if the baseline had been read incorrectly, and what other values were probable. In cases where these decisions had to be made, the noise level was usually very high, and the baseline would be uncertain, even with the most careful measurement, by as much as 0.10" (1/4 cm.). The change in the baseline would then be added or subtracted to the ordinate values on the semilog plot, and the result examined. If no great improvement occurred for any reasonable change in the baseline, the data were not used, but if the semilog plot became linear, the slope was measured and the half-decay time calculated by measuring the time increment that occurred between a given signal level and a signal level half the original.

By exposing the film to many photo-decay traces, it was possible to reduce greatly the effects of irregularity in the intensity of the pulse, pickup, and contact noise. This was done by using the average trace positions on the multiply-exposed film to determine the lifetime.

Once the lifetime, or alternatively, the half-decay time $T_{1/2} = \tau_e \ln 2$, had been determined for a sample as a function of inverse temperature, these data were plotted on semilog paper, and a smoothed curve drawn through the data points. (Figures 22, 30, 28, and 32) Each set of points $(10^3/T, \tau_m)$, where $\tau_m$ is the measured lifetime, was identified by a code number affixed after the sample number, indicating the total number of measurements taken after irradiation, including that set. Thus E5-0 indicates a pre-irradiation measurement, and E5-2 indicates the second post-irradiation measurement. The value of $T_{1/2}$ of the smoothed curve was read from the curve for equally spaced intervals of inverse temperature. If the lifetime was seen to be a

strongly varying function of inverse temperature, the interval chosen was $\Delta(10^3/T) = 0.05$, otherwise an interval of $\Delta(10^3/T) = 0.10$ was chosen. A table was then constructed listing the half-decay time for these values of inverse temperature. This set of points was also given the same code as the original set for which the smoothed curve was drawn. After additional defects had been introduced into the material by irradiation, the lifetime was again measured as a function of inverse temperature, the data plotted, the smoothed curve drawn, and the values of $T_m$ entered into the table mentioned above.

Using the multilevel lifetime formula Eq. (2.1), which can be rewritten as

$$1/\tau_m = 1/\tau_{pre} + 1/\tau_\gamma \tag{3.2}$$

$$\tau_\gamma = \frac{\tau_m \tau_{pre}}{\tau_{pre} - \tau_m} \tag{3.3}$$

where $\tau_\gamma$ is the lifetime which would be measured if the radiation induced defects were the only recombination centers present, $\tau_{pre}$ is the pre-irradiation lifetime, and $\tau_m$ is the lifetime measured after irradiation. The set of points $(10^3/T, \tau_\gamma)$ is defined as a data set, and is identified by the sample code followed by the two code numbers of the smoothed curves. Thus E5-2-0 denotes the data set describing the lifetime change caused by defects introduced between the pre-irradiation measurement (the -0) and the second post-irradiation measurement (the -2).

It was noted earlier that the surface states contribute to the lifetime, and hence there are more terms than indicated above in the formula relating pre-irradiation and post-irradiation lifetimes. The pre-irradiation lifetime will be given by

$$1/\tau_{pre} = 1/\tau_{bo} + 1/\tau_{so} \qquad (3.4)$$

where $\tau_{bo}$ is the lifetime due to bulk defects present before irradiation, and $\tau_{so}$ is the effective pre-irradiation surface lifetime. After irradiation the lifetime will be given by

$$1/\tau_{m} = 1/\tau_{bo} + 1/\tau_{\gamma} + 1/\tau_{sf} \qquad (3.5)$$

where $\tau_{sf}$ is the effective surface lifetime for the post-irradiation measurement. If the two surface lifetimes are greatly different, and are comparable with the other lifetimes involved, large errors can arise in the measurement of the radiation induced lifetime. In this experiment, the surface lifetimes were, with one exception, sample I4, much longer than any of the other lifetimes. Thus the effect of errors introduced by considering the two surface lifetimes to be equal is small. It should be noted that the error will be smaller the greater the ratio of $\tau_{11}$ to $\tau_{bo}$. It follows, therefore, that lifetimes calculated from data measured after two different doses will be more accurate than that calculated from data measured prior to and after one irradiation, if the pre-irradiation lifetime is of the order of the surface decay time. For data calculated from two post-irradiation measurements, the effective $\tau_{bo}$ will be $\tau_{m}$ of the first post-irradiation measurement. The error introduced by the difference in surface decay times is relatively insensitive to moderate changes in the post-irradiation lifetime, if that lifetime is much less than the pre-irradiation lifetime, and so the error is experimentally indistinguishable from an error in the radiation dose. The error in the radiation induced lifetime due to surface lifetime differences was calculated from the data given by Blakemore and Nomura[46] to be less than 5%, and usually 1% or less.

2. Analysis of Lifetime-Temperature Data

The changes in the lifetime due to radiation induced defects were analyzed on an IBM 7094 computer for those cases where measurements could be made over a temperature range large enough to allow meaningful interpretation of computer fits to the S-R theory, and in other cases the slope of the $\ln\tau$ vs $10^3/T$ plots were measured and corrected for the density-of-states temperature correction. The computer analyses were done with the simplest approximations to S-R type formulae (fits), that had the same qualitative behavior, and also with more complicated formulae that were thought to be more correct if the simpler fits gave ambiguous results.

The main computer program can be described as a "lesser squares fitting program," in that it adjusts the parameters $A_j$ of the lifetime formula supplied to it, so that the quantity

$$\chi^2 = \sum_{j=1}^{N} \left( \frac{\tau_j - \tau_{\gamma j}}{W_j} \right)^2 \tag{3.6}$$

is constantly reduced. In the above expression the sum runs over the N data points $(10^3/Tj, \tau_{\gamma j})$, $W_j$ is the estimated probable error of the jth value of $\tau_{\gamma j}$, and $\tau_j$ is the lifetime calculated for that value of $10^3/T$. The $W_j$ were chosen to be equal to $\tau_{\gamma j}/20$, since the error in the lifetime measurement is a percentage error. It was also possible to weight a given temperature region by increasing the density of data points in that region, so that that region contributed more to $\chi^2$ than the other region(s). With the weights as chosen, $\chi^2$ should be equal to the number of points less the number of parameters if the random error is 5%.

The vast majority of data was taken for temperatures for which the approximation $n_o + p_o = n_o(p_o) = N_d(N_a)$ for n-type (p-type) was valid to

better than 1%. Under these circumstances the S-R formula becomes

$$\tau = \tau_{po}(1+n_1/N_d) + p_1/N_d \, \tau_{no} \quad \text{for n-type, and} \tag{3.7a}$$

$$\tau = \tau_{no}(1+p_1/N_a) + n_1/N_a \, \tau_{po} \quad \text{for p-type .} \tag{3.7b}$$

Unless the defect level is very close to the center of the gap, one of the terms $p_1\tau_{n_o}$ and $n_1\tau_{po}$ will be much smaller than the other. Thus, if the defect level in n-type silicon is in the upper half of the gap, the lifetime will be given by

$$\tau = \tau_{po}(1+n_1/N_d) \tag{3.8a}$$

while if it is in the lower half of the gap it will be given by

$$\tau = \tau_{po}(1 + \frac{\tau_{no}}{\tau_{po}} p_1/N_d) \tag{3.8b}$$

This can be seen by examining the ratio $(\tau_{no}/\tau_{po})(p_1/n_1)$. $p_1/n_1$ is given by $(N_v/N_c)\exp[(E_c-2E_r)/kT]$, and $N_c/N_v$ is about 2.8. If the recombination level is more than 0.1 ev (1160$^o$K) from the midgap position $E_c/2$, then $p_1/n_1$ will be equal to $\exp(1\underline{+}5.8)$ at $T = 400^oK$. At lower temperatures the ratio will be more disparate than at this temperature, the highest temperature for which measurements were made in this experiment, where the ratio is 0.0011 or 121. The smaller value is for the level in the upper half of the gap, and the larger to the level in the lower half of the gap. The ratio $\tau_{no}/\tau_{po}$ is roughly equal to $\sigma_p/\sigma_n$, and since one of the capture processes will be favored by coulomb attraction, the ratio should not be near one. Values reported are about 20 or 0.05. Thus we see that the ratio $\tau_{no}p_1/\tau_{po}n_1$ will be about 0.02 or less, or greater than 6. The approximation of dropping the smaller term is always excellent for the first case, which is for a

level in the upper half of the gap, but rather poor for the second, corresponding to a neutral-positive level at $E_v$ + .46 ev. Since all known defects near this position have a neutral-negative nature, the ratio $\tau_{no}p_1/\tau_{po}n_1$ would be greater than 2000, and the approximation justified here also.

For the sake of simplicity, only n-type material will be discussed, since the formulae can be easily converted to apply to p-type material by the interchanging of n's and p's, etc.

The simpliest approximation to Eq. (3.8a) is given by

$$\tau = A_1[1 + (10^3/T)^{-1.5} \exp(A_2 - 11.6(10^3/T)A_3)] \tag{3.9}$$

where $A_1$ will be $\tau_{po}$, and $A_3$ the energy separation of the recombination level from the nearest band edge in electron volts. The factor of 11.6 arises from the conversion 1 ev = 11,600°K. If the level is nearest the conduction band, the constant $A_2$ will be equal to $\ln[\omega N_c(10^3/T)^{3/2}/N_d] + \beta$ with $N_c(10^3/T)^{3/2}$ equal to $1.73\text{x}10^2\ {}^{\circ}K^{-1.5}\ cm^{-3}$. The quantity β arises from the assumption that the energy level has a linear temperature dependence

$$E_r = E_{ro} + \beta kT\ . \tag{3.10}$$

If β is greater than zero, the level will approach the conduction band as the temperature increases.

If the level is nearer the valence band, $A_2$ will be given by

$$A_2 = \ln[\tau_{no}N_v(10^3/T)^{1.5}/N_d\tau_{po}\omega] - \beta \tag{3.11}$$

The above fit was given the code PFZ-1, since it appeared it would fit p-type float zoned material.

In most cases it will be possible to determine which energy band the level is nearest, if all three constants can be determined. As noted

previously the ratio $\tau_{no}/\tau_{po}$ or its reciprocal has been determined to be about 20. The factor $e^{\beta}$, from Hall effect measurements, is about 1/2 for the Si-A center, so that the product $\omega e^{\beta}$ can range from 4 to 1/4. Thus if $A_2$ differs by more than ln4 from $\ln(N_c(10^3/T)^{1.5}/N_d)$, the level most probably lies in the lower half of the gap. If it is within ln4, identification is more difficult. Since $N_c$ is not known very accurately, and $N_d$ is calculated from the conductivity using published rather than measured mobilities, there exists an uncertainty of as much as a factor of two in the ratio of $N_c/N_d$. If $\tau_{no}/\tau_{po} = 20$ and $\omega e^{\beta} = 1/4$ it will be impossible on the basis of the foregoing discussion to distinguish this level from one in the upper half of the gap with $\omega e^{\beta} = 4$. Most previous accounts have tended to neglect these considerations, using $\omega = 1$ and $\beta = 0$.

If the nature of the defect is known from other investigations, then $\omega$ may be known, and the energy level position known, making it possible to determine $\beta$ if the experimental errors are small. Alternatively, if the factor $\omega e^{\beta}$ for a given level is known, it may then be possible to determine whether a level indicated by lifetime measurements is indeed the previously discovered level.

In several experiments it has been determined that the quantities $\tau_{no}$ and/or $\tau_{po}$ are not constant. Bemski[66] reported temperature dependences of $T^n$, with n = 1/2,2 and 7/2 for several of the levels of gold in silicon. By investigating the injection level dependence of the silicon A-center, Galkin, et. al.[33] concluded that the electron capture cross-section was strongly temperature dependent above 250°K. By plotting his data suitably, a reasonably good fit was obtained with $\tau_{no} = \tau_{noo}T^{-1/2}(1+e^{11.5-3.45*(10^3/T)})$.

Baicker's[35] injection level curves also indicate a temperature dependence for $\tau_{no} + \tau_{po}$. In view of these findings, fits PP-1, PFZ-2, and PFZ-3 were used when it was suspected that $\tau_{no}$ and/or $\tau_{po}$ were temperature dependent.

In the n-type float-zoned samples it is evident that either 2 separate levels or a multivalent level controls the lifetime. The data sets for this type of material were fit by

$$\tau = \frac{P*Q}{P+Q}$$

where P and Q are PFZ-1 fits. If both levels are closest to the same band, the $A_2$ of P and $A_2$ of Q are related. Since it was not possible to measure the lifetime at temperatures low enough that the approximation

$$\tau \sim \tau_{po} \frac{N_c}{N_d} e^{\frac{-(E_c - E_R)}{KT}}$$

was not adequate for the shallower level, it was not necessary to take explicit account of the differences (if any) in the degeneracies of the two levels. Fits NFZ-1, NFZ-2, and NFZ-3 are bilevel fits of this type.

In the p-type pulled samples it became evident that two levels were active in the recombination process, and fits NFZ-1 and PP-1 were used on these data sets. Fit PP-2 is also of the form

$$\tau = \frac{P*Q}{P+Q}$$

with P a PFZ-1 fit and Q a PP-1 fit.

For the high resistivity samples at high temperature, the approximation $n_o(p_o) = |N_d - N_a|$ in n-type (p-type) material is no longer valid. Fit NI-1 was programmed to account for this.

Table 4 lists the various fits used in the analysis of the data, along with their formulae and descriptive comments.

Table 4

List of Computer Fits

| Code | Formula | Description |
| --- | --- | --- |
| PFZ-1 | $\tau = P_o(A_1,A_2,A_3) = A_1*[1+(\frac{10^3}{T})^{-1.5} *\exp(A_2-11.6*(\frac{10^3}{T})*A_3)]$ | single S-R level in extrinsic temperature range, constant $\tau_{n_o}, \tau_{p_o}$ |
| PFZ-2 | $\tau = P_o(A_1,A_2,A_3)*(10^3/T)^{A_4}$ $= P_1(A_1,A_2,A_3,A_4)$ | same as PFZ-1 except that $A_1$ now has a temperature dependence of $T$-$A4$ |
| PFZ-3 | $\tau = A_1+(10^3/T)^{A_4-1.5} *\exp(A_2-11.6*(10^3/T)*A_3)$ | formula for recombination level and Fermi level in opposite halves of the gap, and with a temperature dependence of $T^{A4}$ to the capture cross-section ratio. |
| NFZ-1 | $\tau = \frac{P*Q}{P+Q}$ , $P=P_o(A_1(P),A_2(P),A_3(P))=P_o(P)$ $Q = P_o(Q)$ | formula for 2 S-R defects, constant $\tau_{n_o}$ and $\tau_{p_o}$ |
| NFZ-2 | $\tau = \frac{P*Q}{P+Q}$ , $P = P_o(A_1(P),A_2(P),A_3(P))$ $Q = P_o(A_1(Q),A_2(P),A_3(Q))$ | same as NFZ-1 except both levels are fixed to be closer to the same band. |
| NFZ-3 | $\tau = \frac{P*Q}{P+Q}$ $P = P_1(A_1(P),A_2(P),A_3(P),1/2)$ $Q = P_1(A_1(Q),A_2(P),A_3(Q),1/2)$ | same as NFZ-2 except $\tau_{n_o}$ and/or $\tau_{p_o}$ have $T^{-1/2}$ temperature variation |

Table 4 (continued)

| | | |
|---|---|---|
| PP-1 | $\tau = P_2(P) = A_1*(1+\exp(A_4-A_5+(10^3/T)$ <br> $+ (10^3/T)*\exp(A_2-11.6*A_3*(10^3/T))$ | similar to PFZ-3 except 1) $A_1$ in PFZ-3 is replaced by $A_1*(1+\exp(A_4-(10^3/T)A_5))$ and 2) $A_4$ in PFZ-3 is zero for PP-1. |
| PP-2 | $\tau = \frac{P*Q}{P+Q}$ $P = P_o(P)$, $Q = P_2(Q)$ | similar to NFZ-1 except for differences between $P_o(Q)$ in NFZ-1 and $P_2(Q)$ in PP-2 |
| NI-1 | $\tau = \frac{A_1*(n(A_4)+A_2*(10^3/T)^{-1.5}*\exp(47.1-11.6*(10^3/T)*A_3))}{[n(A_4) + p(A_4)]}$ <br> with $[n(A_4+p(A_4)] = 10^{13}*(A_4{}^2+(10^3/T)^{-3}\exp(38.63-14.04*(10^3/T)))^{1/2}$ <br> and $n(A_4) = (A_4*10^{13}+ [n(A_4)+p(A_4)])/2$ | similar to PFZ-1 except intrinsic temperature range included |

Due to trapping and/or contact problems, it was impossible to measure some samples to low enough temperatures that $n_1/n_o$ ($\tau_{no}/\tau_{po}\ p_1/n_o$) became of order unity or less, and hence all that could be determined was the product $\tau_{po}\ n_1/n_o$ ($\tau_{no}/\tau_{po}\ p_1/n_o$) for the level in the upper (lower) half of the gap. In these cases the high temperature slope of the log $\tau_\gamma$ vs. $10^3/T$ plot was measured, and corrected for the temperature dependence of the density of states by subtracting 3/2 kT from the energy determined from the slope. If there is no temperature dependence in $\tau_{no}$ or $\tau_{po}$, and if no other levels are active in the recombination process, the corrected energy obtained will be the energy separation of the level from the nearest band edge.

# IV. DISCUSSION OF RESULTS

## A. Phosphorus Doped Floating Zone Grown Silicon

The pre-irradiation characteristics of the n-type float-zoned samples, along with those of all the other samples used in the experiment, are listed in Table 5. The irradiation histories of the samples are listed in Table 6, and Appendix II contains the calculations justifying the application of the S-R formulae to the data sets. The results of the computer fits to the n-type float-zoned data sets, listed in Table 7, indicate that a deep level, with an energy separation of about 0.4ev from a band edge, was found in all samples, and that a much shallower level was also always seen. The shallow level appeared to have an energy separation of about 0.16ev in all data sets except for the data set B2-2-0 and all data sets of the type XX-1-0, in which the energy separation was about 0.1ev. In view of this apparent correlation between level position and irradiation number, it is not certain whether the 0.1ev level is real or whether it arises from some effect which vanishes when the post-irradiation lifetime is much less than the pre-irradiation lifetime. A similar increase, although of much smaller magnitude, can be seen in the value of the energy separation of the deep level for later irradiations. The data sets and the curves fit to them are shown in Figures 20 to 24.

The quantity $\tau_{p_o}$ was assumed constant in nearly all fits. This assumption implies that the hole capture cross-section $\sigma_p$ has a temperature variation of $T^{-1/2}$, since $1/\tau_{p_o} = N\sigma_p v_p$, and $v_p$ is proportional to $T^{1/2}$. An NFZ-3 fit, which assumes $\sigma_p$ constant, was made to the data set L5-2-0 to determine if this latter assumption might not be more appropriate than

Table 5

Pre-Irradiation Sample Characteristics†

| Sample Code | Material Class | Resistivity (ohm-cm) | Pre-Irradiation lifetime (μsec) | Supplier | Notes |
|---|---|---|---|---|---|
| B2 | nFZ | 18 | 30 | D | |
| B3 | " | 18 | 24 | D | |
| L5 | " | 68 | 52 | M | 1,2 |
| C1 | " | 180 | 155 | D | |
| C3 | " | 137 | 207 | D | |
| C4 | " | 139 | 200 | D | |
| C6 | " | 192 | 180 | D | |
| H1 | nP | 25 | 26 | D | 3,5 |
| H2 | " | 26 | 34 | D | 3,5 |
| T4 | " | 79 | 470 | M | 2,3 |
| I1 | " | 220 | 520 | D | 3 |
| I4 | " | 220 | 87 | D | 3,6 |
| T7 | " | 475 | 290 | M | 2,3,7 |
| E3 | pFZ | 24 | 200 | D | |
| E4 | " | 25 | 270 | D | |
| E5 | " | 25 | 260 | D | |
| M3 | " | 71 | 105 | M | |
| M4 | " | 73 | 98 | M | |
| F3 | " | 222 | 90 | D | |
| F4 | " | 238 | 133 | D | |
| U1 | " | 1160 | 107 | S | 8 |
| U2 | " | 1160 | 125 | S | 8 |
| W1 | " | 6300 | 113 | S | 4,8 |
| W2 | " | 6300 | 127 | S | 4,8 |
| S2 | pP | 11 | 110 | M | 3 |
| O1 | " | 32 | 260 | M | 3,5 |
| P1 | " | 50 | 37 | M | 1,3 |
| R2 | " | 250 | 51 | S | 1,3 |

nFZ: n-type float-zoned nP: n-type pulled PFZ: p-type float-zoned
pP: p-type pulled

D: Dupont M: Monsanto S: Semi-elements, Inc.

1. strong injection level effects seen
2. axial cut crystal (all others radius cut)
3. long time constant traps
4. short time constant traps
5. large minority carrier trap concentration
6. thin (1.4mm) sample
7. lateral resistivity gradients
8. severe lifetime gradients

† at room temperature

Table 6

Radiation History of Samples Used

| Data Set* | Total Dose ($10^6$ Roentgens) | Data Set* | Total Dose ($10^6$ Roentgens) |
|---|---|---|---|
| B2-1 | .2 | I4-1 | 5 |
| B3-1 | .1 | I4-2 | 10 |
| B3-2 | .2 | L5-1 | .1 |
| C1-A1 | 3 | L5-2 | .2 |
| C3-1 | .1 | M3-1 | 2 |
| C4-1 | .2 | M4-1 | 1 |
| C4-2 | .4 | O1-1 | 2.5 |
| C4-3 | .8 | O1-2 | 5 |
| C4-4A | 10 | P1-1 | 5 |
| C6-1 | .2 | R2-1 | 11 |
| C6-2 | .4 | R2-2 | 20 |
| C6-3 | .8 | S2-1 | 2 |
| E3-1 | 4 | S2-2 | 4 |
| E4-1 | 2 | S2-3 | 9 |
| E4-2 | 4 | T4-1 | 2.5 |
| E5-1 | 2 | T4-2 | 5 |
| E5-2 | 20 | T7-1 | 2.5 |
| F3-1 | 2 | T7-2 | 5 |
| F3-2 | 4 | U1-1 | 2.5 |
| F3-3 | 9 | U1-2 | 5 |
| F3-4 | 18 | U2-1 | 5 |
| F4-1 | 2.5 | U2-2 | 10 |
| H1-1 | 5 | W1-1 | 2.5 |
| H2-1 | 2 | W1-2 | 5 |
| H2-2 | 4 | W2-1 | 5 |
| I1-1 | 12 | | |
| I1-3 | 20 | | |

* Sample is denoted by first letter and number. Second number denotes number of irradiation.

Table 7

Computer Results for n-Type Float-Zoned Silicon

| Data Set | $A_1(P)$ | $A_2(P)$ | $A_3(P)$ [a] | $A_1(Q)$ | $A_2(Q)$ | $A_3(Q)$ [a] | Fit | $\chi^2/N$ [b] | $A_{20}$ [c] | $\tau_o\phi$ [d] |
|---|---|---|---|---|---|---|---|---|---|---|
| B2-1-0 | 8.33 | 14.00 | .378 | .0178 | 12.58 | .0894 | NFZ-1 | .743 | 13.5 | 1.66 |
| B3-1-0 | 23.75 | 14.22[e] | .40[f] | .0207 | 14.22 | .1064 | NFZ-2 | .336 | 13.5 | 2.37 |
| B3-1-0 | 10.45 | 14.71[e] | .40[f] | .0204 | 14.71[e] | .175[f] | NFZ-3 | 1.025 | 13.5 | |
| B3-2-0 | 10.85 | 14.63[e] | .402 | .0094 | 14.63[e] | .112 | NFZ-2 | .600 | 13.5 | 2.16 |
| B3-2-0 | 9.25 | 14.30[e] | .389 | .354 | 14.30[e] | .175[f] | NFZ-2 | .958 | 13.5 | 1.85 |
| L5-1-0 | 23.06 | 14.78[e] | .400 | .0016 | 14.78[e] | .103 | NFZ-2 | .554 | 14.95 | 2.31 |
| L5-2-0 | 10.0 | 15.30 | .416 | .117 | 15.30 | .166 | NFZ-1 | .414 | 14.95 | 2.00 |
| L5-2-0 | 5.52 | 15.59[e] | .420 | .051 | 15.59[e] | .174 | NFZ-3 | .554 | 14.95 | |
| L5-1-2 | 19.87 | 15.09[e] | .412 | .126 | 15.09[e] | .151 | NFZ-2 | .441 | 14.95 | 1.99 |
| C1-A1-0 | 1.41 | 16.19 | .429 | | | | PFZ-1 | .300 | 15.80 | |
| C1-A2-0 | 22.1 | 14.66 | .392 | | | | PFZ-1 | .131 | 15.80 | 66 |
| C1-A1-A2 | 1.53 | 16.62 | .442 | | | | PFZ-1 | .333 | 15.80 | 4.6 |
| C3-1-0 | 28.37 | 14.77 | .366 | .179 | 15.09 | .128 | NFZ-1 | .147 | 15.55 | 2.84 |
| C3-1-0 | 28.35 | 14.79[e] | .367 | .268 | 14.79[e] | .130 | NFZ-2 | .148 | 15.55 | 2.84 |
| C4-1-0 | 12.97 | 15.36 | .386 | .053 | 12.38 | .346 | NFZ-1 | .040 | 15.55 | 2.60 |
| C4-1-0 | 12.78 | 15.23[e] | .383 | .037 | 15.23[e] | .078 | NFZ-2 | .044 | 15.55 | 2.52 |
| C4-1-2 | 16.54 | 16.72[e] | .422 | .147 | 16.72[e] | .174 | NFZ-2 | .101 | 15.55 | 3.30 |
| C4-2-0 | 7.07 | 15.61[e] | .391 | .295 | 15.57 | .165 | NFZ-1 | .021 | 15.55 | 2.83 |
| C4-2-0 | 6.87 | 15.55 | .389 | | | | PFZ-1 | .045 | 15.55 | 2.75 |
| C4-3-0 | 3.64 | 15.43[e] | .396 | .137 | 15.43[e] | .181 | NFZ-2 | .105 | 15.55 | 2.91 |
| C4-3-0 | 3.64 | 15.40 | .395 | .119 | 15.67 | .184 | NFZ-1 | .105 | 15.55 | 2.91 |
| C4-4A-0 | 7.64 | 15.5[g] | .439 | | | | NI-1 | .240 | 15.55 | 76. |
| C4-4A-0 | 7.44 | 15.01 | .40 | | | | PFZ-1 | .052 | 15.55 | 74. |
| C6-1-0 | 12.24 | 15.22 | .380 | | | | PFZ-1 | .130 | 15.85 | 2.45 |
| C6-2-0 | 7.59 | 16.09 | .408 | | | | PFZ-1 | .127 | 15.85 | 3.04 |
| C6-2-3 | 8.86 | 17.65 | .461 | | | | PFZ-1 | .164 | 15.85 | 3.54 |
| C6-3-0 | 4.04 | 16.37 | .419 | | | | PFZ-1 | .120 | 15.85 | 3.23 |

a. energy separation from nearest band edge in ev.
b. $\chi^2$ divided by number of data points used in calculation.
c. $A_{20} = \ln(N_c(10^3/T)^{1.5}/N_d)$.
d. given by $A_1(P)$ times flux increment = $\tau_{po}\phi$ for the .4 ev level
e. denotes parameters of some calculation fixed to be equal
f. denotes fixed parameter
g. NI-1 parameter converted to PFZ-1 parameter for comparison

Figure 20. Variation of radiation induced lifetime with reciprocal temperature for 20 ohm-cm n-type float-zoned silicon. Complete parameters for the theoretical curves are given in Table 7. The curve for data set B3-1-0 was calculated by the NFZ-2 fit, and for B3-2-0 the curve was calculated with the shallow level at .112ev from a band edge.

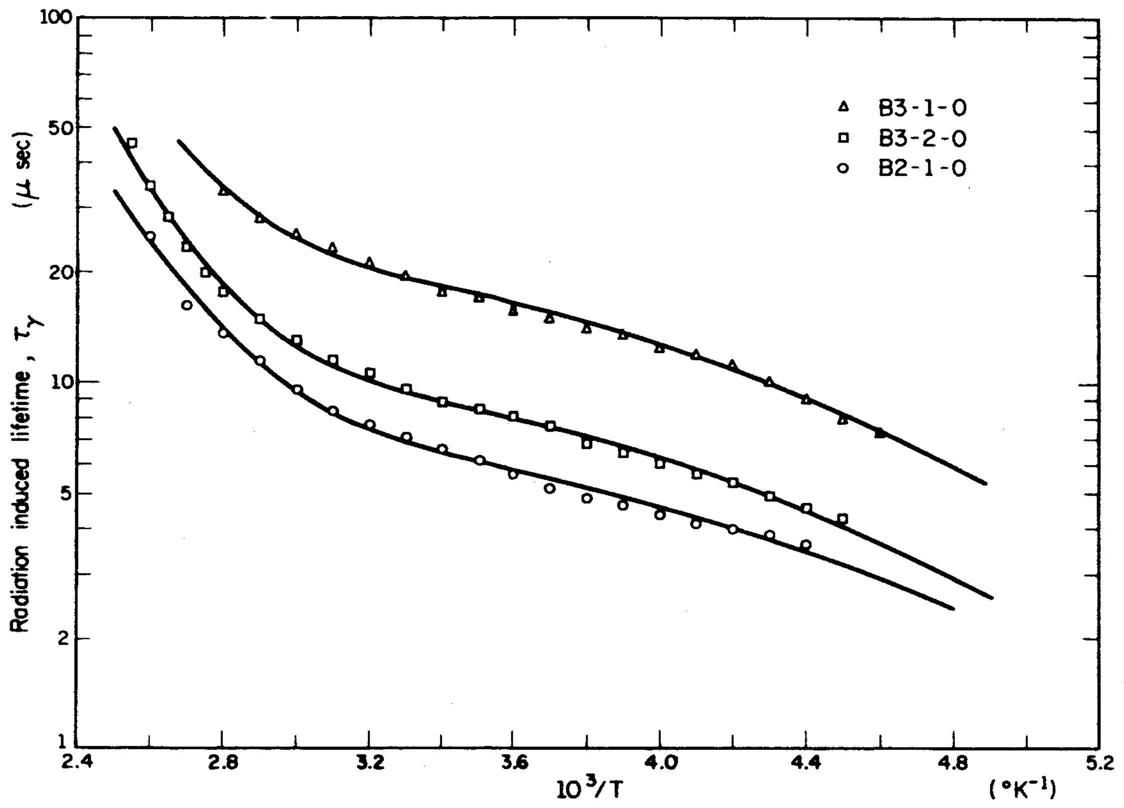


Figure 20

Figure 21. Variation of lifetime with reciprocal temperature for 70 ohm-cm n-type float-zoned silicon. (a) Radiation induced lifetime. The parameters for the theoretical curves are given in Table 7. The solid curve for the L5-2-0 data set is the result of the NFZ-1 fit, and the dashed curve is the result of the NFZ-3 fit. (b) Measured lifetime. The data points for the radiation induced lifetime in the upper figure were obtained from evenly spaced points on the curves hand-drawn through the measured lifetime data points and by use of formula 3.3.

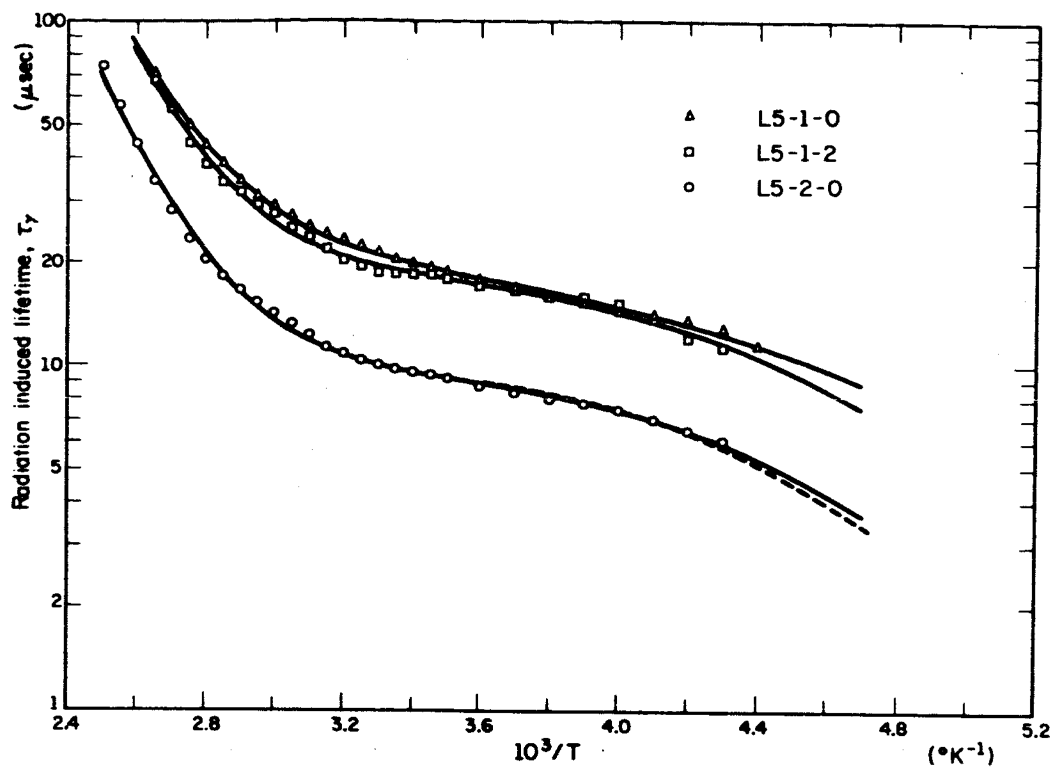


Figure 21a

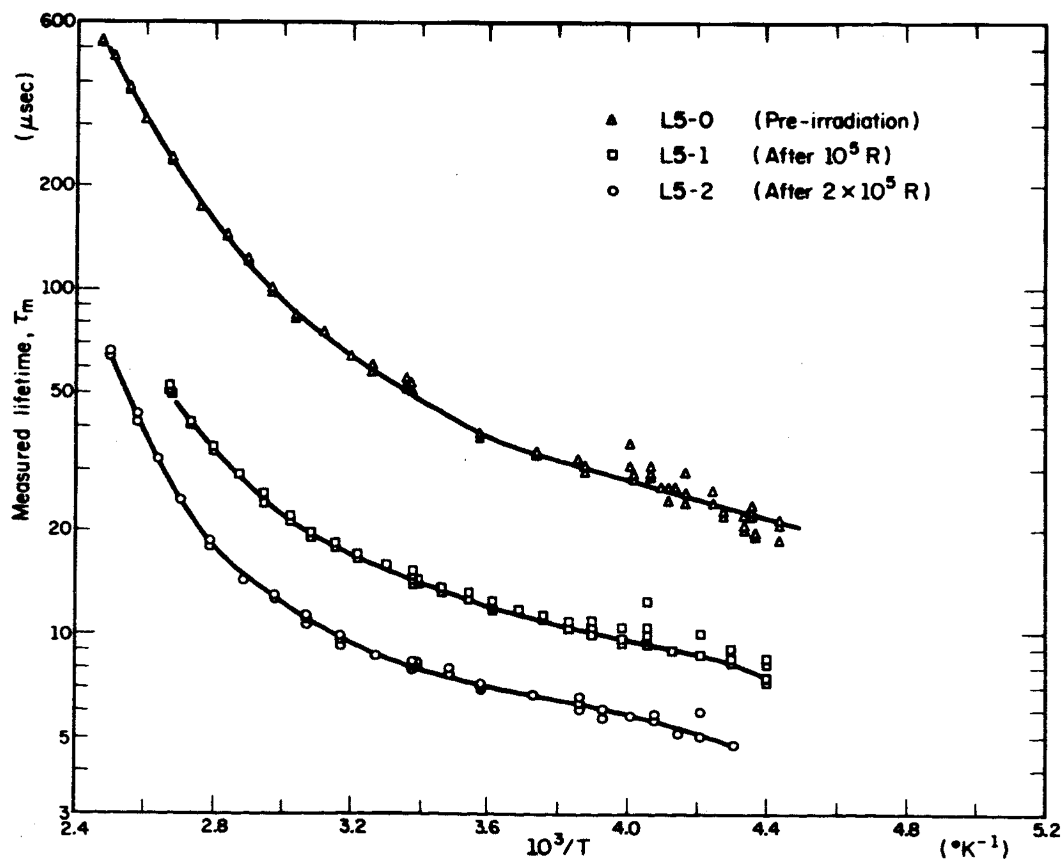


Figure 21b

Figure 22. Variation of radiation induced lifetime with reciprocal temperature for 140 ohm-cm n-type float-zoned silicon. Parameters for the theoretical curves are given in Table 7. The curves resulted from the NFZ-1 fits. A -0 has been omitted from all curve designations.

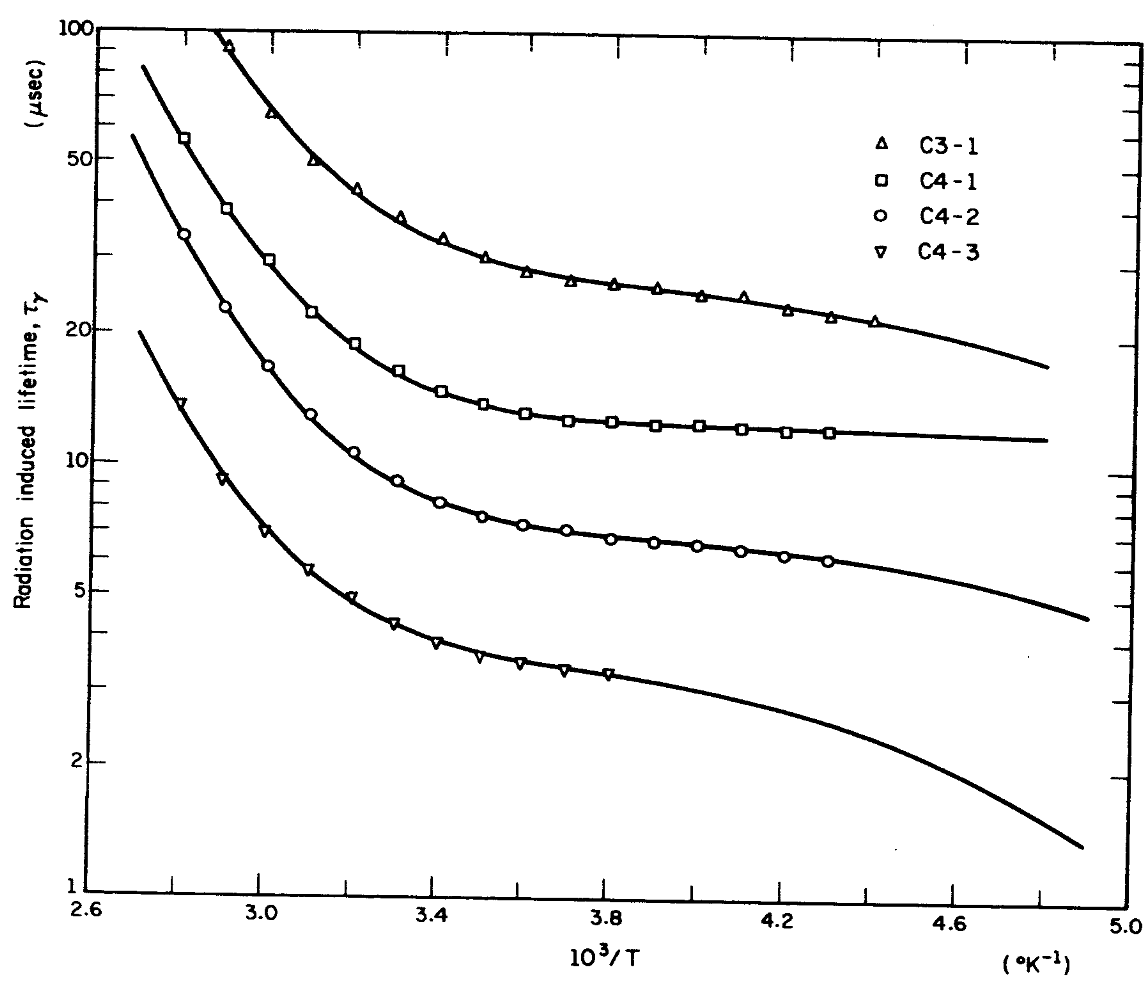


Figure 22

Figure 23. Variation of radiation induced lifetime with reciprocal temperature for 190 ohm-cm n-type float-zoned silicon. Parameters for the theoretical curves are given in Table 7. A -0 has been omitted from all curve designations.

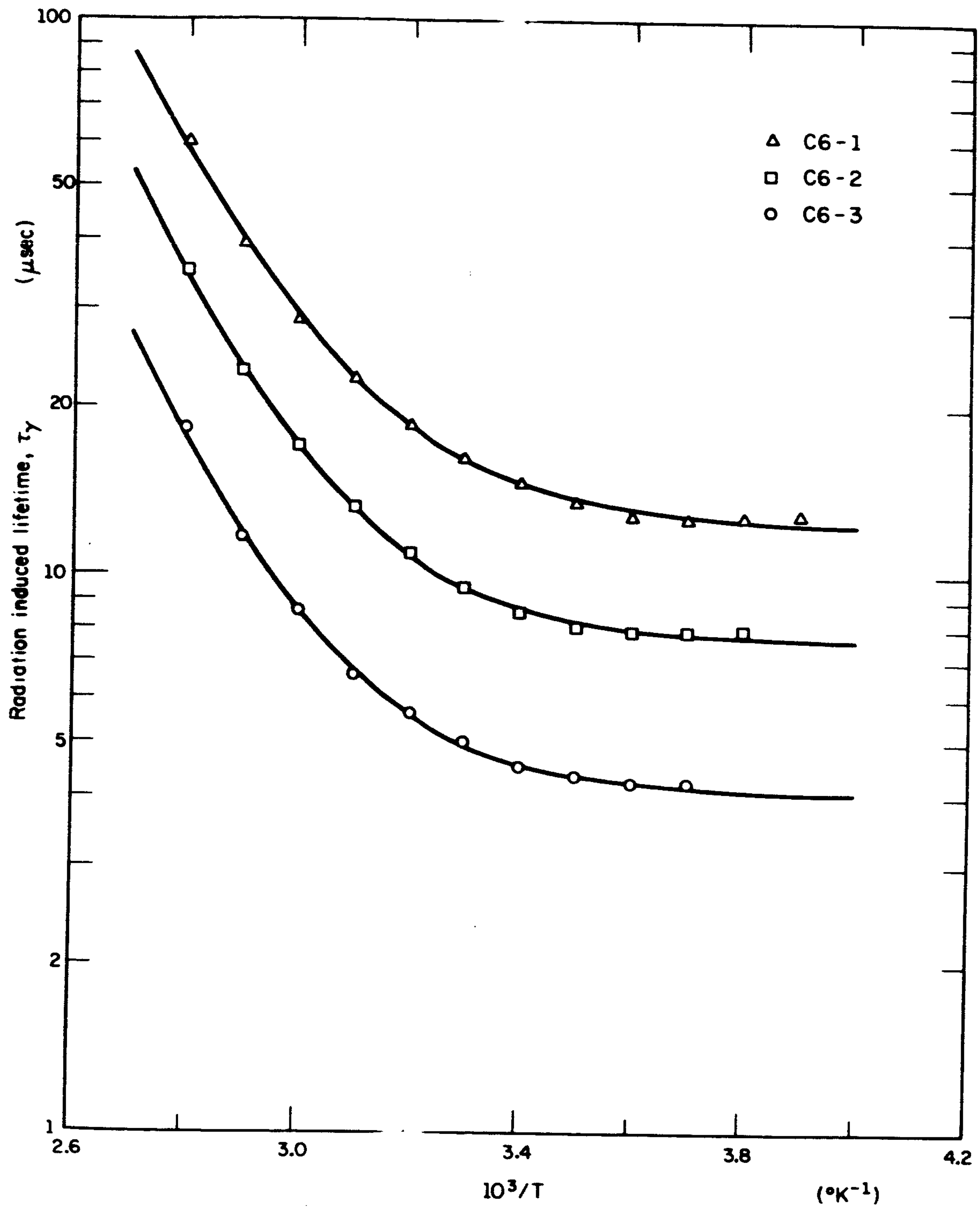


Figure 23

Figure 24. Variation of annealed radiation induced lifetime with reciprocal temperature in 180 ohm-cm n-type float-zoned silicon. A -0 has been omitted from all curve designations except Cl-Al-A2. The dashed curve for C4-4A-0 is for the PFZ-1 fit, and the solid curve is for the NI-1 fit. The parameters for the theoretical curves are given in Table 7.

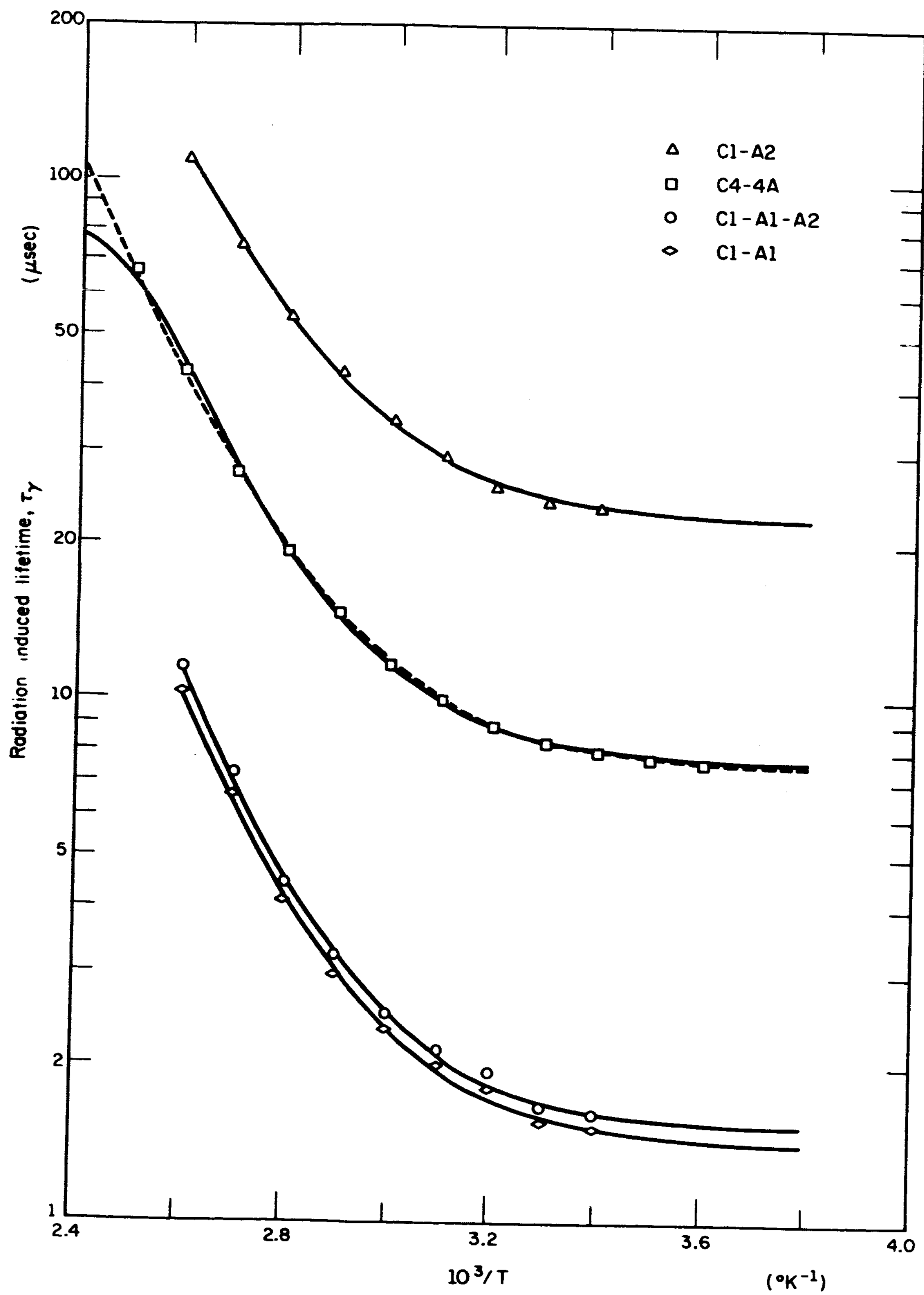


**Figure 24**

the assumption of constant $\tau_{p_o}$. A comparison of the NFZ-2 and NFZ-3 parameters reveals that the effect of constant $\sigma_p$ rather than constant $\tau_{p_o}$ is 1) an increase in the value of the parameter $A_2$, corresponding to an increase in the factor $\omega e^{\beta} N_c/N_d$, 2) essentially no change in the deep level position, 3) an increase in the energy separation of the shallow level from the nearest band edge, and 4) an increase in $\chi^2$, indicating a poorer fit. Both fits are shown in Figure 21a. Since the quality of the fit was not impaired using the simpler assumption of constant $\tau_{p_o}$, all other data sets were processed using the simpler NFZ-1 and NFZ-2 fits.

As is evident from the figures, the shallow level does not have much effect upon the lifetime in the temperature range measured, and therefore the parameters calculated for it are much more uncertain than for the deeper level. Since the lifetime was not measured at temperatures low enough that it approached its minimum value, the parameter $A_2$ in the NFZ-2 and NFZ-3 fits was determined by the deeper level. In the NFZ-1 fit the parameter $A_2$ for the shallow level appeared to be determined more by the original estimate required by the computer program than by anything else. It is therefore impossible to determine whether the level is closest to the conduction band or to the valence band.

All the parameters for the deep level could be determined, with an accuracy roughly proportional to the resistivity of the material. The average of the quantity $[A_2(P)-\ln(N_c'/N_d)]$, where $N_c' = N_c(10^3/T)^{1.5} = 1.73\times10^{20}\,cm^{-3}\,{}^oK^{-1.5}$, over all runs on all samples was 0.36, making it possible that the level could be closest to either band. For a conduction band fit, this requires that $\beta + \ln\omega = 0.36$, so that if $\omega = 1/2$, a rather

large temperature variation of $9.05\times10^{-5}$ ev/$^{o}$C results. If $\omega = 2$, in agreement with the models for all defects known to have levels at this position, a much more reasonable temperature variation of $-2.9\times10^{-5}$ ev/$^{o}$C is the result. Possible errors affecting these values include error in the value of $N_c$ used, and incorrect values of $N_d$ arising from differences between the actual majority carrier mobilities and the value reported by Morin and Maita. The minority carrier mobility was measured in several samples prior to irradiation, using the apparatus shown in Figure 10, and the values obtained ranged from 2/3 to 1 times the value given in the literature. Whether the majority carrier mobility varied similarly could not be determined. Considering these factors, the results are compatible with the interpretation that the deep level is located closest to the conduction band, has a spin degeneracy ratio of 2, and has a slight variation of position with temperature, apparently moving toward midgap as the temperature increases.

The average value of $A_2(P)$ is also consistent with the conclusion that the deep level lies closest to the valence band if the spin degeneracy is 2, and if the level moves toward midgap with increasing temperature. The capture cross-section ratio $\sigma_p/\sigma_n$ is then about 15. For any other combination of degeneracy ratio and reasonable temperature dependence, the ratio of hole to electron capture cross-section is between 2 and 7, a rather unlikely range.

Additional information about the deep level was obtained from the anneals on crystals C1 and C4, which showed annealing at or below 100$^{o}$C. It was assumed that no defects were created as a result of the anneal,

either from components of defects disassociating during the anneal or from any other source. The data set CX-A-0, where A denotes the measurement made after some anneal treatment, and X is either 1 or 4, then contains information about the defects remaining after the anneal, and the data set CX-N-A, where N is the number of the last irradiation performed before the anneal treatment, contains information about the defects that annealed out. A partial anneal on crystal C1 occured at 100°C during exploratory measurements after the room temperature lifetime had been measured. The lifetime was then measured as the temperature was decreased. The crystal was annealed at about 150°C until no further change was seen in the lifetime. The resulting data sets were then processed by the PFZ-1 fit, and a comparison of the C1-A2-0 and C1-A1-A2 parameters indicates that the defects which annealed out had an energy level separated by 0.44ev from a band, while those remaining had an energy level separated by 0.39ev from a band. A difference in $A_2$ was seen between the two fits, indicating that the factor $\omega e^{\beta}$ was smaller for the defects remaining than for those that had annealed out. Sample C4 was given a very large fourth dose, after which its lifetime should have been about 0.3μsec, according to the linear relationship between recombination rate and dose observed for the lower doses. This value could not be checked since it was well below the minimum measurable lifetime. The sample was annealed for 15 minute periods at 10°C temperature intervals, beginning at 95°C. After the 145°C anneal, the lifetime appeared to be about 1 microsecond. Since the indium contacts melt at 153°C, the anneal temperature was not increased, but the sample was annealed at 145°C for 760 minutes. The lifetime after this anneal was 7.6 microseconds, indicating

that about 95% of the pre-irradiation lifetime had been restored by the anneal. The lifetime was measured as a function of temperature, and the resulting data set C4-4A-0 was fit by the PFZ-1 program, with the result that the deep level was definitely at $E_c$ - 0.4ev, and had a temperature dependence in agreement with that found for C1-A2-0. The lifetime had been measured at temperatures for which the approximation $n_o = N_d$ was slightly in error, and so the data set was refit using the NI-1 program, a program valid in the near-intrinsic region. The result of this fit was that the level appeared to be at $E_c$ - 0.44, with $\omega e^{\beta}$ equal to 1. In the NI-1 fit the donor density was fixed at $2.1\times10^{13}cm^{-3}$, which is slightly lower than the calculated donor concentration. The PFZ-1 fit is thus probably more correct, and the result then agrees with that for C1-A2-0, in that the remaining, more stable defects appear to lie closer to the conduction band than the less stable ones.

It is very likely that only one type of defect is present, and that for some reason a small percentage of the defects in the C crystals are more stable than the others. Evidence for this conclusion comes both from a comparison of the lifetime-flux product $\tau_{p_o}\phi$ for the 0.4ev level, which is equal to $(\sigma_p v_p \frac{dN}{d\phi})^{-1}$ where $\sigma_p$ is the hole capture cross-section, $v_p$ the hole thermal velocity, and $dN/d\phi$ the defect introduction rate of the defects with this energy level, for all the n-type float-zoned samples, and from a comparison of the annealing behavior of these crystals. For these calculations $\tau_{p_o}$ was assumed constant. The average of the lifetime-flux product for the B samples was 2.0sec-Roentgen and for the L samples it was 2.2sec-Roentgen, while for the C crystals it was 2.9sec-Roentgen. The differences are in the direction expected for recombination centers involving

donors, and thus from the similarity in introduction rates it appears that the same defects were created in all of these crystals. Samples B and L showed no annealing at temperatures for which a large anneal was seen in the C crystals. This suggests that the annealing behavior of the defects was controlled by some other factor such as oxygen content, dislocation content, or other type of defect which has an effect upon the annealing.

The lifetime results of this experiment agree with those of Glaenzer and Wolf[34], including the lifetime-flux products. They reported that the deep defects in their crystals were stable to $400^{o}K$, which agrees with the results on crystals B and L. However, they did not see a shallow level 0.1ev from a band edge, only a level at about 0.17ev, which they identified as the A center (the substitutional oxygen center with a level at $E_c$ - 0.16ev and with $\omega = 1/2$) on the basis of the experiments of Watkins and Corbett,[23,32] Sonder and Templeton[22], and Saito, Hirata, and Horiuchi[28]. The defect level seen at $E_c$ - 0.16ev in this experiment is also identified with the A center for the same reasons. The level 0.1ev from a band edge, if real, might be the level reported by Iniushi and Matsuura,[26] and also by Wertheim and Buchanan[25].

The deep level found in this experiment agrees with the energy level position found by Watkins and Corbett[39], and the spin degeneracy ratio found appears to be that predicted by their model for the E center (phosphorus atom and vacancy as nearest neighbors). Sonder and Templeton[27] reported the E center to be somewhat deeper, at $E_c$ - 0.47ev, and to have annealing behavior similar to that seen in this experiment for the C samples. It therefore appears that the lifetime in the n-type float-zoned crystals investigated was controlled by two types of defects, the A center and the E center.

## B. Phosphorus Doped Crucible Grown Silicon

An examination of the data sets (Figure 25-28) for lifetime changes due to irradiation in the n-type pulled materials suggests that if trapping did not prevent measurement of the lifetime of the higher resistivity crystals at lower temperatures, the behavior would qualitatively be the same as that observed in the n-type float-zoned samples.

The slopes of the lines drawn through the H data sets (Figure 25) are somewhat less than might be expected if the recombination centers are A centers, since the energy separation, after correction for the temperature variation of the effective density of states of the conduction band, is about 0.14ev. This value is actually slightly high, if the deeper level, which appears to be formed in all other n-type samples, is present in this material. The effect of the deeper level can be seen in Figure 4 by comparing the slope of the curve for the net lifetime to that for the curve of the shallow level for values of $10^3/T$ greater than 4.8.

By assuming that the lifetime in the irradiated H samples is controlled by A centers, and that the introduction rate for A centers in this material is typical, the A center lifetime-flux product $\tau_{p_o} n_1/N_d \phi$ of 81.5sec-Roentgen at $10^3/T = 3.0$ can be used to estimate the lifetime due to A centers in the other n-type samples. Differences in the resistivities of the various samples are accounted for by multiplying the lifetime-flux product by $N_{dH}/N_{dX} = \rho_X/\rho_H$ where $N_{dH}$ and $N_{dX}$ are the donor concentrations of sample H and of the sample for which the calculation is to be performed, and $\rho_H$ and $\rho_X$ are the resistivities of these materials, respectively. Such calculations show that except for sample T4, the calculated lifetimes are compatible with the measured lifetimes. This agrees with the conclusion of Sonder and

Figure 25. Variation of radiation induced lifetime with reciprocal temperature for 20 ohm-cm n-type pulled silicon. The lines were drawn through the high temperature points and the slopes on the curves measured.

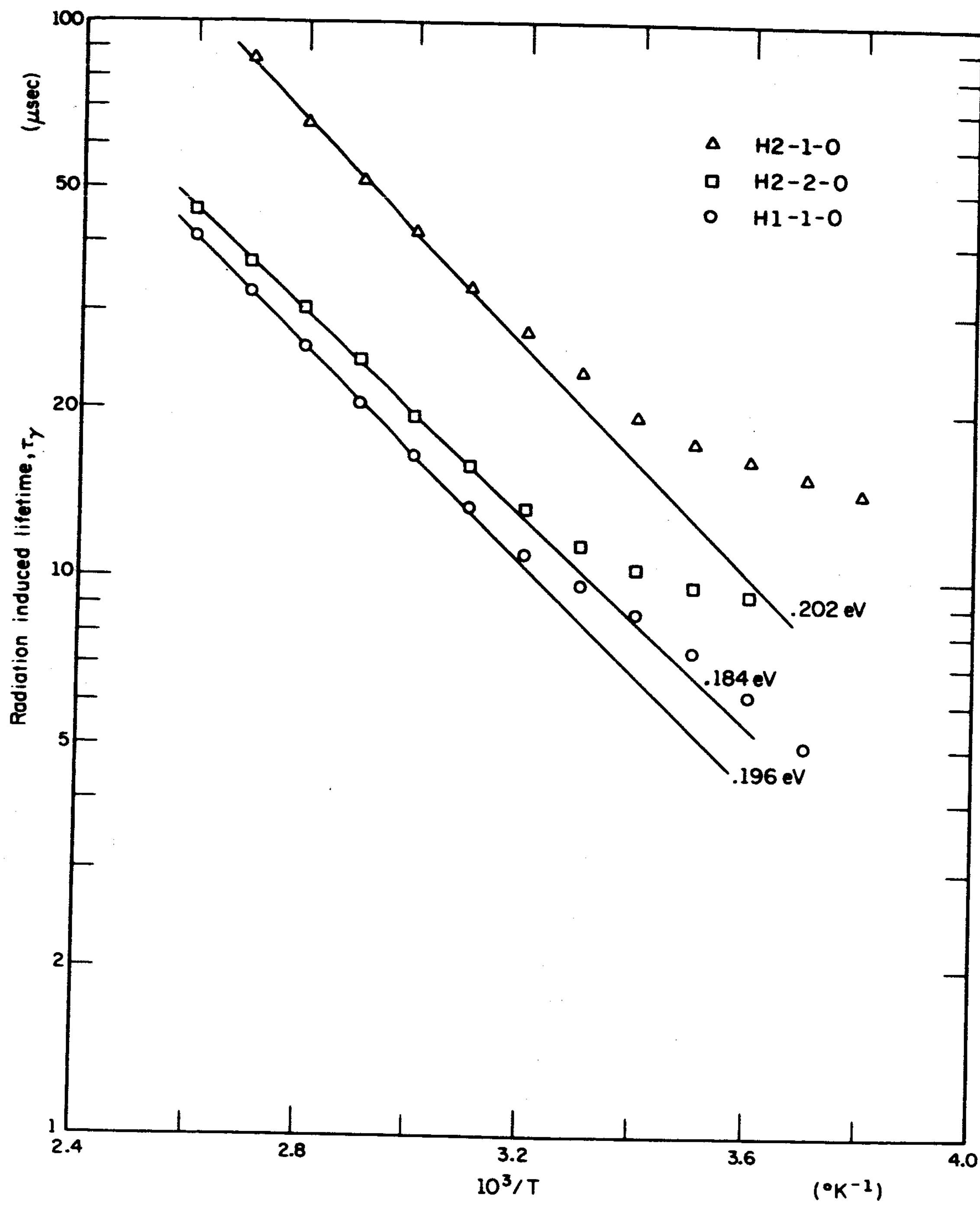


Figure 25

Figure 26. Variation of radiation induced lifetime with reciprocal temperature for 80 ohm-cm n-type pulled silicon. A -0 has been omitted from the data set designations.

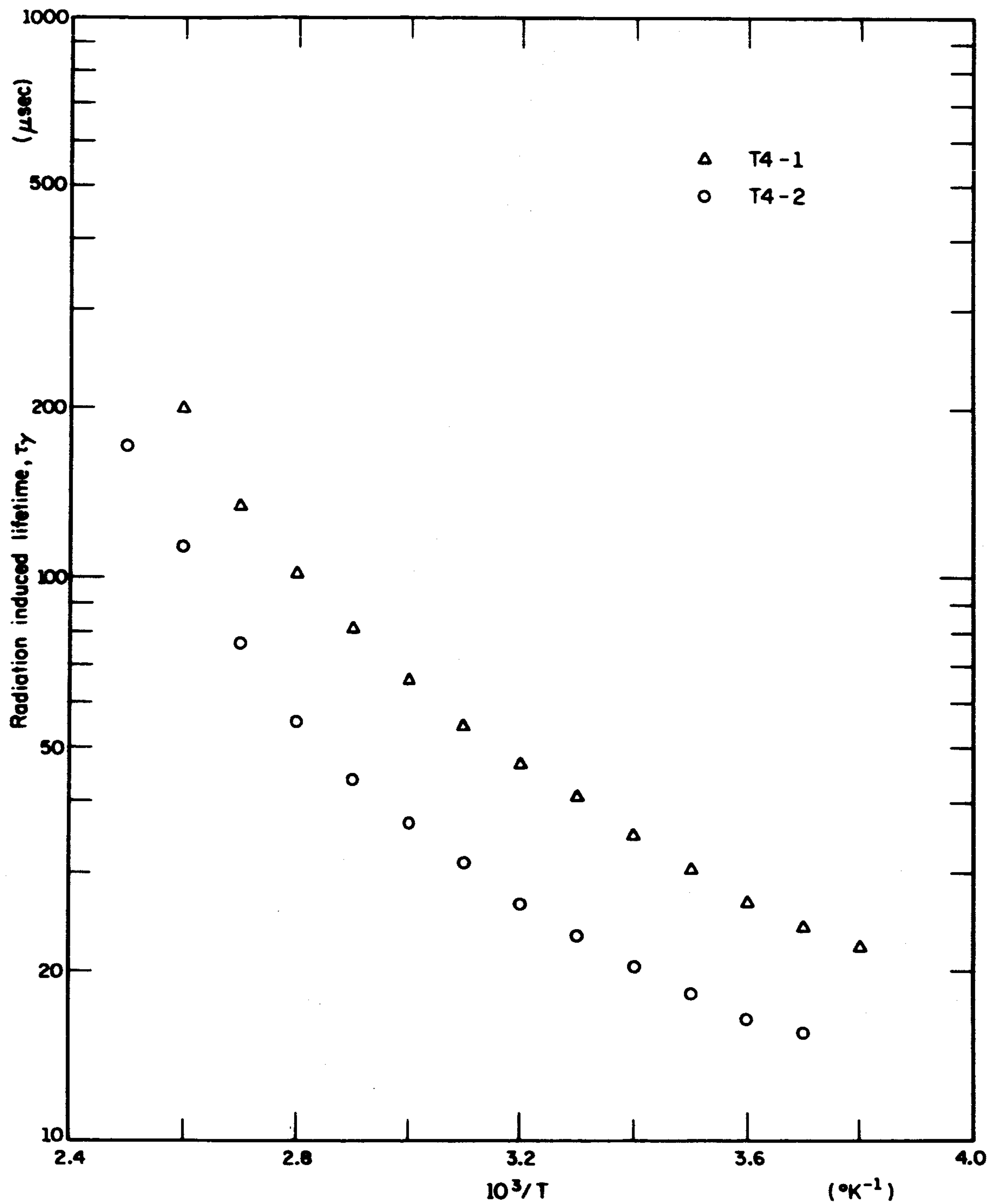


Figure 26

Figure 27. Variation of radiation induced lifetime with reciprocal temperature and variation of measured lifetime with reciprocal temperature in 220 ohm-cm n-type pulled silicon. (a) Radiation induced lifetime and annealed lifetime (I1-3A1-3A2). Parameters for the theoretical curves (I4-1-0 and I4-2-0) are given in Table 8. (b) The curves drawn through the measured data points were used to obtain the radiation induced lifetime at evenly spaced values of $10^3/T$ by means of formula 3.3. The pre-irradiation lifetime in sample I4 appears to be dominated by surface recombination due to its small (.14 cm) thickness.

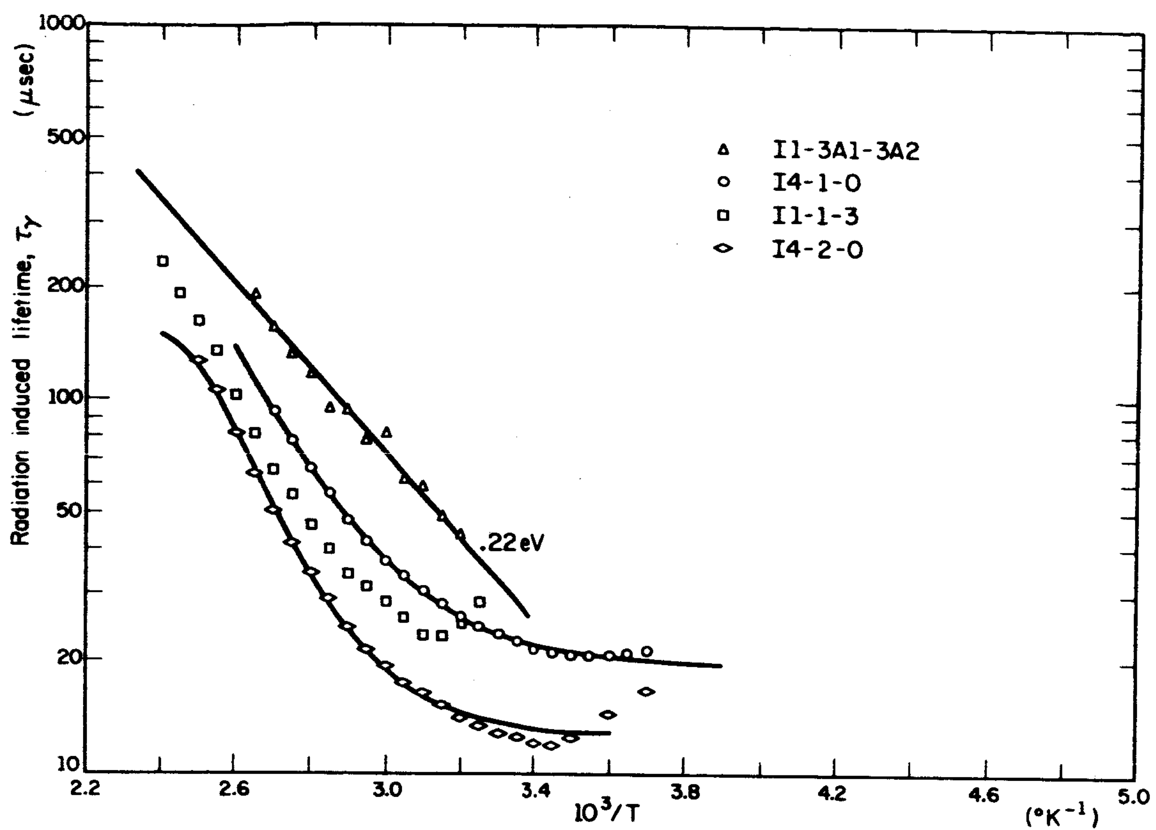


Figure 27a

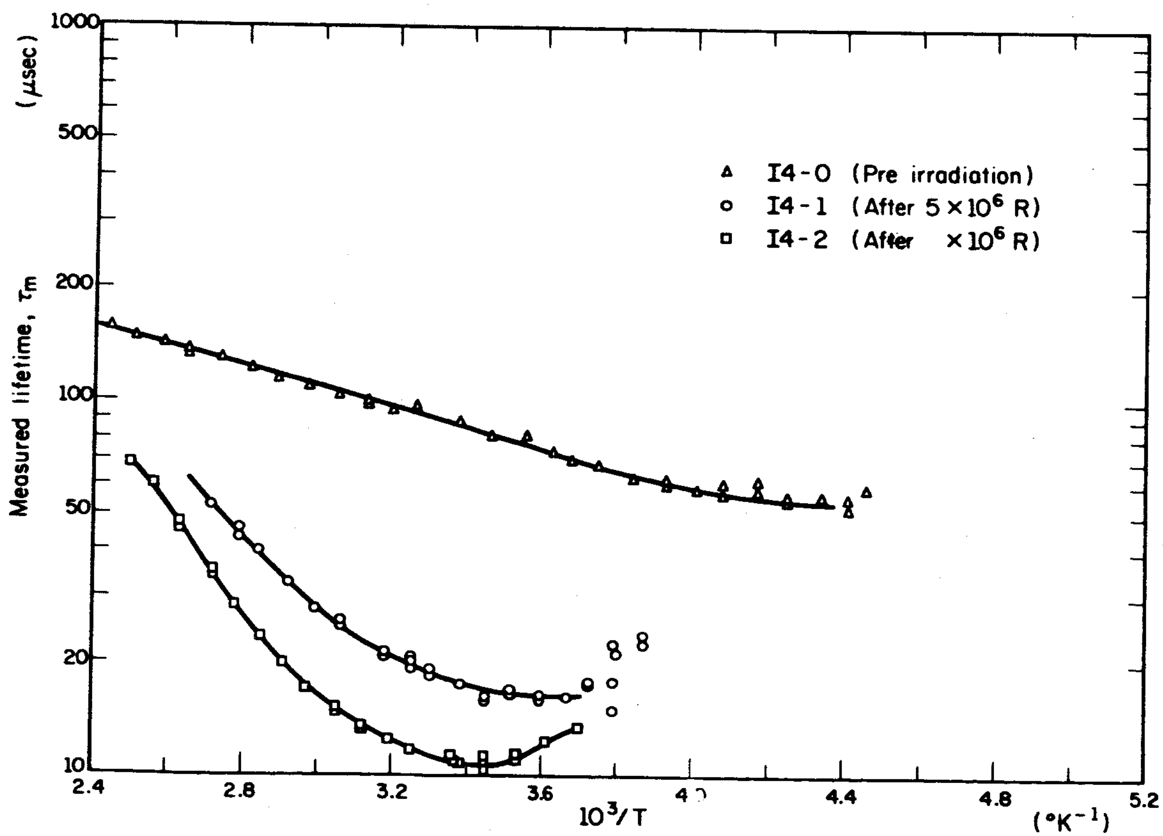


Figure 27b

Figure 28. Variation of radiation induced lifetime with reciprocal temperature in 475 ohm-cm n-type pulled silicon. The parameters for the theoretical (heavy line) curve are given in Table 8. The light lines were drawn through the high temperature points and the slopes measured. A -0 has been omitted from all data set designations except T7-1-2.

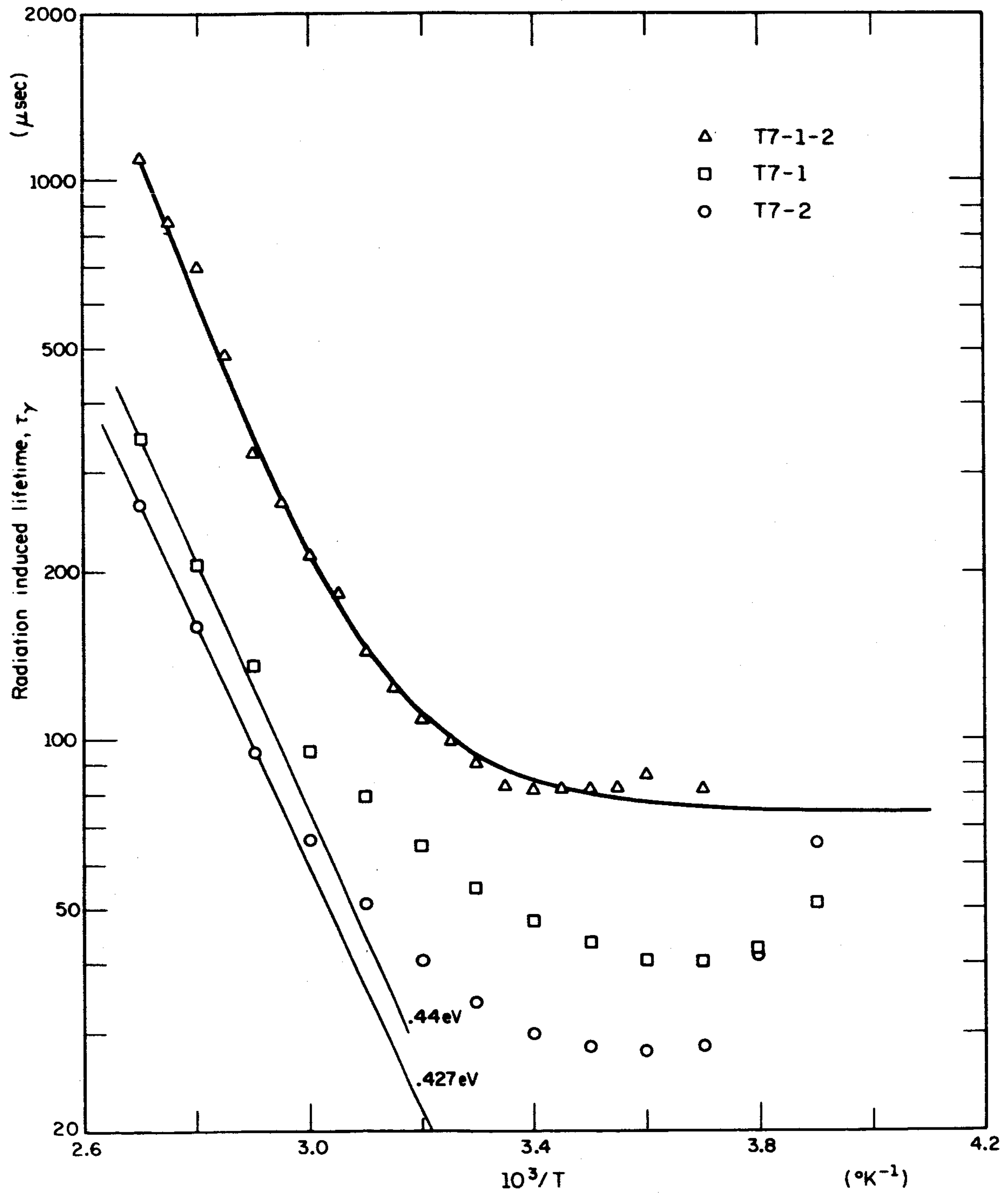


Figure 28

Templeton[27] that the A center introduction rates in pulled and float-zoned materials were nearly the same.

The lifetime variation with reciprocal temperature seen in the data sets for sample T4 (Figure 26) appears to correspond to that calculated for the curve with $\alpha$ (the ratio of the quantities $\tau_{p_o}$ for the two levels) equal to 0.01 in Figure 7, remembering that the lifetime at low temperatures is increased by trapping. From the calculation of the A center lifetime using the lifetime-flux product of the H samples, it appears that the A center introduction rate in this material is down by a factor of 3 or more from its value in the H samples.

The results of the computer fits to the data sets I4-1-0, I4-2-0, and T7-1-2 are listed in Table 8. They indicate that the deep level in sample I4 is definitely near the conduction band, if the room temperature lifetime is not greatly affected by trapping so as to indicate a much larger value of $\tau_{p_o}$ than is actually the case. While the behavior of the data set I1-1-3 indicates that trapping can affect the lifetime in this temperature region, the point at which the lifetime reaches its minimum moves to higher temperatures as the total dose increases. It follows, therefore, that the data set I4-1-0, which resulted from the lightest dose, is less affected by trapping than the others, and it is felt that the results of the fit to this data set are not greatly in error.

The results of the fit to the data set T7-1-2 should be regarded lightly, since the constant lifetime for $10^3/T$ greater than 3.4 appears to be an accident, for the data sets T7-1-0 and T7-2-0, while similar, do not resemble the T7-1-2 data set. More weight should be attached to the -0 data sets, shown in Figure 28, which have slopes of 0.427 and 0.44ev at

Table 8

Computer Results for n-type Pulled Silicon

| Data Set | $A_1$ | $A_2$ | $A_3$† | Fit | $\chi^2$ | pts | $\ln[N_c(10^3/T)^{3/2}/N_d]$ |
|---|---|---|---|---|---|---|---|
| I4-1-0 | 19.37 | 14.06 | .358 | PFZ-1 | .776 | 19 | 15.8 |
| I4-2-0 | 12.68 | 17.75* | .483 | NI-1 | 2.61 | 15 | 15.8 |
| T7-1-2 | 74.5 | 20.55 | .525 | PFZ-1 | 24.1 | 20 | 16.7 |

*Parameters converted for comparison with PFZ-1 fits.

†energy separation from nearest band edge in ev.

high temperatures. The opposite effects of the density of states variation and of the non-validity of the high temperature approximation $\tau = \tau_{p_o} n_1/n_o$ make it impossible to accurately determine the level position, but it is safe to say that it lies between 0.38 and 0.47ev from a band edge.

Samples T4 and T7 were cut from the same boule, with their long dimensions along the boule axis, so that there is a resistivity variation across the sample thickness due to the radial resistivity variation in the boule. This variation is negligible in T4, since it was cut from the center of the boule, while it is perhaps appreciable in T7, which was cut from a portion closer to the outside (see Figure 12). The lifetime data from sample I4, which was a very uniform crystal, agrees well with that obtained on T7, indicating that the effect of the resistivity variation upon the lifetime in T7 is not as severe as might be supposed from consideration of the S-R equations.

The deep level defects, like those seen in samples B and L, were stable to $400^{o}$K. The lifetime-flux product for this deep level calculated for the I samples and sample T7, ranges between 125 and 170sec-Roentgen, compared to the 2 to 3sec-Roentgen values in the float-zoned samples. Assuming that the less stable defects in crystals C1 and C4 annealed completely, and that no anneal of the more stable defects had occurred, the lifetime-flux product for these two samples after anneal was about 70sec-Roentgen. This result may indicate that only the more stable defects are formed in the material containing appreciably more oxygen.

Evidence that A centers were formed by irradiation of the higher resistivity materials came from a series of anneal treatments on sample I1.

The final anneal consisted of a six hour anneal at about $250^{o}C$, and the data set I1-3A1-3A2 indicated that only A centers had annealed, since the data points all lie close to a line of slope 0.22ev, so that the energy separation, after correction for the density of states variation, was about 0.16ev. Comparison of the results on the n-type pulled materials and on the float-zoned materials obtained in this experiment with the results of previous experiments suggests that the same levels are formed in the pulled materials as in the float-zoned materials, but that the effect of higher oxygen concentration is to decrease the introduction rate of the deeper level.

C. Boron Doped Crucible Grown Silicon

A brief examination of the data sets for p-type pulled material (Figures 29-32) reveals that the lifetime in this type of material is also controlled by two types of defects. The effect of the deeper level is seen best in the data sets for sample R2 (Figure 32). Even in this high resistivity material at high temperatures it appears that the lifetime of the deep level is approximately equal to its low temperature value, and thus the energy separation cannot be determined from the slope of the lifetime-reciprocal temperature plot. To agree with the observed behavior, the level must lie in the range $E_v$ + 0.4ev to $E_c$ - 0.25ev, and if it is in the upper half of the gap the capture cross-section of the defect for holes must be larger than for electrons.

The lifetime in sample S2 was relatively uninfluenced by the deeper level, showing only a very slight bend-over at high temperatures (Figure 29). The PFZ-1 fits to the shallow level can be analyzed either for a level 0.18ev from the conduction band or for one 0.18ev from the valence band. For the

Figure 29. Variation of lifetime with reciprocal temperature in 10 ohm-cm p-type pulled silicon. (a) Radiation induced lifetime. The parameters for the theoretical curves are given in Table 9. The curves for data sets S2-1-0, S2-2-0, and S2-3-0 resulted from PP-1 fits, and the curve for S2-2-3 resulted from the PFZ-1 fit which used 15 data points. (b) Measured lifetime. The curves were drawn by hand through the measured data points, and the data points of the upper figure were obtained by means of formula 3.3.

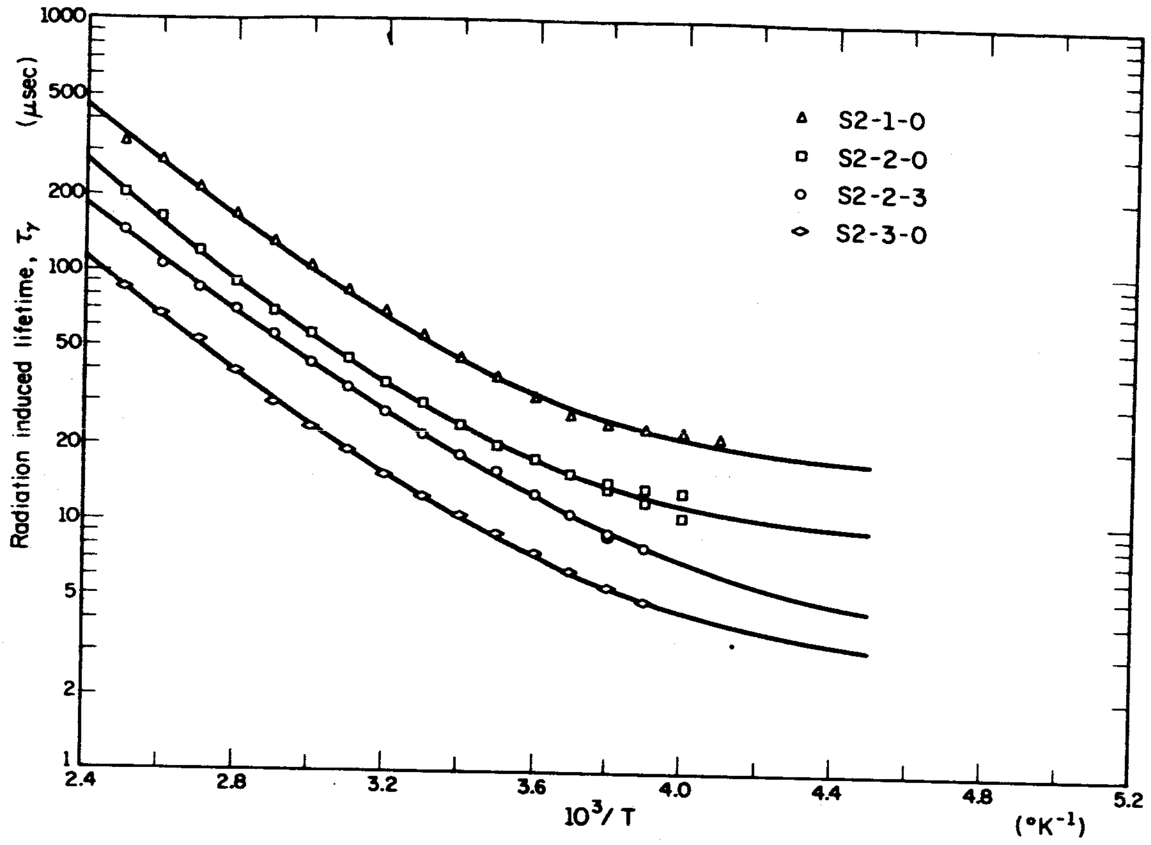


**Figure 29a**

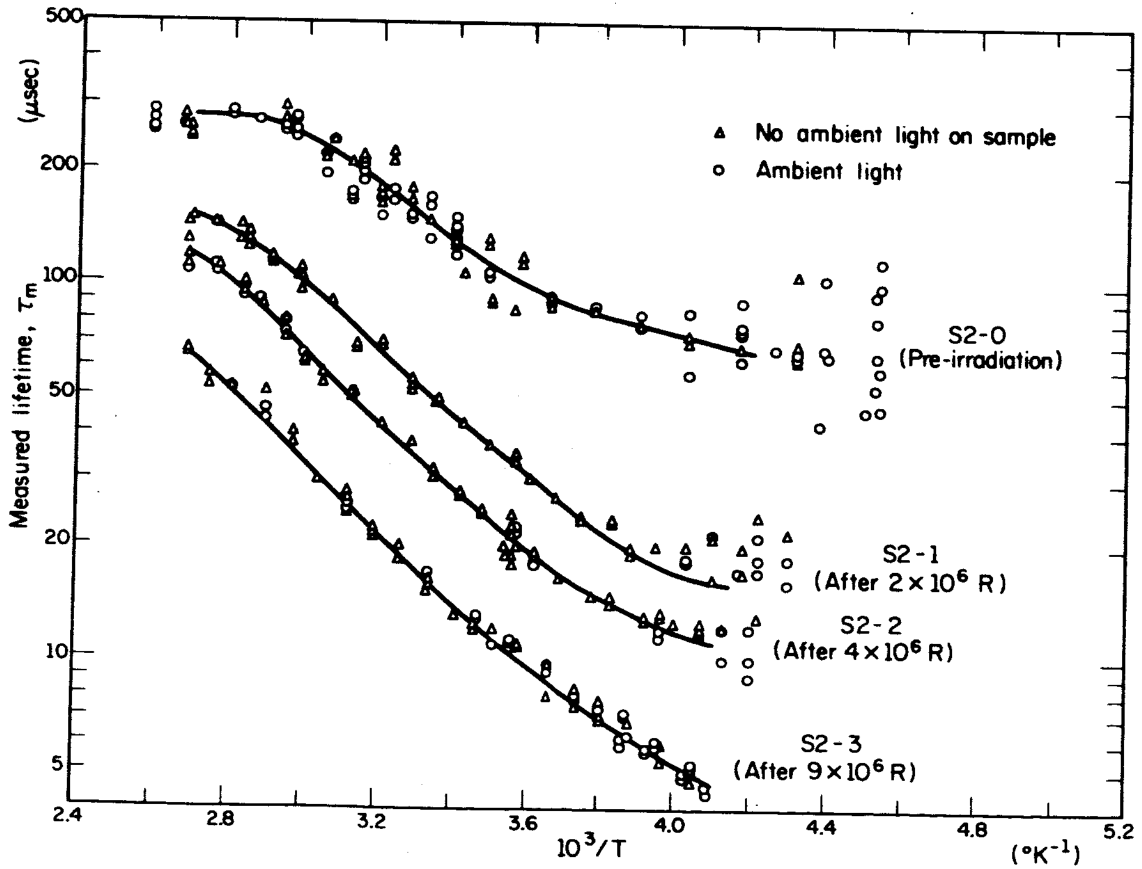


**Figure 29b**

Figure 30. Variation of radiation induced lifetime with reciprocal temperature for 32 ohm-cm p-type pulled silicon. The parameters for the theoretical curves are given in Table 9. The dashed curve for the data set 01-1-0 is the result of the PFZ-1 fit, and the solid curve is the result of the PP-1 fit. For the data set 01-2-0, the solid curve is the result of the NFZ-1 fit, and the dashed curve the result of the second PP-2 fit, in which certain parameters were fixed at the values determined in the analysis of the S2 data and which should be applicable for all p-type pulled silicon.

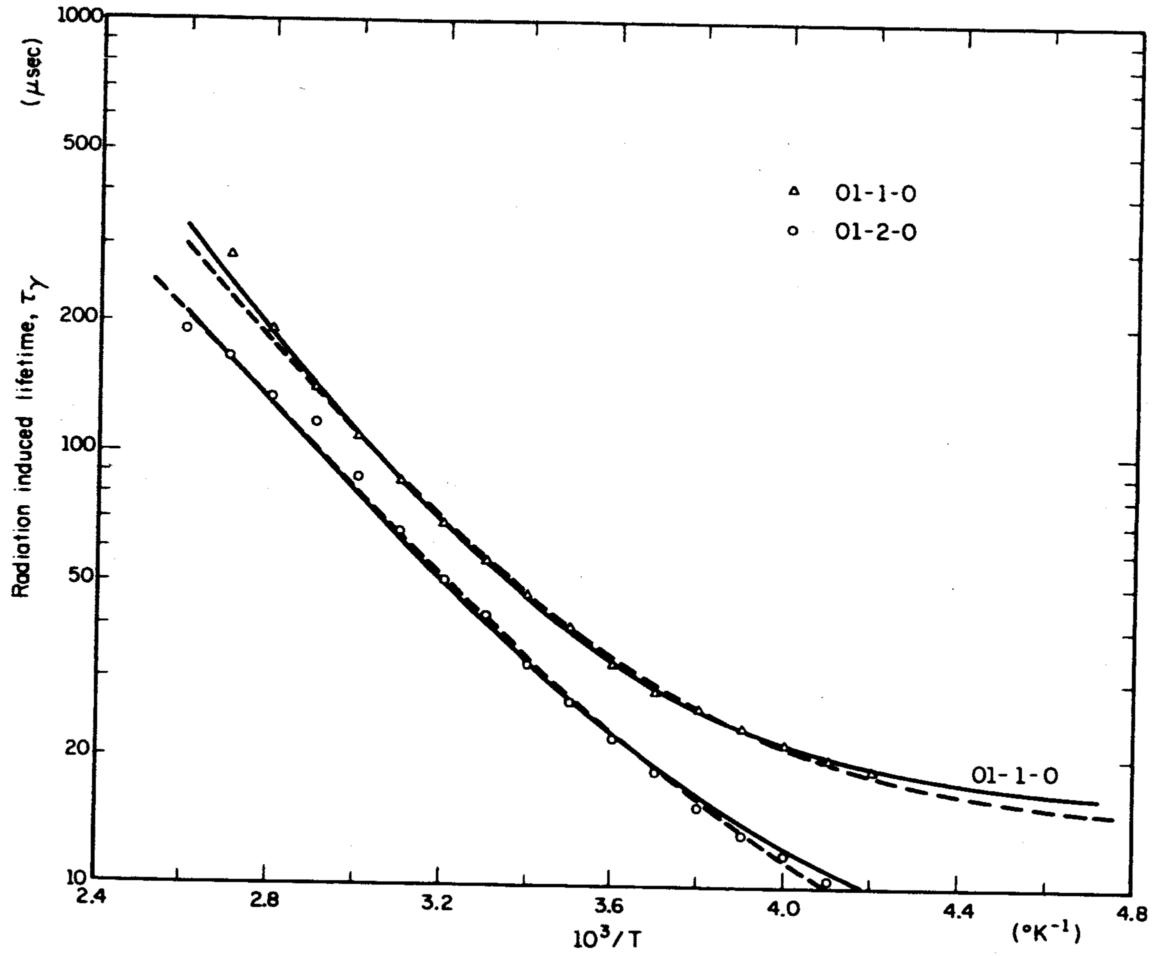


Figure 30

Figure 31. Variation of lifetime with reciprocal temperature in 50 ohm-cm p-type pulled silicon. (a) Radiation induced lifetime. The theoretical curve resulted from an NFZ-1 fit. The parameters are given in Table 9. (b) Measured lifetime. The data points for the radiation induced lifetime were obtained from points from the hand-drawn curves at evenly spaced values of $10^3/T$ and formula 3.3. The dashed pre-irradiation curve was used to obtain the points shown in Figure 32a. The solid curve was used for the PP-2 fit listed in the table, and also for an NFZ-1 fit that differed little from the one listed. A -0 has been omitted from the radiation induced lifetime data set designation.

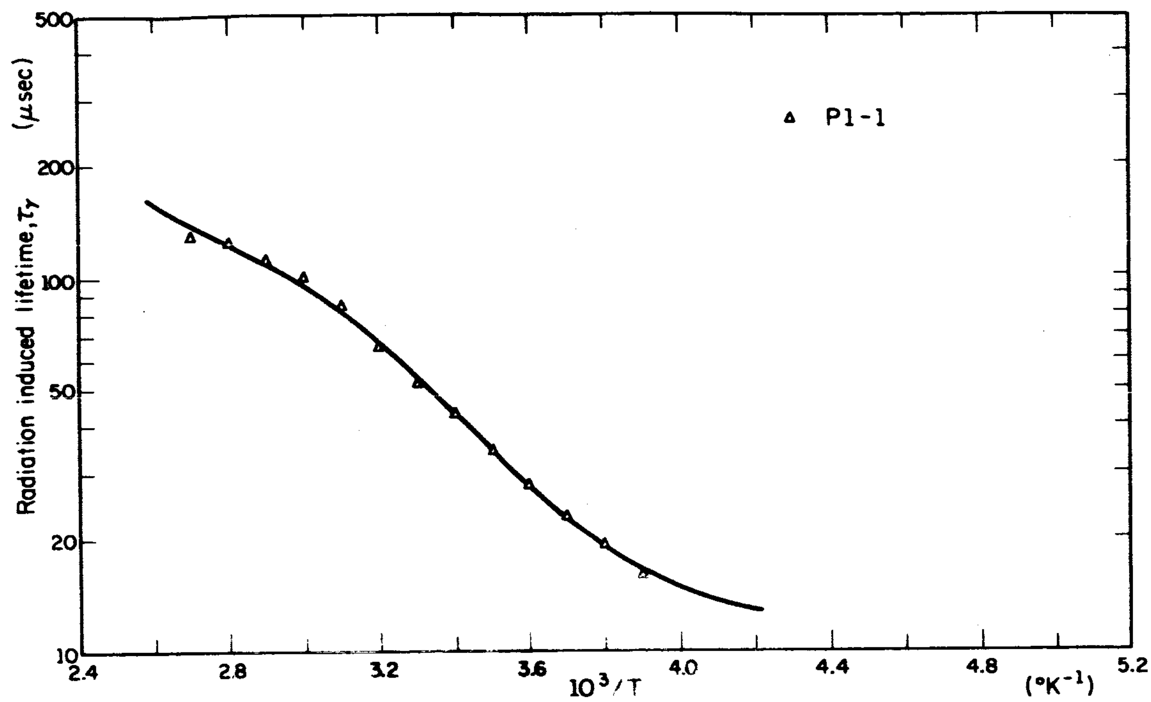


Figure 31a

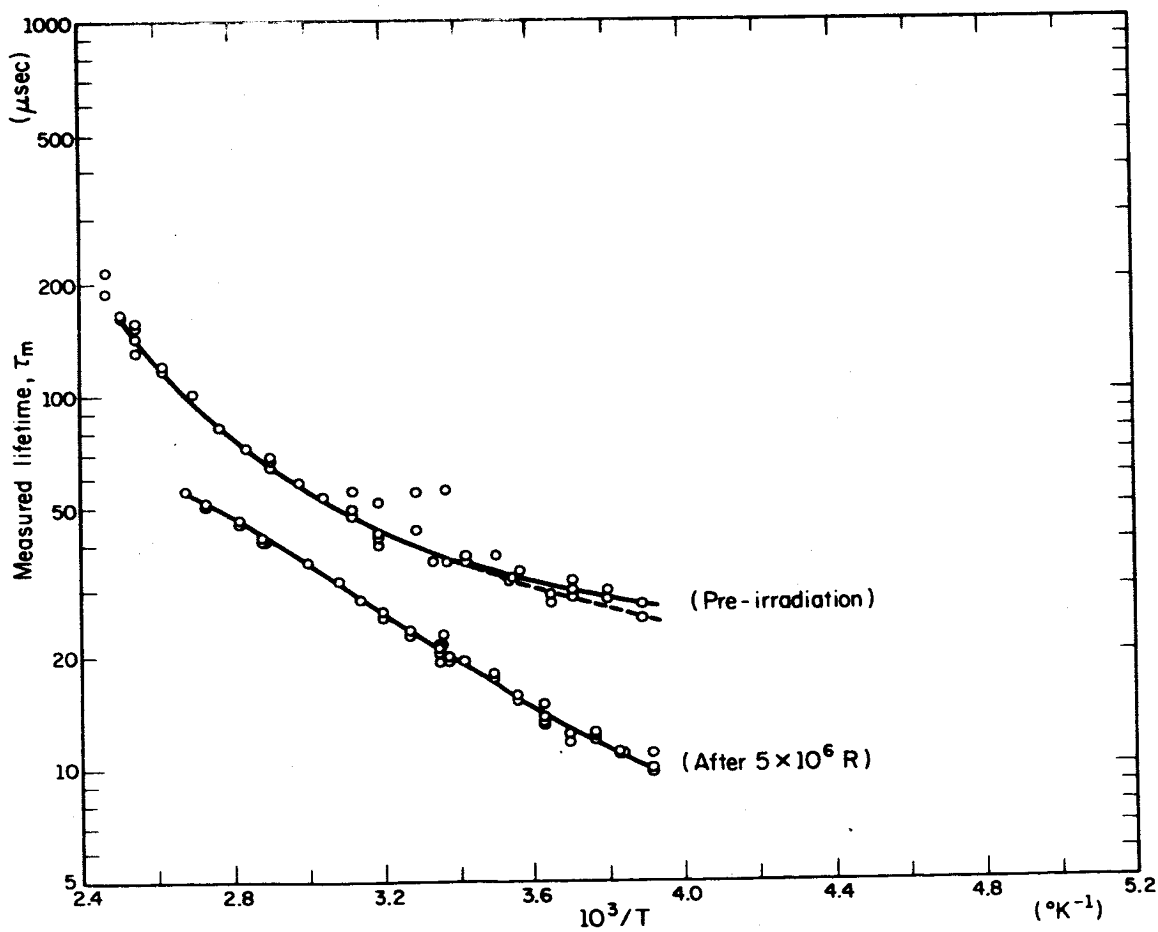


Figure 31b

Figure 32. Variation of radiation induced lifetime with reciprocal temperature for 250 ohm-cm p-type pulled silicon. The twin set of points for R2-1-0 resulted from two choices for the pre-irradiation curve. Fits were tried to the two data sets but were regarded as worthless because of the great difference in results.

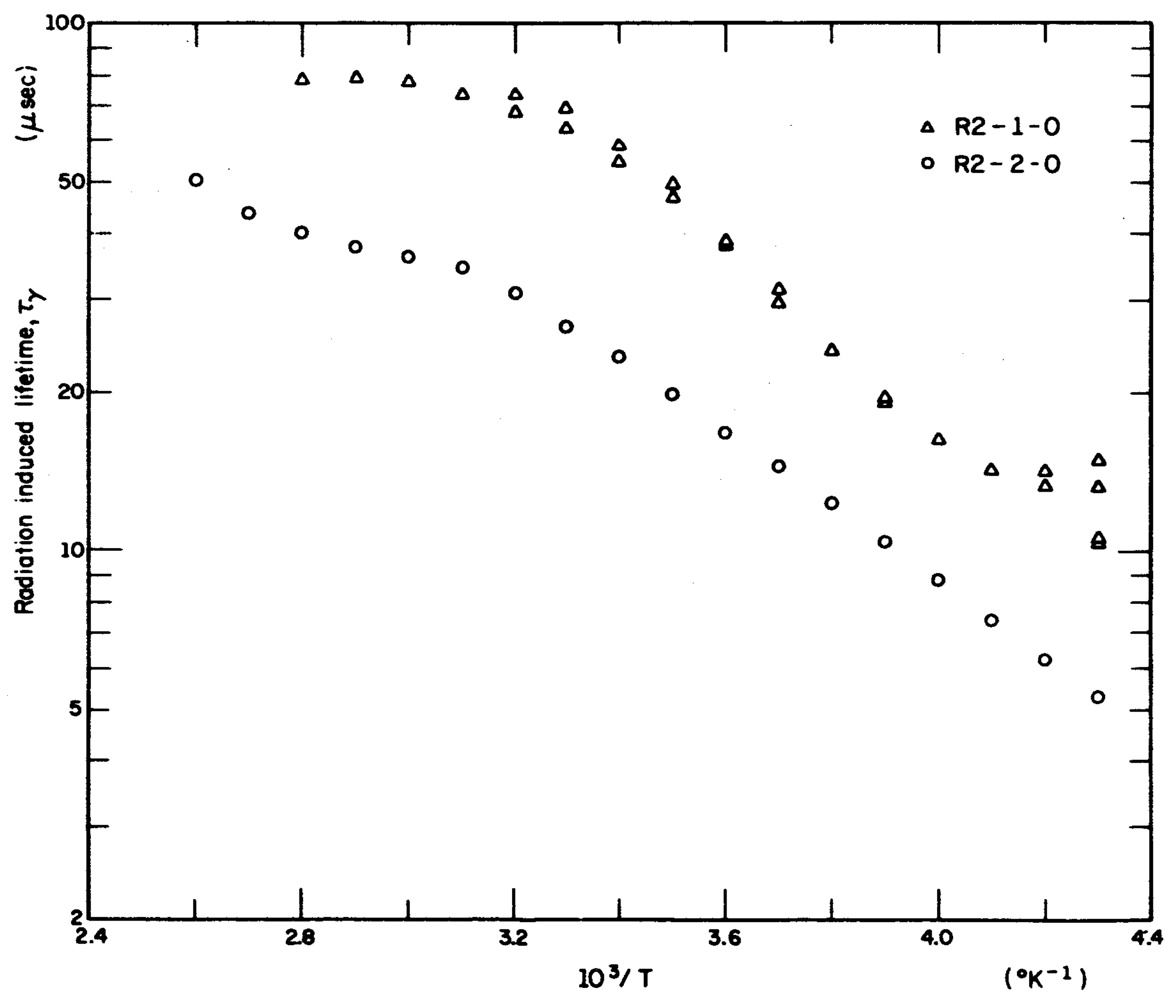


Figure 32

valence band fit, the parameter $A_2$, which averaged 9.9, computed from the values in Table 9, for the S2 data sets, should be equal to $\ln[N_v(10^3/T)^{1.5}/(\omega N_a)]-\beta$. Using the value of $\ln[N_v(10^3/T)^{1.5}/N_a]$ of 10.7 obtained from the published value of $N_v$ and the value of $N_a$ obtained from the resistivity measurement and the hole mobility determined by Morin and Maita, the factor $\beta + \ln\omega$ is 0.8. If $\omega$ is two, $\beta$ becomes 0.11, and if $\omega$ is 1/2, $\beta$ is 1.5. In either case the level moves toward midgap as the temperature increases. Baicker[35] reported a level at $E_v + 0.17$ev in p-type silicon with $\tau_{p_o}/\tau_{n_o} = 12$ as determined by injection level measurements. Since $\tau_{p_o}/\tau_{n_o} \approx \sigma_n/\sigma_p$, it appears that the level has either neutral and positive, or positive and double positive charge states. If only silicon atoms are present in the vicinity of the defect, then the first set of charge states would correspond to $\omega = 2$, and the second set to $\omega = 1/2$. However, neither these nor Baicker's results give any indication of the nature of the defect, so that $\omega$ could have either value.

If the shallow level lies in the upper half of the gap, $A_2$ is given by $A_2 = \ln(\tau_{p_o}/\tau_{n_o}) + \beta + \ln\omega + \ln[N_c(10^3/T^{1.5}/N_a]$, and since $N_c/N_v \approx e$, the last quantity in the preceding expression has the value 11.7. If the defect is the A center, then the factor $\omega e^{\beta}$ should have the value reported by Wertheim[21], and by Sonder and Templeton[22] of 1/4, which would make $\tau_{n_o}/\tau_{p_o} \approx \sigma_p/\sigma_n = 1.4$ for a defect known to have neutral and negative charge states. Baicker[35] and Galkin, et. al.[33] both report values of $\sigma_p/\sigma_n$ of about 20 for the A center. Only if the value of $\omega e^{\beta}$ is assumed to be 4 instead of 1/4 will the capture cross-section have a reasonable value. When PP-1 fits were used, which provided for the temperature variation of $\sigma_n$ found

Table 9

Computer Results for p-type Pulled Silicon

| Sample | $A_1(Q)$ | $A_2(Q)$ | $A_3(Q)$ [a] | $A_4(Q)$ | $A_5(Q)$ | $A_1(P)$ | $A_2(P)$ | $A_3(P)$ [a] | Fit | $\chi^2$ | pts | $\ln[N_v(\frac{10^3}{T})^{3/2}/N_A]$ |
|---|---|---|---|---|---|---|---|---|---|---|---|---|
| S2-1-0 | 15.11 | 11.79 | .175* | 9.52 | 2.96 | | | | PP-1 | 11.93 | 17 | 10.7 |
| S2-1-0 | 15.18 | 10.00 | .189 | | | | | | PFZ-1 | 8.48 | 16 | 10.7 |
| S2-2 | 8.23 | 11.314 | .175* | 10.88 | 3.50 | | | | PP-1 | 16.52 | 19 | 10.7 |
| S2-2-0 | 8.34 | 11.31 | .175 | 10.88 | 3.50 | | | | PP-1 | 5.45 | 17 | 10.7 |
| S2-1-2 | 17.89 | 12.09 | .175* | 12.13 | 3.88 | | | | PP-1 | 96.92 | 19 | 10.7 |
| S2-3-0 | 2.62 | 10.35 | .167 | 10.91 | 3.54 | | | | PP-1 | 2.264 | 15 | 10.7 |
| S2-3-0 | 2.61 | 10.02 | .180 | | | | | | PFZ-1 | 2.96 | 15 | 10.7 |
| S2-2-3 | 5.27 | 9.76 | .176 | | | | | | PFZ-1 | 24.06 | 28 | 10.7 |
| S2-2-3 | 3.25 | 9.97 | .167 | | | | | | PFZ-1 | 12.11 | 15 | 10.7 |
| 01-1-0 | 15.09 | 11.06 | .164 | 11.5* | 3.46* | | | | PP-1 | 1.61 | 13 | 11.7 |
| 01-1-0 | 13.61 | 10.09 | .186 | | | | | | PFZ-1 | 3.44 | 13 | 11.7 |
| 01-2'-0 | 7.8 | 5.67 | .374 | 12.04 | 3.16 | 421 | 13.0* | .56* | PP-2 | 4.70 | 16 | 11.7 |
| 01-2'-0 | 5.93 | 10.27 | .175 | | | 2062 | 12.0* | .45* | NFZ-1 | 22.65 | 16 | 11.7 |
| 01-2'-0 | 3.60 | 11.38 | .156 | 10.90* | 3.50* | 8080 | 12.0* | .50* | PP-2 | 17.87 | 16 | 11.7 |
| P1-1-0 | 1.107 | 12.64 | .175* | 11.5* | 3.46* | 260 | 14.0* | .56* | PP-2 | 15.09 | 13 | 12.2 |
| P1-1-0 | 138 | 14.0* | .46* | | | 12.14 | 15.85 | .32 | NFZ-1 | 5.91 | 13 | 12.2 |

*Fixed parameter

[a] energy separation from nearest band edge in ev.

by Galkin, the capture cross-section ratio as calculated from the computer results ranged between 2.5 and 3.5, using the value of $\omega e^{\beta}$ reported for the A center. Thus the analysis indicates that for reasonable capture cross-section values, the level must have a value of $\omega e^{\beta}$ different than that of the A center, if it is to lie close to the conductor band. In view of the agreement of the several authors upon the reported value of $\omega e^{\beta}$ for this defect, it seems unlikely that they are wrong, and thus it must be concluded that if the defect level lies in the upper half of the gap, the defect is not the A center.

The data set O1-1-0 was fit by PFZ-1 to give $A_2 = 10.09$. For a valence band fit, this gives $\ln\omega + \beta = 1.6$, and if $\omega = 2$, $\beta$ becomes +0.9, somewhat larger than the value obtained for sample S2. For an A center conduction band fit, the ratio $\tau_{n_o}/\tau_{p_o}$ is 3.7, still rather low compared to earlier reports. The remarks made earlier about the factor $\omega e^{\beta}$ apply here also. When a PP-1 fit was made to the data, the value of $\tau_{n_o}/\tau_{p_o}$ was found to be about 21, in agreement with Galkin. A PP-2 fit to the data set O1-2-0, which appeared to have two levels instead of the one in O1-1-0, gave ratios of $\tau_{n_o}/\tau_{p_o}$ between 3.6 and 4.5, which does not agree with the O1-1-0 results but agrees with the S2 results. An NFZ-1 fit to the data set O1-2-0 indicated that the shallow level was closest to the valence band with $\omega = 2$ and $\beta = +.74$. The deep level in the PP-2 and NFZ-1 fits was fixed arbitrarily to have approximately the behavior indicated by the R2 data sets.

Only one irradiation was performed on sample P1. A PP-2 fit to the resulting data set with the energy level fixed at $E_c - 0.175$ resulted in a very small value of 1.32 for the ratio $\sigma_p/\sigma_n$. For the NFZ-1 fit, the

energy level was not fixed, and the computer results gave an energy separation of 0.32ev from a band edge. For a valence band fit, $\beta + \ln\omega$ was -3.65, requiring a very large temperature dependence. For a conduction band fit, the computer results required $\omega(\tau_{p_o}/\tau_{n_o})e^{\beta} = 14.2$. If $\omega$ is taken as 1/2 with $\beta$ equal to zero, then $\sigma_n/\sigma_p$ is about 30. This would indicate an entirely different level than that seen in sample S2 or O1. This difference of behavior may not be real, and may be due to trapping, contact difficulties or differences in the annealing behavior of the materials.

The results of irradiation of sample R2 indicate that the effects mentioned above can indeed affect the lifetime. The data sets R2-1-0 and R2-2-0 agree qualitatively only, as seen by the difference in the slopes of the lifetime at low temperature (Figure 32). It appeared that some annealing of the lifetime occurred in this sample at temperatures near 100°C, while no annealing was seen in sample S2. As a result of the differences in the data sets for R2, no computer analysis was done. The low temperature behavior of R2 appeared to be compatible with that of samples S2 and O1.

It then appears, that with the exception of sample P1, the observed lifetime temperature dependence in p-type pulled silicon can be described by two sets of levels, one near midgap, and one probably located 0.18ev from the valence band edge. The same deep level was seen in sample P1, and it appeared that all the samples could be described fairly well by the shallow level nearer the conduction band, if the defect had a spin degeneracy-temperature coefficient product markedly different from that reported for the A center.

The recent luminescence data of Spry[67], taken on material from boule R, can be interpreted equally well for the shallow level to be near the conduction and/or the valence band. On the basis of available data, it is not possible to explain why the A center is not seen in this type of material, except that other defects with more favorable values of capture cross-sections have introduction rates as large as or larger than the introduction rate of the A center.

D. Boron Doped Float-Zoned Silicon

Except for samples from boule E, there was no evidence of the 0.18ev level in the p-type float-zoned crystals. The data sets of samples E3, E4, and E5 (Figure 33) resemble those of sample O1 (Figure 30). Since trapping appeared to affect the lifetime at low temperature in the E samples, it was felt that the average lifetime calculated from the data sets E3-1-0 and E4-2-0 would be more representative of the material than either set alone. An NFZ-1 fit was made to the averaged points, and the results are listed in Table 10, along with the computer results for the other p-type float-zoned data sets. The result for the shallow level was in complete agreement with the results on samples S2 and O1. Although the theoretical curve is not shown in Figure 33, it is pertinent to remark that the measured slope of the curve was 0.11ev, indicating that all the data sets for the E samples are in agreement with the computer calculation.

The results on the other samples, while quite similar qualitatively (Figures 34-37), do not show the agreement seen in the n-type float-zoned samples. The M and U data sets exhibit an apparent temperature dependence of $\tau_{n_o}$, and one of the W1 data sets shows such an effect, as does the W2

Figure 33. Variation of radiation induced lifetime with reciprocal temperature in 20 ohm-cm p-type float-zoned silicon. The lines were drawn through the points to obtain the slopes listed. A -0 has been omitted from all data set designations.

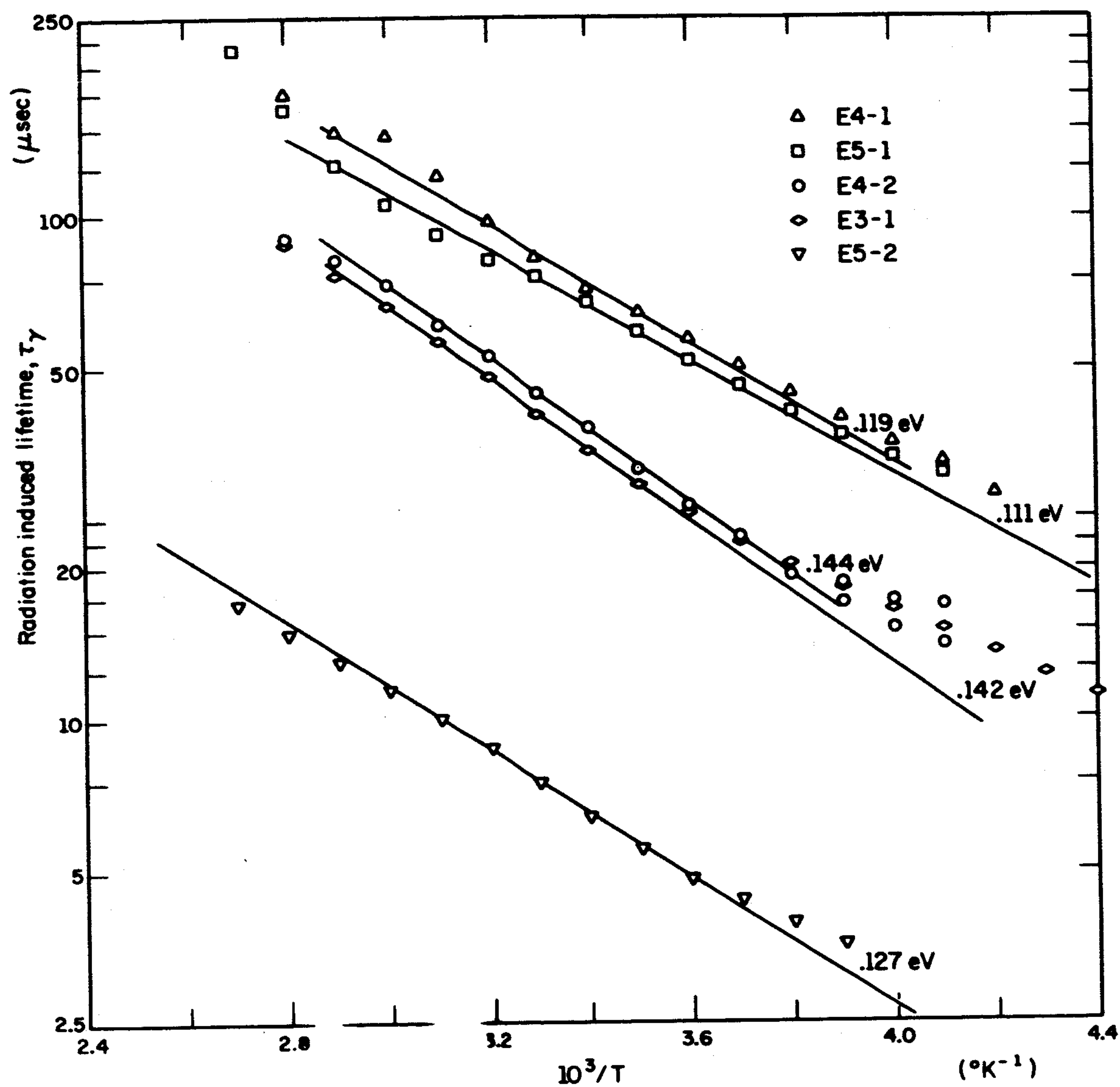


Figure 33

Table 10

Computer Results for p-type Float-zoned Silicon

| Sample | $A_1$ | $A_2$ | $A_3$ [a] | $A_4$ | Fit | $\chi^2$ | Points | $A_{20}$ [b] |
|---|---|---|---|---|---|---|---|---|
| {E4-2-0<br>E3-1-0} | P 183<br>Q 9.71 | 10.8*<br>10.18 | .46*<br>.1784 | | NFZ-1 | 2.8 | 17 | 11.40 |
| M3-1-0 | 11.52 | 10.97 | .33 | -1.0 | PFZ-2 | 1.20 | 21 | 12.65 |
| M4-1-0 | 26.96 | 18.20 | .56* | -1.10 | PFZ-2 | 11.87 | 14 | |
| F3-1-0 | 35.7 | 11.07 | .311 | | PFZ-1 | .383 | 12 | 13.6 |
| F3-2-0 | 21.1 | 10.57 | .302 | | PFZ-1 | 1.09 | 15 | 13.6 |
| F3-1-2-0 | 50.8 | 8.10 | .236 | | PFZ-1 | 1.68 | 15 | 13.6 |
| F3-3-0 | 9.94 | 11.92 | .339 | | PFZ-1 | 1.23 | 14 | 13.6 |
| F3-4-0 | 5.38 | 9.06 | .250 | | PFZ-1 | .164 | 12 | 13.6 |
| F4-1-0 | 65.7 | 13.70 | .40 | | PFZ-1 | .40 | 11 | 13.6 |
| F4-A1-0 | 85.8 | 10.78 | .307 | | PFZ-1 | 1.25 | 13 | 13.6 |
| F4-A2-0 | 1445. | 21.10 | .68 | -1.0* | PFZ-2 | 7.66 | 11 | 13.6 |
| F4-A1-A2 | 106.1 | 10.83 | .306 | | PFZ-1 | 2.02 | 11 | 13.6 |
| F4-A1-A2 | 109.4 | 15.1† | .423 | 2.5 | PFZ-3 | 1.92 | 11 | 13.6 |
| U1-1-0 | 38.6 | 13.20 | .355 | -.655 | PFZ-2 | 1.33 | 13 | 15.4 |
| U1-1-2 | 27.6 | 18.55 | .498 | | PFZ-1 | 5.70 | 12 | 15.4 |
| U2-1-0 | 15.0 | 12.57 | .328 | -.5* | PFZ-2 | 1.94 | 14 | 15.4 |
| U2-2-0 | 5.66 | 12.44 | .318 | | PFZ-1 | .37 | 10 | 15.4 |
| W1-1-0 | 17.91 | 16.42 | .416 | | PFZ-1 | 3.05 | 16 | 16.8 |
| W1-2-0 | 26.3 | 16.57 | .432 | -.5* | PFZ-2 | 2.28 | 15 | 16.8 |

* Parameters fixed.

† normalized at $10^3/T = 3.4$

a energy separation from nearest band edge in ev.

b $A_{20} = \ln[N_v(10^3/T)^{1.5}/N_a]$

Figure 34. Variation of radiation induced lifetime with reciprocal temperature in 70 ohm-cm p-type float-zoned silicon. The parameters for the theoretical (heavy line) curve are given in Table 10. The light line was drawn through the data points to obtain the slope listed. A -0 has been omitted from all data set designations.

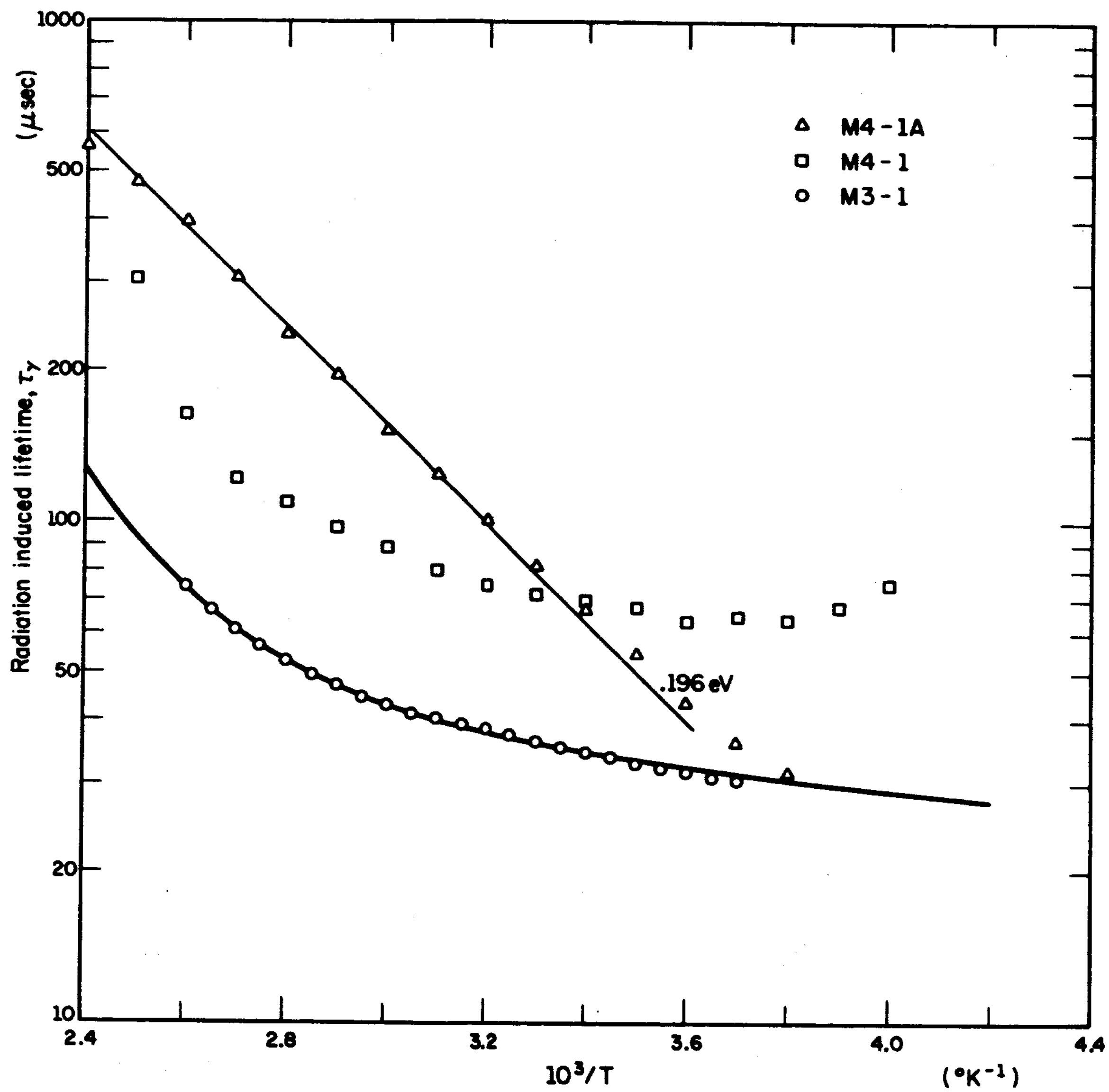


Figure 34

Figure 35. Variation of radiation induced lifetime with reciprocal temperature in 200 ohm-cm p-type float-zoned silicon. A -0 has been omitted from the data set F4-A1-0. The parameters for the theoretical curves are given in Table 10.

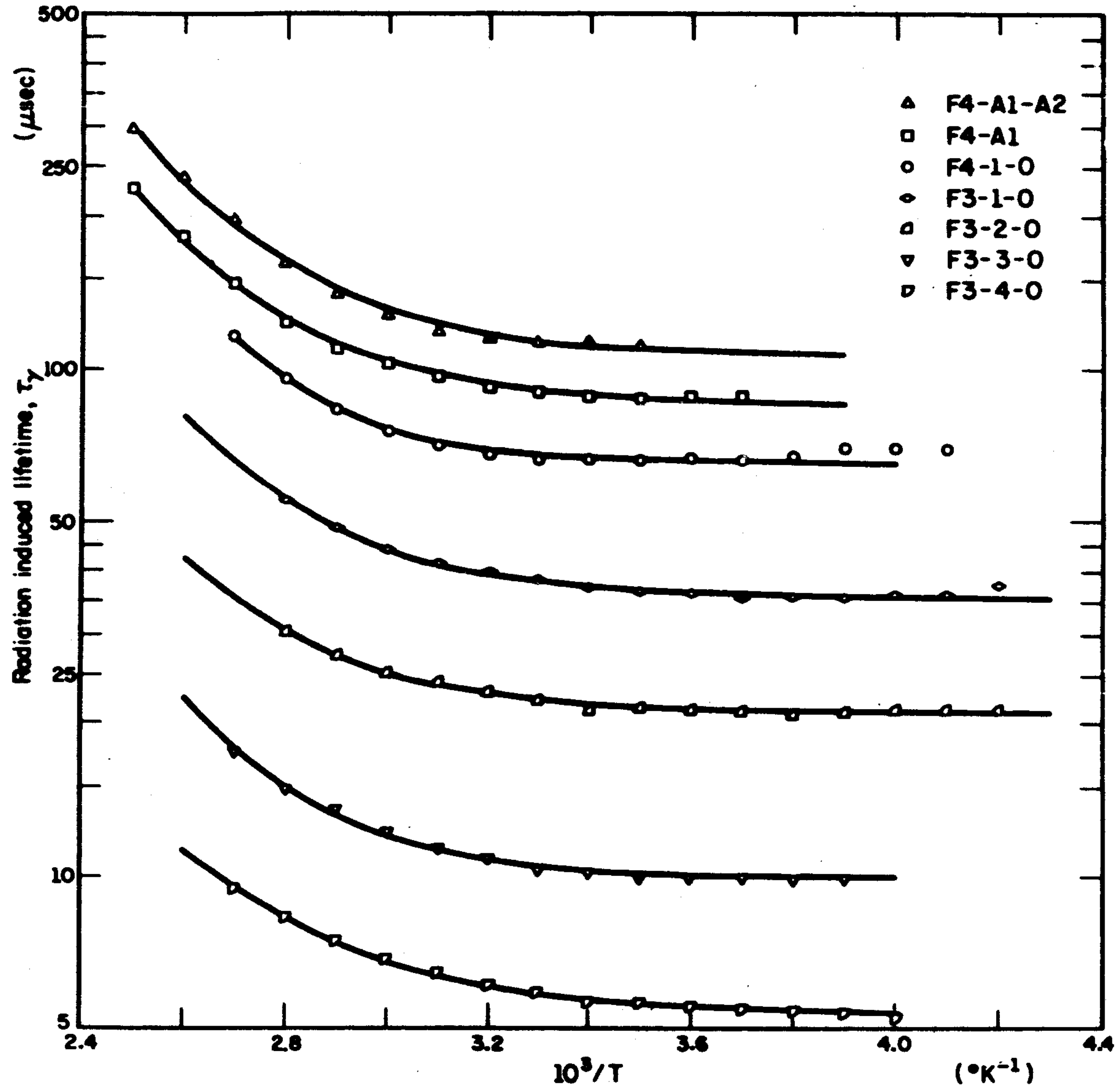


Figure 35

Figure 36. Variation of radiation induced lifetime with reciprocal temperature in 1200 ohm-cm p-type float-zoned silicon. The parameters for the theoretical curves are given in Table 10.

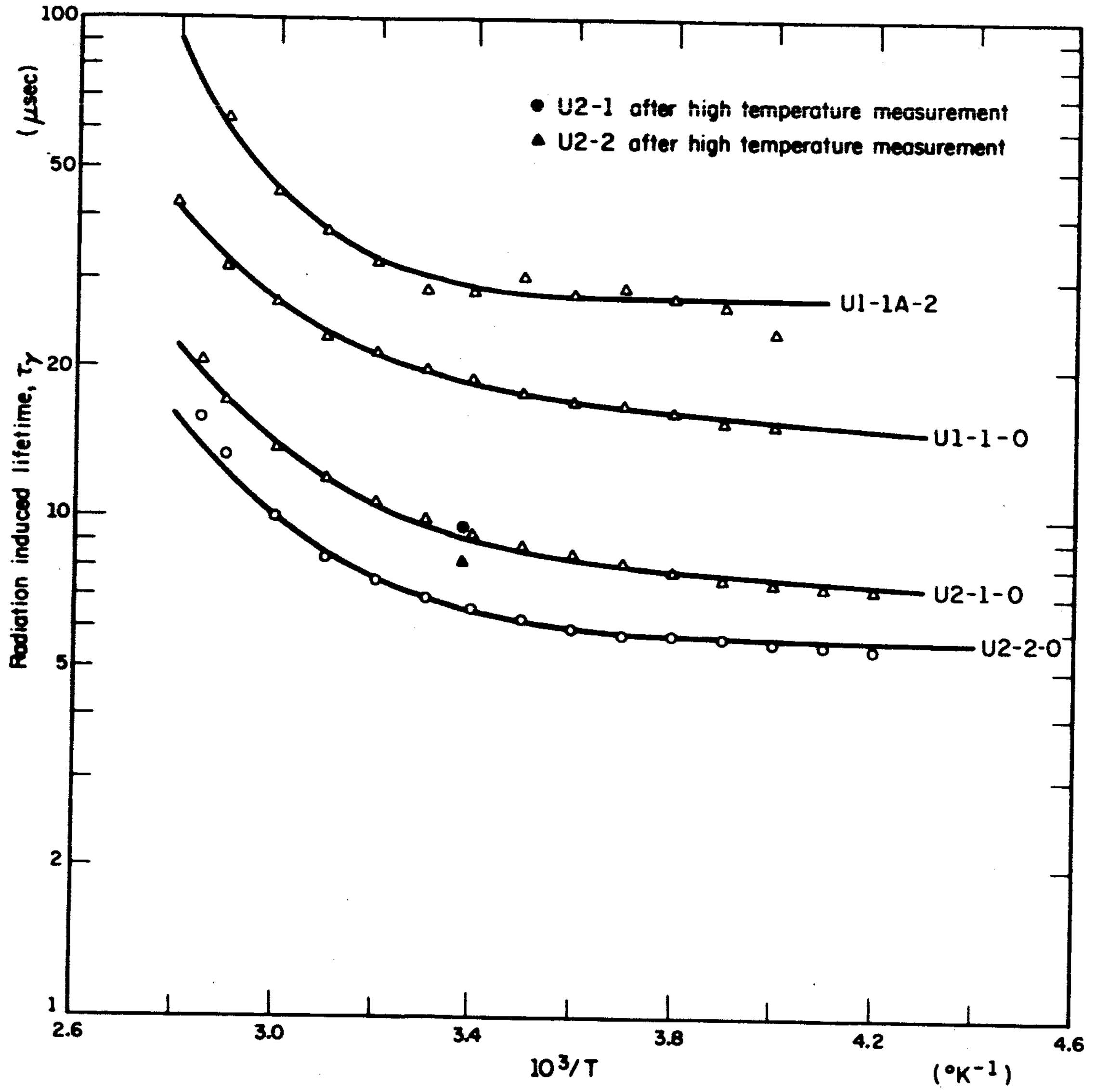


Figure 36

Figure 37. Variation of radiation induced lifetime with reciprocal temperature in 5000 ohm-cm p-type float-zoned silicon. The parameters for the theoretical curves are given in Table 10. A -0 has been omitted from all data set designations.

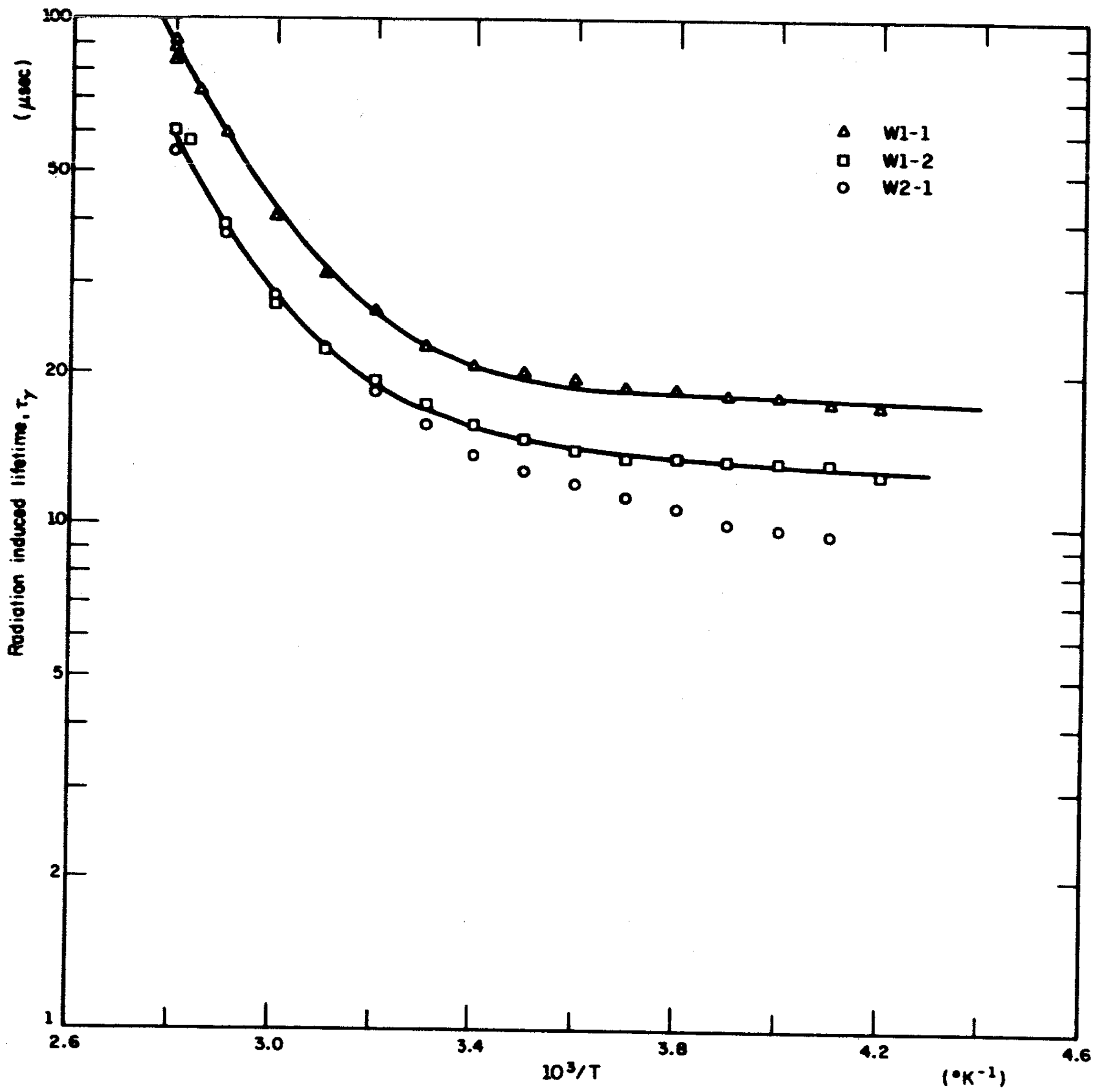


Figure 37

data set. None of the F data sets show any such temperature dependence. An examination of the computer parameters (Table 10) shows that the temperature coefficient varied between 1/2 and 1. With the exception of the W data sets and the F4-1-0 set, the p-type float-zoned data sets indicate a level approximately 0.3ev from the conduction band edge. This value is not very certain, since the annealing of defects prevents the measurements from being taken at temperatures sufficiently high to observe the increase in the lifetime. In such circumstances, both the energy separation and the parameter $A_2$ in the PFZ fits were greatly susceptible to slight errors in measurement. If the lifetimes were measured at a temperature at which the sample had annealed slightly, the effect would be to increase the value of the energy separation from what it would have been had that data point not been used in the calculation. Such is perhaps the case for the data set F4-1-0, since the F4 data set does not agree with any of the other F data sets, and for the U1-1A-2 set since the $U_2$ data sets indicates that annealing takes place at very low temperatures in the U samples (Figure 37).

Since the U1-1A and U1-2 data sets were not well separated, subtraction errors in U1-1A-2 are large, which might account for the different computer results for this data set. With these remarks in mind, the U and M data sets agree well, and except for the temperature dependence of $\tau_{n_o}$, they agree well with the F data sets, in indicating the previously mentioned level in the upper half of the gap. The parameter $A_2$ for these fits indicates that the level has the capture cross-section for holes larger than for electrons by a factor of 15 to 40. Since the level definitely was in the upper half of the gap, a PFZ-3 fit, which allowed a temperature

variation in $\tau_{p_o}$, was fit to the data set F4-A1-A2, and the computer output indicated that the level could be at $E_c - 0.42$ev if $\tau_{p_o}$ had a temperature dependence of $T^{-2.5}$, as well as its PFZ-1 calculated position of $E_c - 0.3$ev. This level seemed to anneal simply in sample F4, with no new defects formed. In sample M4, however, a reverse anneal was seen, and after the anneal the lifetime appeared to be controlled by defects with an energy level separated by about 0.16ev from a band edge (Figure 34). Whether this is the same level as seen in the E samples and the p-type pulled samples cannot be determined since the contacts were of such poor quality after the anneal that the lifetime could not be measured to temperatures low enough that the lifetime reached its minimum value. The decrease of slope at high temperatures indicates that not all of the $E_c - 0.3$ev defects have annealed out.

The W samples showed somewhat anomalous behavior, which tends to discredit the level at $E_v + 0.42$ev indicated by the computer calculations. Severe trapping was seen in these samples at all times, and to obtain unique lifetimes it was necessary to use d.c. light injection for all measurements. Since this material was of very high resistivity, this procedure can easily lead to injection level effects which would tend to invalidate the interpretation of the lifetimes as based upon the simple Shockley-Read theory. In addition, the effect of very small gamma ray doses on the material was to change its resistivity from $\approx$ 6300 ohm-cm to $\approx$ 4800 ohm-cm. The usual effect of irradiation upon silicon is to increase the resistivity due to carrier removal by defects created. In this material the same change in resistivity was seen for the first dose in both

samples, even though that dose was $2.5 \times 10^6$ R in W1 and $5 \times 10^6$ R in W2.

It is of interest to attempt to correlate the effects of radiation upon the p-type materials by using the lifetime-flux products determined in one growth method to predict lifetime values for other type of material, assuming equal defect introduction rates. The product $\tau\phi$ was about 70sec-Roentgens for samples M, F, U, and W, at $10^3/T = 3.4$. Using this value for the p-type pulled samples, the lifetimes calculated for the doses received by various crystals are less than the lifetimes measured, and of course the temperature dependence is much different. If now the lifetime-flux product of 216sec-Roentgens of sample S2 (at $10^3/T = 3.0$) is used to calculate the lifetime in the float-zoned material, taking into account the differences in resistivity as was done for the A center in n-type material, the result is that except for samples E and M, the calculated lifetime is several orders of magnitude greater than the measured lifetime. For the data set M3-1-0, the calculated shallow level lifetime is 756 microseconds, compared to the measured lifetime of 43 microseconds, so that except at low temperatures, the shallow level should not affect the lifetime of the M crystals noticeably.

It is not certain that the $E_c$ - 0.3ev level seen in the float-zoned materials is the same as the deep level seen in the pulled p-type crystals. Assuming that they are the same, it thus appears that the presence of the much larger concentrations of oxygen in the pulled p-type materials inhibits the formation of the defects seen in the float-zoned materials. This could be done by any type of complex involving oxygen and the primary defects, presumably vacancies, which form the defects having levels at

$E_c$ - 0.3ev, and they need not be active in the recombination process. If they were not, this would account in part for the greater resistance to lifetime degradation seen in the p-type materials.

# V. SUMMARY AND RECOMMENDATIONS

The conclusions made on the basis of the experimental results may be summarized as follows:

1) The recombination centers active in n-type silicon are not the same as those active in p-type silicon. In each type of material the recombination process could be described by two sets of recombination centers.

2) The recombination centers dominant in float-zoned material appeared to anneal at lower temperatures than those dominant in crucible grown material, although in some of the n-type float-zoned materials the defects appeared to be equally stable at the temperatures investigated.

3) The defects controlling the lifetime in n-type material appeared, by comparison to earlier work, to be the A and E centers, located at $E_c$ - 0.17 and $E_c$ - 0.4 ev, respectively. The deep level showed partial anneal in one sample at 145°C, indicating that either two or more types of defects, with energy levels at the same position, were present or that some of the E centers annealed at lower temperatures than the rest. Anneal of the A center was seen at 250°C, in material in which the deep level did not anneal at this temperature.

4) The defects controlling the lifetime in p-type material appeared to have energy levels at $E_v$ + .18 ev and at $E_c$ - .3 ev. The first level might equally well be located at $E_c$ - .18 ev, but the parameters of the lifetime formula, when compared to the results of the Hall effect measurements of others, suggest that the defect is not the A center. The level at $E_c$ - .3 ev, in contrast to the defects seen in the n-type material and the

$E_v$ + .18 ev level, has not been seen previously. From the lifetime parameters, it appears that the capture cross-section ratio $\sigma_p/\sigma_n$ is about 20. In some cases it appeared that either or both of the capture cross-sections was temperature dependent. In one sample, upon which only one post-irradiation measurement was made, the strongly varying portion of the lifetime appeared to be due to a level at $E_c$ - .3 ev, but with $\sigma_p/\sigma_n$ equal to .03. Since the lifetime data fit nearly as well with the shallow level .18 ev from the conduction band, but with nearly equal capture cross-sections, the position of the level is rather uncertain.

5) There appears to be no strong dependence of the introduction rates for the defects upon resistivity. Oxygen content appeared to have a much larger effect in the p-type than in the n-type silicon in determining which defects controlled the lifetime.

There are several suggestions for further work:

1) Crystals of much lower resistivity should be investigated. This would permit the determination of all the parameters for the shallow level in n-type material, and a better determination in p-type material. It will be necessary to use a different source for the creation of the excess carrier pulse in order to achieve a satisfactory signal to noise ratio.

2) Hall effect studies should be done upon the n-type crystals to determine the magnitude of the hole capture cross-sections of the defects.

3) Higher resistivity p-type float-zoned material should be investigated to obtain a more accurate value of the energy level at $E_c$ - .3 ev. It might be possible to heat-treat boule W to eliminate the traps and the anomalous resistivity change from irradiation.

4) An attempt should be made to determine the introduction rate of A centers into p-type material by some unambiguous procedure. A study of the 12 micron absorption band might prove fruitful.

5) The study of materials doped with substances other than boron or phosphorus should be informative. According to Sonder and Templeton, the E center energy level for phosphorus doped silicon lies deeper than for antimony doped silicon. A change of acceptor dopant would have an effect upon the lifetime if either of the levels seen in p-type silicon involved an acceptor atom.

6) Further work should be done on high resistivity p-type pulled samples to determine if the deep level is the same as in the float-zoned material, and if the level seen in sample P1 is located at $E_c - .3$ or at some other position.

7) A comprehensive study of the thermal annealing of the radiation induced defects would be useful with the crystals already measured. If the defects anneal without the formation of new types of defects, it should be possible to determine the activation energy for disassociation of the defects. If new defects are formed, the measurement of the lifetime with temperature should give information on their position and characteristics.

# APPENDIX I

## LIFETIME IN THE PRESENCE OF TWO TYPES OF MONOVALENT DEFECTS

For a system of two S-R defects the solution for the lifetime will be found according to the method of Wertheim. If the quantities $C_{nj}$, $C_{pj}$, $E_{nj}$, $E_{pj}$, $f_j$, $N_j$, are defined analogously to $C_n$, $C_p$, $E_n$, $E_p$, f, N, for a single type of S-R defects, then the electron, hole, and defect occupancy equations are

$$-\frac{dn}{dt} = \sum_{j=1}^{2} [C_{nj}nN_j(1-f_j) - E_{nj}N_jf_jN_c] \quad (A1.1)$$

$$-\frac{dp}{dt} = \sum_{j=1}^{2} [C_{pj}pN_jf_j - E_{pj}N_j(1-f_j)N_v] \quad (A1.2)$$

$$\frac{df_j}{dt} = \frac{d\delta f_j}{dt} = [C_{nj}n(1-f_j) - E_{nj}f_jN_c] - [C_{pj}pf_j - E_{pj}(1-f_j)N_v] \quad (A1.3)$$

where $n = n_o + \delta_n$, $p = p_o + \delta p$, $f_j = f_{jo} + \delta f_j$, and as before, the zero subscript denotes the thermal equilibrium value. The electrical neutrality equation

$$n - p + \sum_j N_j \delta f_j = 0 \quad (A1.4)$$

can be used in place of one of the two defect occupancy equations.

If we consider the electron equation in the case of thermal equilibrium, and demand that both of the terms are identically zero, implying we do not have a net generation of electrons in one set of defects and a net recombination through the other, then as for the S-R analysis we can relate $C_{nj}$ and $E_{nj}$: $E_{nj} = C_{nj}(n_o/N_c)\frac{(1-f_{jo})}{f_{jo}}$. If we now define $n_j = \frac{n_o(1-f_{jo})}{f_{jo}} = N_c\omega_j \exp[(E_{rj}-E_c)/kT]$ similarly to $n_1$ in the previous treatment, with $E_{rj}$ the defect energy level, and $\tau_{nj} = (N_j\sigma_{nj}v_n)^{-1}$, then the electron equation becomes

$$-\frac{dn}{dt} = \sum_j \left[ \frac{1}{\tau_{nj}} \left[ \frac{\delta n\, n_j}{n_o+n_j} - [\delta n + n_o + n_j]\delta f_j \right] \right] \quad \text{(A1.5)}$$

and similarly the hole equation becomes

$$-\frac{dp}{dt} = \sum_j \frac{1}{\tau_{pj}} \left[\frac{p_j \delta p}{p_o+p_j} + (p_o + p_j + \delta p)\delta f_j\right] \quad \text{(A1.6)}$$

where we have used the fact that $f_{jo} = n_o/n_o+n_j$, $1-f_{jo} = n_j/n_o+n_j$. The differential equation for $N_1\delta f_1 = \delta N_1$ is

$$\frac{dN_1}{dt} = -\frac{1}{\tau_{p_1}}\left[\frac{p_1\delta p}{p_o+p_1} + (p_o+p_1+\delta p)\frac{\delta N_1}{N_1}\right] + \frac{1}{\tau_{N_1}}\left[\frac{n_1\delta n}{n_o+n_1} - \frac{(n_o+n_1+\delta n)\delta N_1}{N_1}\right] \quad \text{(A1.7)}$$

By using Eq. (A1.4) in the form

$$N_2\delta f_2 = \delta p - \delta n - N_1\delta f_1$$

the above equations can be put in the form

$$\frac{d\delta n}{dt} + \left[\frac{1}{\tau_{n_1}}\frac{n_1}{n_o+n_1} + \frac{1}{\tau_{n_2}}\frac{n_2}{n_o+n_2} + \frac{(n_o+n_2+\delta n)}{N_2\tau_{n_2}}\right]\delta n - \frac{1}{\tau_{n_2}}\frac{(n_o+n_2+\delta n)\delta p}{N_2}$$

$$+ \left[\frac{(n_o+n_2+\delta n)}{N_2\tau_{n_2}} - \frac{(n_o+n_1+\delta n)}{N_1\tau_{n_1}}\right]\delta N_1 = 0 \quad \text{(A1.8a)}$$

$$-\left[\frac{p_o+p_2+\delta p}{N_2\tau_{n_2}}\right]\delta n + \frac{d\delta p}{dt} + \left[\frac{p_1}{\tau_{p_1}(p_o+p_1)} + \frac{p_2}{\tau_{p_2}(p_o+p_2)} + \frac{(p_o+p_2+\delta p)}{N_2\tau_{p_2}}\right]\delta p$$

$$+ \left[\frac{(p_o+p_1+\delta p)}{N_1\tau_{p_1}} - \frac{(p_o+p_2+\delta p)}{N_2\tau_{p_2}}\right]\delta N_1 = 0 \quad \text{(A1.8b)}$$

$$-\left[\frac{n_1}{\tau_{n_1}(n_o+n_1)}\right]\delta n + \left[\frac{p_1}{\tau_{p_1}(p_o+p_1)}\right]\delta p + \frac{d\delta N_1}{dt} + \left[\frac{p_o+p_1+\delta p}{N_1\tau_{p_1}} + \frac{n_o+n_1+\delta n}{N_1\tau_{n_1}}\right]\delta N_1 = 0 \quad \text{(A1.8c)}$$

The third order equation

$$[D^3 + pD^2 + qD + r]\delta n = 0 \tag{A1.9}$$

can be formed, whose roots, if real, negative, and distinct are $m_1$, $m_2$, and $m_3$ found by factoring the equation into

$$[D+m_1]\ [D+m_2]\ [D+m_3]\delta n = 0\ . \tag{A1.10}$$

The solution of the equation is then $\delta n = Ae^{-m_1 t} + Be^{-m_2 t} + Ce^{-m_3 t}$. By comparing terms in Eqs. (A1.9) and (A1.10) we see that $p = (m_1+m_2+m_3)$, $q = (m_1m_2+m_2m_3+m_3m_1)$ and $r = m_1m_2m_3$. If we suppose $m_1 \gg m_2 \gg m_3$, then $m_1 \approx p$, $m_2 \approx q/m_1 \approx q/p$, and $m_3 \approx r/q$. If the time constant observed is the longest one, it will be equal to $1/m_3$, or $q/r$. Thus we have the system

$$\begin{vmatrix} (D+a_{11}) & a_{12} & a_{13} \\ a_{21} & (D+a_{22}) & a_{23} \\ a_{31} & a_{32} & (D+a_{33}) \end{vmatrix} \quad \delta n = 0 \tag{A1.11}$$

where the quantities $a_{ij}$ can be found by comparing Eqs. (A1.8) and (A1.11). For this set of equations, the quantities p, q, and r are given by

$$p = (a_{11}+a_{22}+a_{33}) = [\frac{n_1}{\tau_{n_1}(n_o+n_1)} + \frac{n_2}{\tau_{n_2}(n_o+n_2)} + \frac{(n_o+n_2+\delta n)}{N_2\tau_{n_2}}$$

$$+ \frac{p_1}{\tau_{p_1}(p_o+p_1)} + \frac{p_2}{\tau_{p_2}(p_o+p_2)} + \frac{(p_o+p_2+\delta p)}{N_2\tau_{p_2}}$$

$$+ \frac{(p_o+p_1+\delta p)}{N_1\tau_{p_1}} + \frac{(n_o+n_1+\delta n)}{N_1\tau_{n_1}}\ ] \tag{A1.12a}$$

$$q = (a_{11}a_{22}+a_{11}a_{33}+a_{22}a_{33}-a_{13}a_{31}-a_{12}a_{21}-a_{23}a_{32})$$

$$= \frac{1}{\tau_{p_1}\tau_{p_2}}\left[\frac{n_o(p_o+p_1+\delta p)}{N_1(n_o+n_2)} + \frac{n_o(p_o+p_2+\delta p)}{N_2(n_o+n_1)} + \frac{(p_o+p_2+\delta p)(p_o+p_1+\delta p)}{N_1N_2}\right]$$

$$+ \frac{1}{\tau_{p_1}\tau_{n_1}}\left[\frac{n_o(n_o+n_1+\delta n)}{N_1(n_o+n_1)} + \frac{n_1(p_o+p_1+\delta p)}{N_1(n_o+n_1)} + \frac{n_o n_1}{(n_o+n_1)^2}\right]$$

$$+ \frac{1}{\tau_{p_2}\tau_{n_2}}\left[\frac{n_o(n_o+n_2+\delta n)}{N_2(n_o+n_2)} + \frac{n_2(p_o+p_2+\delta p)}{N_2(n_o+n_2)} + \frac{n_o n_2}{(n_o+n_2)^2}\right]$$

$$+ \frac{1}{\tau_{n_1}\tau_{p_2}}\left[\frac{n_2(n_o+n_1+\delta n)}{N_1(n_o+n_2)} + \frac{n_1(n_o+n_2+\delta n)}{N_2(n_o+n_1)} + \frac{(n_o+n_2+\delta n)(n_o+n_1+\delta n)}{N_1N_2}\right]$$

$$+ \frac{1}{\tau_{p_1}\tau_{n_2}}\left[\frac{n_o(n_o+n_2+\delta n)}{N_2(n_o+n_1)} + \frac{n_2(p_o+p_1+\delta p)}{N_1(n_o+n_2)} + \frac{n_o n_2}{(n_o+n_2)(n_o+n_1)}\right.$$

$$\left.+ \frac{(n_o+n_2+\delta n)(p_o+p_1+\delta p)}{N_1N_2}\right] + \frac{1}{\tau_{p_2}\tau_{n_1}}\left[\frac{n_o(n_o+n_1+\delta n)}{N_1(n_o+n_2)} + \frac{n_1(p_o+p_2+\delta p)}{N_2(n_o+n_1)}\right.$$

$$\left.+ \frac{n_o n_1}{(n_o+n_2)(n_o+n_1)} + \frac{(n_o+n_1+\delta n)(p_o+p_2+\delta p)}{N_1N_2}\right] \quad \text{(A1.12b)}$$

and

$$r = (a_{11}a_{22}a_{33}+a_{12}a_{23}a_{31}+a_{13}a_{32}a_{21}-a_{11}a_{32}a_{23}-a_{22}a_{13}a_{31}-a_{33}a_{12}a_{21})$$

$$= \frac{1}{\tau_{p_1}\tau_{p_2}\tau_{n_1}}\left[\frac{(p_o+p_1+\delta p)}{n_1}\,\frac{n_o}{(n_o+n_2)}\,\frac{n_1}{(n_o+n_1)} + \frac{(p_o+p_1+\delta p)(p_o+p_2+\delta p)n_1}{N_1N_2(n_o+n_1)}\right.$$

$$\left.+ \frac{n_o(p_o+p_2+\delta p)(n_o+n_1+\delta n)}{(n_o+n_1)N_1N_2} + \frac{n_o n_1(p_o+p_2+\delta p)}{(n_o+n_1)^2\,N_2}\right] + \frac{1}{\tau_{p_1}\tau_{p_2}\tau_{n_2}}$$

$$\left[\frac{(p_o+p_1+\delta p)n_o n_2}{N_1(n_o+n_2)^2} + \frac{(p_o+p_1+\delta p)(p_o+p_2+\delta p)n_2}{N_1N_2(n_o+n_2)} + \frac{(p_o+p_1+\delta p)(n_o+n_2+\delta n)n_o}{N_1N_2(n_o+n_2)}\right.$$

$$+ \frac{n_o n_2 (p_o+p_2+\delta p)}{(n_o+n_1)(n_o+n_2) N_2}] + \frac{1}{\tau_{n_1} \tau_{n_2} \tau_{p_1}} [ \frac{n_o n_1}{(n_o+n_1)^2} \frac{(n_o+n_2+\delta n)}{N_2}$$

$$+ \frac{(p_o+p_1+\delta p)(n_o+n_2+\delta n) n_1}{N_1 N_2 (n_o+n_1)} + \frac{(n_o+n_1+\delta n)(n_o+n_2+\delta n) n_o}{N_1 N_2 (n_o+n_1)}$$

$$+ \frac{(n_o+n_1+\delta n) n_2 n_o}{N_1 (n_o+n_2)(n_o+n_1)}] + \frac{1}{\tau_{n_1} \tau_{n_2} \tau_{p_2}} [\frac{n_1 n_o (n_o+n_2+\delta n)}{(n_o+n_1)(n_o+n_2) N_2}$$

$$+ \frac{(n_o+n_1+\delta n)(n_o+n_2+\delta n) n_o}{N_1 N_2 (n_o+n_2)} + \frac{(n_o+n_1+\delta n) n_o n_2}{N_1 (n_o+n_2)^2} + \frac{(n_o+n_1+\delta n)(p_o+p_2+\delta p) n_2}{N_1 N_2 (n_o+n_2)} ] . \quad \text{(A1.12c)}$$

By considering the case of n-type material with $N_1+N_2 < n_o x p_o$, most of the insignificant terms, Wertheim obtained the solution $m_3 = r/q = 1/\tau$ given by

$$\frac{1}{\tau} = \frac{[(1+\mu_1)\tau_1^{-1} + (1+\mu_2)\tau_2^{-1}]}{1+\mu_1(1+\nu_1) + \mu_2(1+\nu_2)} \quad \text{(A1.13a)}$$

where

$$\mu_j = N_j \frac{n_j}{n_o+n_j} [p_o+p_j+(n_o+n_j)(\tau_{p_j}/\tau_{n_j})]^{-1} \quad \text{(A1.13b)}$$

$$\nu_1 = C_{n_1}(n_o+n_1)/[C_{n_2}(n_o+n_2) + C_{p_2}(p_o+p_2)] \quad \text{(A1.13c)}$$

$$\nu_2 = C_{n_2}(n_o+n_2)/[C_{n_1}(n_o+n_1) + C_{p_1}(p_o+p_1)] , \quad \text{(A1.13d)}$$

and

$$\tau_j = [\tau_{p_j}(n_o+n_j+N_j n_j/n_o+n_j)+\tau_{n_j}(p_o+p_j+N_j p_j/p_o+p_j)]/$$

$$[n_o+p_o+N_j n_o n_j/(n_o+n_j)^2] . \quad \text{(A1.13e)}$$

For sufficiently high temperatures or sufficiently low $N_j$, this reduces to Eq. (2.1), $1/\tau = \sum_j 1/\tau_j$. The effect of the additional terms for both levels

near the conductor band is to increase the net lifetime at low temperatures, decreasing the effective energy separation of the shallower level.

Using the parameters from the NFZ-2 fit to the data set L5-2-0, reasonable values for $N_1/n_o$ and $N_2/n_o$, Eq. (A1.13) was used to calculate the lifetime. At $10^3/T = 3.6$, the lifetime from Eq. (A1.13) was 1% greater than the NFZ-2 result, at $10^3/T = 4.0$ it was 3% larger and at 4.4 it was 5% greater, indicating that the use of NFZ-2 rather than Eq. (A1.13) to calculate the lifetime parameters was not significantly in error.

To obtain the result for trapping in n-type material, for recombination through level 1 at $E_c$ - .17 ev and trapping at some level in the lower half of the gap, $1/\tau_{n_2}$ is set to zero, and $p_o$, $p_1$, and $n_2$ neglected. The result for the small signal case ($\delta n$ and $\delta p$ neglected)

$$q = \frac{1}{\tau_{p_1}\tau_{p_2}}\left[\frac{n_o p_2}{N_2(n_o+n_1)}\right] + \frac{1}{\tau_{p_1}\tau_{n_1}}\left[\frac{n_o}{N_1}\right] + \frac{1}{\tau_{n_1}\tau_{p_2}}\left[\frac{n_o}{N_1} + \frac{(n_o+n_1)p_2}{N_1 N_2}\right]$$

and

$$r = \frac{1}{\tau_{p_1}\tau_{p_2}\tau_{n_1}}\left[\frac{n_o p_2}{N_1 N_2}\right] ,$$

or

$$\tau = \tau_3 = \tau_{n_1}\frac{N_1}{n_o+n_1} + \tau_{p_2}\frac{N_2}{p_2} + \tau_{p_1}\left(1 + \frac{n_1}{n_o}\right)\left(1 + \frac{N_2}{p_2}\right) , \qquad \text{(A1.14)}$$

which is obtainable from the result of Wertheim for this case. When $N_2/p_2$ is much less than one, and if $N_1 \ll n_o+n_1$, then the lifetime will be given by the simple S-R value $\tau = \tau_{p_1}(1 + n_1/n_o)$. As the temperature decreases and $p_2$ falls, the lifetime will increase, and if $n_1/n_o \gg 1$, will be given by

$$\tau = \tau_{p_2}\frac{N_2}{p_2} + \tau_{p_1}\frac{N_2}{n_o}\frac{n_1}{p_2} . \qquad \text{(A1.15)}$$

The second term will usually predominate, and will be given by

$$\tau_{p_1} \frac{N_2 N_c}{N_d N_v} e^{-(E_c - E_1 - E_2)/kT} \tag{A1.16}$$

so that the effective energy separation is the difference between the recombination level and the trapping level separations.

In the n-type pulled materials, the photo-decay signal was clearly of the form $V = V_1 e^{-t/T_1} + V_2 e^{-t/T_2}$ , with $T_2$ much longer than the fundamental surface decay time, and $T_1$ comparable with the lifetime in similar resistivity n-type float-zoned samples. Assuming that only one type of recombination center (subscript 1) and one type of trap (subscript 2) is active in the recombination process, and that the long time constant $T_2$ of the decay is the last term of Eq. (A1.14), so that $p_2 \ll N_2$, it is of interest to examine the middle time constant $\tau_2 = p/q$ to see if any relationship between it and the S-R lifetime exists. $\tau_2$ is given by

$$\tau_2 = \frac{\dfrac{n_o}{\tau_{p_1}(n_o+n_1)} + \dfrac{1}{\tau_{p_2}(1+p_2/N_2)} + \dfrac{1}{\tau_{n_1}}\left[\dfrac{n_o+n_1}{N_1} + \dfrac{n_1}{n_o+n_1}\right]}{\dfrac{1}{\tau_{p_1}\tau_{p_2}} \dfrac{n_o p_2}{(n_o+n_1)N_2} + \dfrac{n_o}{\tau_{p_1}\tau_{n_1}N_1} + \dfrac{1}{\tau_{p_2}\tau_{n_1}}(1+p_2/N_2)\dfrac{n_o+n_1}{N_1}} \tag{A1.17}$$

Using $p_2 \ll N_2$ and $n_1 \gg n_o$, this simplifies to

$$\tau_2 = \frac{\dfrac{n_o}{\tau_{p_1}(n_o+n_1)} + \dfrac{1}{\tau_{p_2}} + \dfrac{1}{\tau_{n_1}} \dfrac{n_o+n_1}{N_1}}{\dfrac{1}{\tau_{p_1}\tau_{n_1}} \dfrac{n_o}{N_1} + \dfrac{1}{\tau_{p_2}\tau_{n_1}} \dfrac{n_o+n_1}{N_1}} \tag{A1.18}$$

If $n_o/\tau_{p_1} = n_o N_1 \sigma_{p_1} v_p >> n_o + n_1/\tau_{p_2} = N_2 \sigma_{p_2} (n_o + n_1) v_p$, so that the first term in the denominator is much larger than the second, $\tau_2$ becomes $\tau_{p_1}(1 + n_1/n_o)$, the S-R result. If the inequality is reversed, then $\tau_2$ will be given by

$$\tau_2 = \tau_{p_2} + \tau_{n_1} \frac{N_1}{n_1} \quad .$$

Since the observed behavior fits well the first case ($\tau_2$ increasing with increasing temperature) and not at all the second ($\tau_2$ constant or decreasing with increasing temperature), it appears that if only one type of traps is active, measurement of the middle decay constant $\tau_2$ yields the Shockley-Read lifetime. It is possible that many sets of traps cause the behavior observed, in which case the analysis would be so complex as to be uninformative as to the meaning of the measured time constant, due to the large number of unknown quantities involved. Perhaps the best justification of the identification of the measured time constant with the S-R lifetime is the overall similarity between the results for the n-type pulled and float-zoned crystals.

# APPENDIX II

## VERIFICATION OF THE VALIDITY OF THE SHOCKLEY-READ FORMULA

The criterion of Nomura and Blakemore[55] for the validity of the S-R formula is

$$N \ll \frac{(n_o+n_1)^2}{n_o} \frac{(n_o\tau_{p_o}+p_1\tau_{n_o})}{|\tau_{n_o}n_o-n_1\tau_{p_o}|} \quad \text{for n-type material, and} \tag{A2.1a}$$

$$N \ll \frac{(p_1+p_o)^2}{p_o} \frac{(\tau_{n_o}p_o+\tau_{p_o}n_1)}{|\tau_{p_o}p_o-\tau_{n_o}p_1|} \quad \text{for p-type material.} \tag{A2.1b}$$

When this criterion is not met, the lifetime should be given by the solution of Sandiford[5] and Wertheim[6],

$$\tau = \frac{\tau_{p_o}\left[n_o+n_1+N\frac{n_1}{n_o+n_1}\right] + \tau_{n_o}\left[p_o+p_1+N\frac{p_1}{p_o+p_1}\right]}{n_o+p_o+N\frac{n_o n_1}{(n_o+n_1)^2}} \ . \tag{A2.2}$$

This expression can be expressed in terms of the S-R formula for several cases. If p-type material is considered, then for the level in the same half of the gap, the large defect concentration formula is

$$\tau = \tau_o + \frac{\tau_{p_o}\frac{N}{p_o}\frac{p_o}{p_o+p_1}}{1+\frac{N}{p_o}\frac{p_o p_1}{(p_o+p_1)^2}} = \tau_o + \frac{\tau_{p_o}\frac{N}{p_o}}{1+\frac{p_1}{p_o}+\frac{N}{p_o}\frac{p_1}{p_o+p_1}} \ , \tag{A2.3}$$

where $\tau_o$ is the S-R lifetime formula, and if the level is in the upper half of the gap it becomes

$$\tau = \tau_{n_o} + \tau_{p_o}\left(\frac{N}{p_o}+\frac{n_1}{p_o}\right) . \tag{A2.4}$$

The latter equation can be put in the form

$$\tau = \tau'_{n_o} \left(1 + \frac{\tau_{p_o}}{\tau'_{n_o}} \frac{n_1}{p_o}\right) \tag{A2.5}$$

where $\tau'_{n_o}$ is equal to $\tau_{n_o} + N/p_o \, \tau_{p_o}$.

This equation has the same temperature behavior as the S-R equation for this case, and so only defects in the same half of the gap as the fermi level need be considered. For such levels, when $\tau_{n_o}$ is much larger than $\tau_{p_o}$, the Nomura-Blakemore criterion will be met except for such large defect concentrations that carrier removal is seen. Since no changes were seen in the resistivity after irradiation, this case need not be considered further.

A. The case of the level seen at $E_v + 0.18$ ev in p-type material.

The criterion will be satisfied at all temperatures if the low temperature criterion of

$$N \ll p_o \, \tau_{n_o} / \tau_{p_o} \tag{A2.6}$$

is satisfied. Assuming the value of $\tau_{n_o}/\tau_{p_o}$ equal to .05 (Baicker's injection level result)[35], for sample S2, where $p_o$ is $10^{15}$ $cm^{-3}$, we must have

$$N \ll 5 \times 10^{13} \; cm^{-3}.$$

If the typical introduction rate of $1.5 \times 10^6$ defects $/cm^3$-R is assumed,[22] the result for a dose of $5 \times 10^6$ R (corresponding to data set S2-2-0) is

$$N = 7.5 \times 10^{12} \; .$$

The calculated electron capture cross-section for these values is then $10^{-15}$ $cm^2$, using a value of $2 \times 10^7$ cm/sec for $v_n$. This value is certainly

not large, and the effect of increasing the defect concentration would be to decrease the capture cross-section value. Hence it appears that the S-R theory is valid for this case.

B. The level at $E_c$ -0.17ev in n-type material.

In this material for all samples $n_1$ is much larger than $n_o$ at all temperatures measured. Using the least favorable case of 20 ohm-cm material, with $10^3/T$ equal to 4.0, $n_1/n_o$ is 8. Since previous experiments indicated $\tau_{n_o}/\tau_{p_o} = 20$, the Nomura-Blakemore criterion is then

$$N \ll 0.05\ (1+8)^2 \frac{(n_o \tau_{p_o})\, n_o}{\left| 8n_o \tau_{p_o} - 20 n_o \tau_{p_o} \right|} = 7\ n_o$$

With a flux of $5 \times 10^6$ R, and an introduction rate of $1.5 \times 10^6$ defects $cm^3$ R, and $n_o$ equal to $2 \times 10^{14}$ $cm^{-3}$, we have

$$N = 7.5 \times 10^{12} \approx 0.04\ n_o$$

and the criterion is satisfied for this level.

C. The level at $E_c$ -0.4 ev in n-type material.

Again the worst case will be at low temperatures, and for this level $n_1$ will then be much less than $n_o$. Assuming the usual value of 0.05 for $\tau_{p_o}/\tau_{n_o}$, the Nomura-Blakemore criterion is

$$N \ll 0.05\ n_o$$

For the data set L5-2-0, which was typical of the n-type float-zoned samples, the dose was $2 \times 10^5$ R. Using $n_o$ equal to $6 \times 10^{13}$ $cm^{-3}$, and an introduction rate of $1.5 \times 10^6$ defects $cm^3$ R, a value high according to the

findings of Sonder and Templeton,[27] the ratio of the estimated defect concentration to the donor density is

$$N/n_o = 5 \times 10^{-3}$$

and the criterion for the validity of the S-R theory is satisfied for the float-zoned samples. For the higher doses given the n-type pulled samples, the above result indicates that use of the S-R theory would be improper. However the much higher lifetime-flux products in the latter materials indicates that the introduction rate in the pulled materials for the deep levels is about 2% of the introduction rate in the float-zoned materials, and since the doses received by the pulled samples were less than ten times the doses for the other material, the S-R theory is an even better approximation in the pulled material.

D. <u>The level at $E_v$ + 0.4 ev seen in 5000 ohm-cm p-type material.</u>

Since this material seems anomalous, the fits were regarded lightly. For this material, the S-R formula cannot be shown to be valid for $\tau_{p_o} >> \tau_{n_o}$ unless very small defect introduction rates are supposed, due to the high resistivity of the material. The use of reasonable (according to other samples) introduction rates indicates that for the doses received, $N/p_o$ will be about 1. If the radiation induced lifetime is compared to the lifetime predicted by the theory of Sandiford and Wertheim for this case, or even for $N/p_o$ equal to .1, it will be seen that the calculated lifetime at $10^3/T$ equal to 3.2 is less than that at 3.6, which is not true for the data sets shown in Figure 37. Hence if these data are to be trusted, the level at $E_v$ + 0.4 ev either has an exceptionally low introduction rate,

with the introduction rates of all other defects much less in this material, or more probably, the electron capture cross-section is much larger than the hole capture cross-section.

# REFERENCES


1. C. Kittel, Introduction to Solid State Physics, 2nd ed., John Wiley and Sons, New York, pp. 477-48 (1959).

2. Ibid., pp. 561-569.

3. J. N. Hobstetter, "Effects of Imperfections on Germanium and Silicon," Semiconductors, N. B. Hannay, ed., Reinhold Publishing Co., New York, pp. 508-540 (1959).

4. R. G. Rhodes, Imperfections and Active Centers in Semiconductors, The MacMillan Co., New York, pp. 151-159 (1964).

5. C. D. Thurmond, "Control of Composition in Semiconductors by Freezing Methods," Semiconductors, Ed., N. B. Hannay, Reinhold Publishing Co., New York, pp. 145-191 (1959).

6. M. Tannenbaum, "Semiconductor Crystal Growing," Semiconductors, ed. N. B. Hannay, Reinhold Publishing Co., New York, pp. 87-144 (1959).

7. W. Kaiser, P. H. Keck, and C. F. Lange, Phys. Rev., 101, 1264 (1956).

8. C. S. Fuller, "Defect Interactions in Semiconductors," Semiconductors, ed., N. B. Hannay, etc., pp. 217-219.

9. P. H. Keck and W. Van Horn, Phys. Rev., 91, 512 (1953).

10. J. H. Crawford, Jr., "Radiation Effects and Defect Structures in Diamond Structure Semiconductors," The Interaction of Radiation with Solids, eds. Strumane, Nihoul, Gevers, and Amelinckx, pp. 421-470.

11. G. D. Watkins, 7th Int. Conf. on Phys. of Semiconductors, Paris, 1964, 3, 97, Academic Press, New York, 1964.

12. S. G. Kalashnikov and N. A. Penin, Zhur. Tekn. Fiz. 25, 1111 (1955).

13. R. H. Kingston, Proc. Inst. Radio Engrs., 42, 829 (1954).

14. A. P. Ramsa, H. Jacobs, and F. A. Brand, J. Appl. Phys., 30, 1054 (1959).

15. V. S. Vavilov and A. F. Plotnikov, Proc. of Int. Conf. on Crystal Lattice Defects, J. Phys. Soc. Japan, 18, Suppl. III, p. 230 (1963).

16. H. Y. Fan and A. K. Ramdas, J. Appl. Phys., 30, 1127 (1959).

17. M. I. Iglitsyn and Yu A. Kontsevoi, Soviet Physics-Solid State, 2, 1039 (1960).

18. T. Nakano and Y. Inuishi, J. Phys. Soc. Japan, 19, 851 (1964).

19. T. Nakano, K. Nakamura, and Y. Inuisi, J. Phys. Soc. Japan, 20 2140 (1965).

20. H. M. James and K. Lark-Horowitz, Z. Physic Chem. (Leipzig) 198, 107 (1951).

21. G. K. Wertheim, Phys. Rev., 110, 1272 (1958).

22. E. Sonder and L. C. Templeton, J. Appl. Phys., 31, 1279 (1960).

23. G. D. Watkins and J. W. Corbett, Phys. Rev., 121, 1001 (1961).

24. G. D. Watkins, J. Phys. Soc. Japan, Suppl. II, 22 (1963).

25. G. K. Wertheim and D.N.E. Buchanan, J. Appl. Phys., 30, 1232 (1959).

26. Y. Inuishi and K. Matsuura, J. Phys. Soc. Japan, Suppl. III, 240, (1963).

27. E. Sonder and L. C. Templeton, J. Appl. Phys., 34, 3295 (1963).

28. H. Saito, M. Hirata and T. Horuichi, J. Phys. Soc. Japan, Suppl. III., 246 (1963).

29. N. A. Vitovskii, D. P. Lukirskii, T. V. Mashovets, and V. I. Myakota, Soviet Physics-Solid State, 4, 840 (1962).

30. D. E. Hill, Phys. Rev., 114, 1414 (1959).

31. T. Tanaka and Y. Inuishi, J. Phys. Soc. Japan, 19, 167 (1964).

32. J. W. Corbett, G. D. Watkins, R. M. Chrenko, and R. S. MacDonald, Phys. Rev., 121, 1015 (1961).

33. G. N. Galkin, N. S. Rytova, and V. S. Vavilov, Soviet Physics-Solid State, 2, 1819 (1961).

34. R. H. Glaenzer and C. J. Wolf, J. Appl. Phys., 36, 2197 (1965).

35. J. A. Baicker, Phys. Rev., 129, 1174 (1963).

36. V. S. Vavilov, S. I. Vintovkin, A. S. Lyutovich, A. F. Plotnikov, and A. A. Sakolova, Soviet Physics-Solid State, 7, 399 (1965).

37. G. D. Watkins and J. W. Corbett, Phys. Rev., 138, A543 (1965).

38. G. D. Watkins and J. W. Corbett, Disc. Faraday Soc., 31, 86 (1961).

39. G. D. Watkins and J. W. Corbett, Phys. Rev., 134, A1359 (1964).

40. E. Sonder and L. C. Templeton, J. Appl. Phys., 36, 1811 (1965).

41. V. S. Vavilov, G. N. Galkin, V. M. Malovetskaya, and A. F. Plotnikov, Soviet Physics-Solid State, 4, 1442 (1963).

42. T. Tanaka and Y. Inuishi, Jap. J. Appl. Phys., 4, 725 (1965).

43. V. M. Malovetskaya, G. N. Galkin, and V. S. Vavilov, Soviet Physics-Solid State, 4, 1008 (1962).

44. B. R. Gossick, J. Appl. Phys., 30, 1214 (1959).

45. Gladys W. Grodstein, "X-ray Attenuation Coefficients from 10kw to 100 Mev," National Bureau of Standards Circular 583, U. S. Gov't. Printing Office, Washington, D. C., 1957, p. 31.

46. J. S. Blakemore and K. C. Nomura, J. Appl. Phys., 31, 753 (1960).

47. J. S. Blakemore, Semiconductor Statistics, Pergamon Press, London, p. 195, 1962.

48. W. van Rooskeck and W. Shockley, Phys. Rev., 94, 1558 (1954).

49. R. N. Hall, Phys. Rev., 83, 228 (1951).

50. W. Shockley and W. T. Read, Phys. Rev., 87, 835 (1952).

51. D. J. Sandiford, Phys. Rev., 105, 524 (1957).

52. G. K. Wertheim, Phys. Rev., 109, 1086 (1958).

53. J. A. Hornbeck and J. R. Haynes, Phys. Rev., 97, 311 (1955).

54. J. R. Haynes and J. A. Hornbeck, Phys. Rev., 100, 606 (1955).

55. K. C. Nomura and J. S. Blakemore, Phys. Rev., 112, 1067 (1958) and Phys. Rev., 121, 734 (1961).

56. C. B. Collins, et. a., Phys. Rev., 105, 1168 (1957) and references therein, H. H. Woodbury and W. W. Tyler, Phys. Rev., 105, 84 (1957) and references therein.

57. C. T. Sah and W. Shockley, Phys. Rev., 109, 1103 (1958).

58. M. Bernard, J. Electr. Control, 5, 15 (1958).

59. N. G. Zhdanova, et. al., Soviet Physics-Solid State, 1, 481 (1959).

60. M. Nagae, J. Phys. Soc., Japan, 18, 207 (1963).

61. P. Handler, J. Phys. Chem. Solids, 14, 1 (1960).

62. J. S. Blakemore, Semiconductor Statistics, Pergamon Press, London, Ch. 10, 1962.

63. F. J. Morin and J. P. Maita, Phys. Rev., 96, 28 (1954).

64. N. B. Hannay, Semiconductors, Rheinhold Publishing Co., New York, p. 40, 1959.

65. R. K. Swank, Lifetimes of Excited States in Alkali Halide Crystals Containing F Centers, Thesis, University of Illinois, Urbana, 1962, (unpublished).

66. G. Bemski, Phys. Rev., 111, 1515 (1958).

67. R. J. Spry, Bull. Am. Phys. Soc., 11, 193 (1966).

# VITA

Ralph Allan Hewes was born [redacted]. He attended public schools in Clark County, Ohio, and in May 1957 graduated from Northeastern High School. He enrolled at Case Institute of Technology, Cleveland, Ohio, in September 1957 as a Freshman Prize Scholarship Winner. He was elected a member of Tau Beta Pi, was named a Senior Thesis Honors Student, and received his B.S. in physics with honors in June 1961. Since September 1961 he has been a student at the University of Illinois and received the degree of Master of Science in Physics in February 1963. While a graduate student he held teaching and research assistantships from the physics department. He is a member of the American Physical Society.